REPUBLIC OF IRAQ

MINISTRY OF HIGHER EDUCATION AND

SCIENTIFIC RESEARCH

AL-FURAT AL-AWSAT TECHNICAL UNIVERSITY

ENGINEERING TECHNICAL COLLEGE NAJAF

THERMAL AND ELECTRICAL EFFICIENCIES ENHANCEMENT OF A SOLAR PV/T SYSTEM USING POROUS METALLIC MEDIA

By

AMJAD HAMEED HAMZAWY

IN MECHANICAL ENGINEERING TECHNIQUES OF POWER

2024

**THERMAL AND ELECTRICAL EFFICIENCIES
ENHANCEMENT OF ASOLAR PV/T SYSTEM
USING POROUS METALLIC MEDIA**

A THESIS
SUBMITTED TO THE DEPARTMENT OF MECHANICAL
ENGINEERING TECHNIQUES OF POWER
IN PARTIAL FULFILLMENT OF THE REQUIREMENTS FOR
THE DEGREE OF MASTER OF THERMAL TECHNOLOGIES IN
MECHANICAL ENGINEERING TECHNIQUES OF POWER
(M.TECH)

BY

AMJAD HAMEED HAMZAWY

Supervisor By

Prof. Dr.Qahtan Adnan Abed

2024

بِسْمِ اللَّهِ الرَّحْمَنِ الرَّحِيمِ

يَرْفَعِ اللَّهُ الَّذِينَ آمَنُوا مِنْكُمْ وَالَّذِينَ أُوتُوا الْعِلْمَ دَرَجَاتٍ وَاللَّهُ بِمَا تَعْمَلُونَ خَبِيرٌ

المجادلة ﴿11﴾

DISCLAIMER

I confirm that the work submitted in this thesis is my own work and has not been submitted to an organization or for any other degree.

Signature:

Name: Amjad Hameed Hamzawy

Date: /   / 2024

ACKNOWLEDGMENT

I would like to express my deep gratitude to God for granting me success and assisting me in completing my scientific study. I would also like to extend my highest appreciation and thanks to my supervisor Prof. Dr. Qahtan Adnan Abed, who generously devoted his valuable time and shared his extensive knowledge, rich experience, and valuable advice to enhance my research. I pray that God rewards him abundantly. I am grateful to the scientific department and my professors for the help provided throughout my studies.

To my beloved parents, I cannot forget your continuous support and everything you have done for me. You both deserve all the appreciation and love and no matter how much I express my thanks and gratitude, it will never truly reflect what you have done for me.

To my wife, my companion in life and partner on this journey, I thank you for your support and assistance in every difficult situation. I am grateful for everything she has done.

I would also like to express my thanks and gratitude to all my colleagues for their support and encouragement.

Expressing gratitude and appreciation to those who supported you throughout your journey is very important. Your words of thanks reflect your ability to appreciate and acknowledge the efforts they made to help you in your scientific journey. I wish you a bright future and continued success.

Amjad Hameed Hamzawy
2024

SUPERVISORS CERTIFICATION

I certify that the thesis entitled "**Thermal and Electrical efficiencies enhancement of a Solar PV/T system using porous metallic media**" submitted by **Amjad Hameed Hamzawy** has been prepared under my supervision at the Department of Mechanical Engineering Techniques of Power, College of Technical Engineering-Najaf, AL-Furat Al-Awsat Technical University, as partial fulfillment of the requirements for the degree of Master of Techniques in Thermal Engineering.

Signature:

Name: Prof. Dr. Qahtan A. Abed

(Supervisor)

Date: /   / 2024

In view of the available recommendation, we forward this thesis for debate by the examining committee.

Signature:

Name: Asst. Prof. Dr. Adel A. Eidan

Head mechanical Eng Tech of power Dept.

Date: /   / 2024

COMMITTEE CERTIFICATION

We certify that we have read the thesis entitled "**Thermal and Electrical efficiencies enhancement of a Solar PV/T system using porous metallic media**" submitted by **Amjad Hameed Hamzawy** and, as examining committee, examined the student's thesis in its contents. And that, in our opinion, it is adequate as a thesis for the degree of Master of Techniques in Thermal Engineering.

Signature:

Name: Prof. Dr. Qahtan A. abed

(Supervisor)

Date: /   / 2024

Signature: Signature:

Name: Prof. Dr. Mohammed W. Aljibory   Name: Dr. Basil N. Merzah

(Member)   (Member)

Date: /   / 2024   Date: /   / 2024

Signature:

Name: Prof. Dr. Hyder H. Abed Balla

(Chairman)

Date: /   / 2024

Approval of the Engineering Technical College- Najaf

Signature:

Name: Asst. Prof. Dr. Hassanain Ghani Hameed

Dean of Engineering Technical College- Najaf

Date: /   / 2024

LINGUISTIC CERTIFICATION

This is to certify that this thesis entitled "**Thermal and Electrical efficiencies enhancement of a Solar PV/T system using porous metallic media**" was reviewed linguistically. Its language was amended to meet the style of the English language.

Signature:

Name:

Date:

ABSTRACT

Due to the detrimental effects associated with the utilization of fossil fuels, it has become imperative to identify alternative sources of energy. One of the primary avenues for renewable energy generation is solar power. Solar energy can be harnessed and converted into usable electrical energy through the utilization of photovoltaic (PV) cells. The efficiency of solar cells is significantly influenced by their operating temperature, and therefore, it is crucial to mitigate high temperatures to enhance their electrical performance. In this study, an extensive theoretical and practical investigation is conducted with the objective of reducing the operating temperature of photovoltaic (PV) panels and augmenting their overall efficiency. The proposed approach involves employing forced airflow within an air duct located beneath the solar panel, utilizing porous metal media. The optimal design of the PV/T (photovoltaic/thermal) system is determined through theoretical analysis using COMSOL Multiphysics 5.5, which subsequently facilitated experimental work. Simulation findings indicate that incorporating 14 ribs within the porous media and an air mass flow rate of 0.111kg/s yielded optimal results. The experimental study is conducted at AL-Rumaitha Technical Institute, Al-Furat Al-Awsat Technical University in Iraq (coordinates: 31°42′ - 45°12′).

During the experimental work, two monocrystalline silicon solar panels are employed, with one panel integrated into a PV/T module, while the other panel serves as a control without any cooling mechanism. The airflow channel, a critical component of the PV/T system, is constructed using aluminum measuring 0.7 mm in thickness, 115 mm in depth, 2000 mm in length, and 1000 mm in width. Airflow is facilitated through the use of an air intake fan. The experimental investigations was conducted on several different days throughout the year, using three air mass flow rates of 0.057 kg/s, 0.096 kg/s, and 0.111 kg/s. The results demonstrate that the best mass flow rate of air is 0.111 kg/s, where the maximum achieved electrical efficiency reached 19%. This represents a 6.9% enhancement, with a peak output power of

330.7W. Furthermore, the maximum incident radiation was measured at 1192.14 W/m2, with a temperature difference of 6.7°C between the inlet and outside air. The amount of heat gained was about 378.6 watts, and the thermal efficiency was about 29.57%. Thus, a total efficiency of 48.53% was achieved, which confirms the effectiveness of the applied photovoltaic system.

CONTENTS

Contents

LIST OF TABLES

NOMENCLATURE

Symbol	Definition	Unit
PV	Photovoltaic	——
PV/T	Photovoltaic thermal	——
DC	Constant current	Amp.
A	Area of PV panel	m^2
AC	Alternating current	Amp
PPFHS	Plate pin fin heat sink	——
PFHS	Plate fin heat sink	——
TMS	Thin metal plates suspended	——
SAC	Solar Air Collector	——
CFD	Computational fluid dynamic	——
T_{pv}	Photovoltaic temperature	°C
PMP	Maximum power point	W
G	Solar irradiance	W/m^2
V_W	Wind speed	m/s
T_{amb}	Ambient temperature	°C

P_m	Maximum power	W
I_m	Maximum current	Amp.
V_m	Maximum voltage	V
FF	Fill factor	—
I_{sc}	Short circuit current	A
V_{oc}	Open circuit voltage	V
S	PV cell temperature	°C
T_{ref}	PV reference temperature	°C
Q_u	Heat gained	W
$\dot{m}$	Mass flow rate	Kg/s
cp	Specific heat	kJ/kg.K
ΔT	Difference of incoming and outgoing temperatures	°C
RMSE	Root mean square error	—
M	total quantity of values for the efficiency	—
Greek Symbols		
η_{cel}	PV efficiency %	—
η_{Tref}	Electrical efficiency at T_{ref} %	—
β_{ref}	Temperature coefficient (0.0045)	k^{-1}
η_{th}	Termal efficiency %	—
η_O	Overal efficiency %	—
ρ	Density of air	Kg/m^3
k-ε	Physics of turbulent flow	—

Chapter one: Introduction

1.1. Introduction

The majority of the energy on earth comes from the sun. Today, solar energy is gaining popularity worldwide, particularly in nations with more solar potential. Various technologies, including solar thermal electricity, solar heating, and solar photovoltaic cells can be used to harness the sun's energy [1]. Solar photovoltaic systems use a collection of tiny parts known as solar cells to transform light from the sun directly to electrical current. The rising cell operating temperature, particularly in regions with hot weather and intense sunlight, is one of the main interests of researchers in the field of energy solar photovoltaic technology. According to studies, more than 80% of the sunlight that strikes PV cells' surface is converted to heat, and about 20% of it is turned directly into energy [2].

A small portion of the solar radiation is converted into electrical energy by the solar panel, while most of the radiation is converted into heat. The temperature inside the cell increases as a result. The build up of heat decreases the performance of the panel which is typically around 15% in a basic test scenario at a temperature of 25 °C and an intensity of 1000 w/m^2 [3]. However, as the temperature rises, the electrical output of cells will decrease due to losses in the conversion of solar energy to electricity. Furthermore, persistently high operating temperatures may permanently damage the cells. Solar cells should remain cool to avert temperature increases, efficiency decreases, and irreversible breakdown. There are numerous ways to keep the PV's temperature limit constant. PV temperature adjustment techniques might be passive, active, or a combination of both[4].

1.2. Solar Energy

Solar energy is a term that refers to the combined radiant light and heat from the sun which is harnessed using different energy conversion and transfer technologies such as the photovoltaic cell and solar thermal collector, etc. This technology's main benefit is its energy source. The sun is limitless and cannot run out. Additionally, solar energy technologies are a practical choice for all since the sun shines everywhere. It is essential to keep in mind that the strength of solar energy might change from one location to another. However, in general, solar energy is split into two processes, which are as follows:

1. The photoelectric effect is the transformation of visible light into electricity.
2. Solar thermal refers to collecting and distributing its heat component for heating purposes.

Solar radiation, which is the sum of the Sun's visible and near-visible (ultraviolet and near-infrared) radiations, is emitted into space. The areas of solar radiation can be found at various wavelengths. These ranges fall within 0.2 to 4.0-micron broadband range. Figure (1.1) shows the areas of the solar Spectrum.

This radiation's power per square meter (W/m^2) is measured on a plane to the Sun. Figure (1.2) depicts the position of the earth and sun in space. It is commonly believed that solar radiation outside earth is constant at about 1367 W/m^2, and due to differences in the distance between the Earth and the Sun, this number varies by $\pm 3\%$. The properties of the solar irradiance within the earth's atmosphere might vary depending on the barriers and media the radiation may pass through. Figure (1.3) shows the types of solar radiation[5].
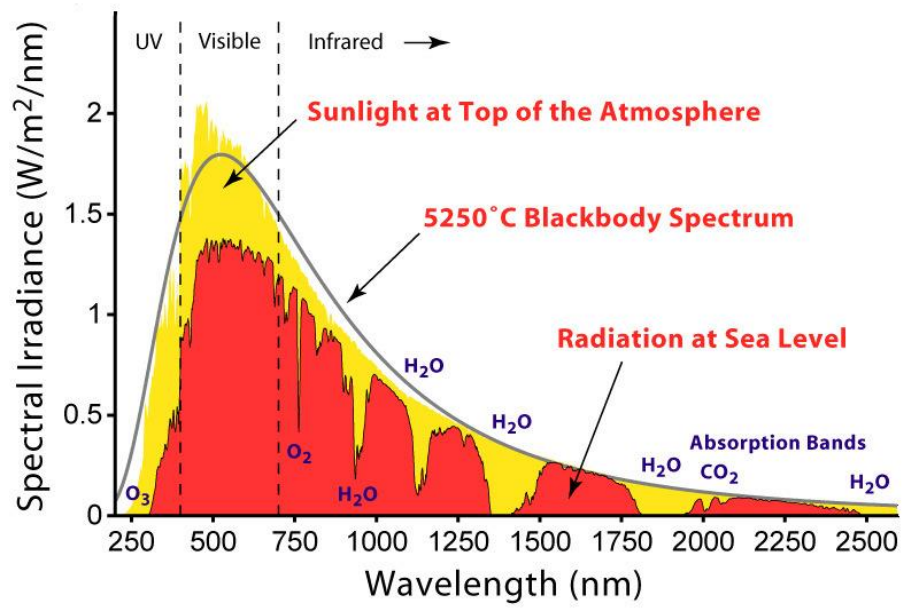
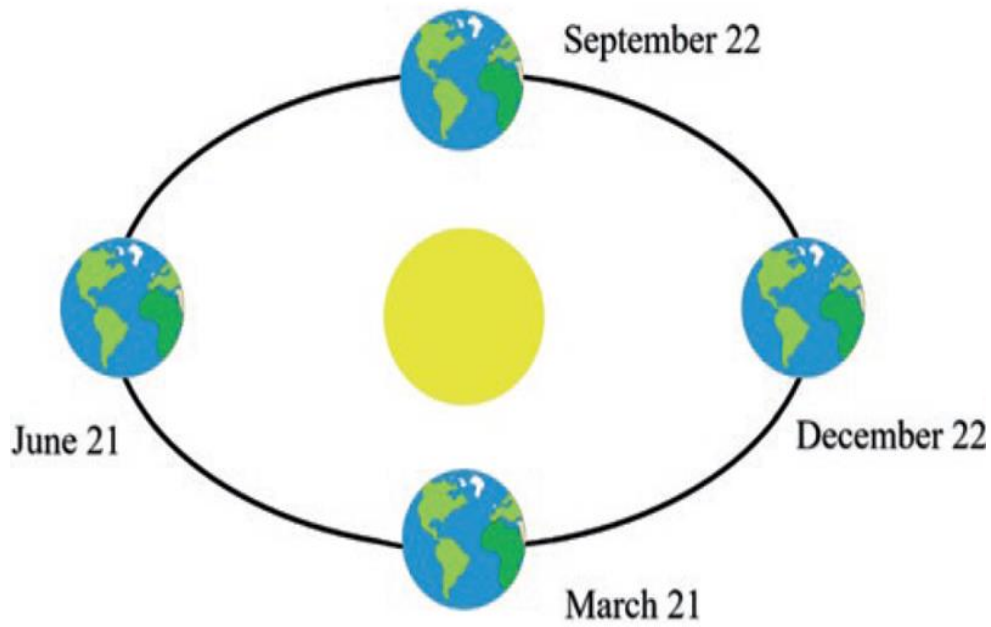Figure 1.1. The areas of the solar Spectrum [6].

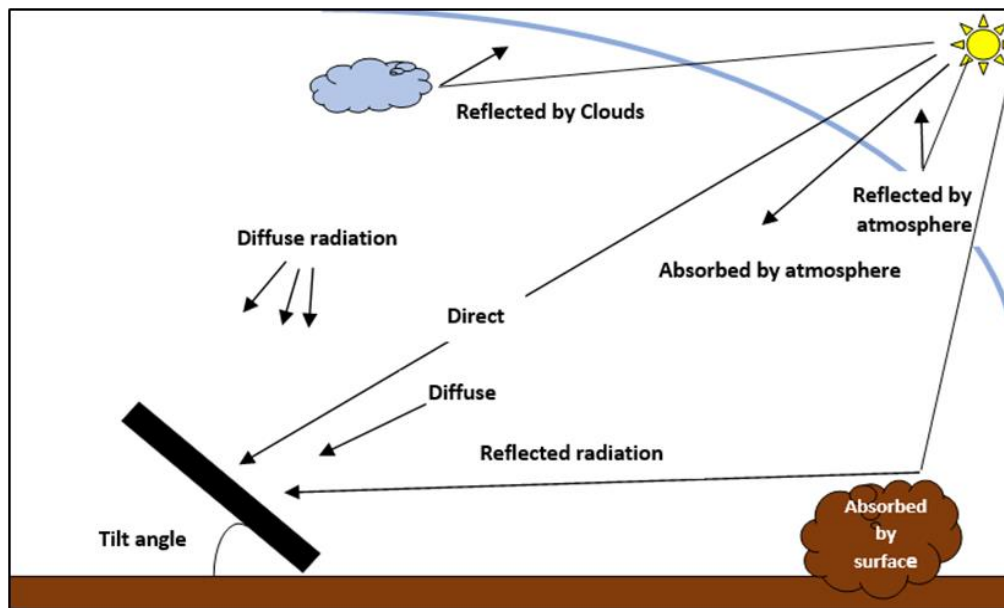Figure 1.2. The position of the Earth and Sun in space [7].

Figure 1.3. Type of solar radiation

1.3. Photovoltaic Panel Types

In general, there are several technologies for solar cells. In addition to the existence of these technologies, the solar PV sector now uses two fundamental commercial PV module technologies that are readily available on the market, these are solar cell Wafers Made from a monocrystalline or polycrystalline wafer of crystalline silicon, and thin film technologies use very thin layers of photovoltaic active material deposited using vacuum deposition manufacturing processes on a glass or metal substrate [5]. Figure (1.4) shows the types of PV panels.
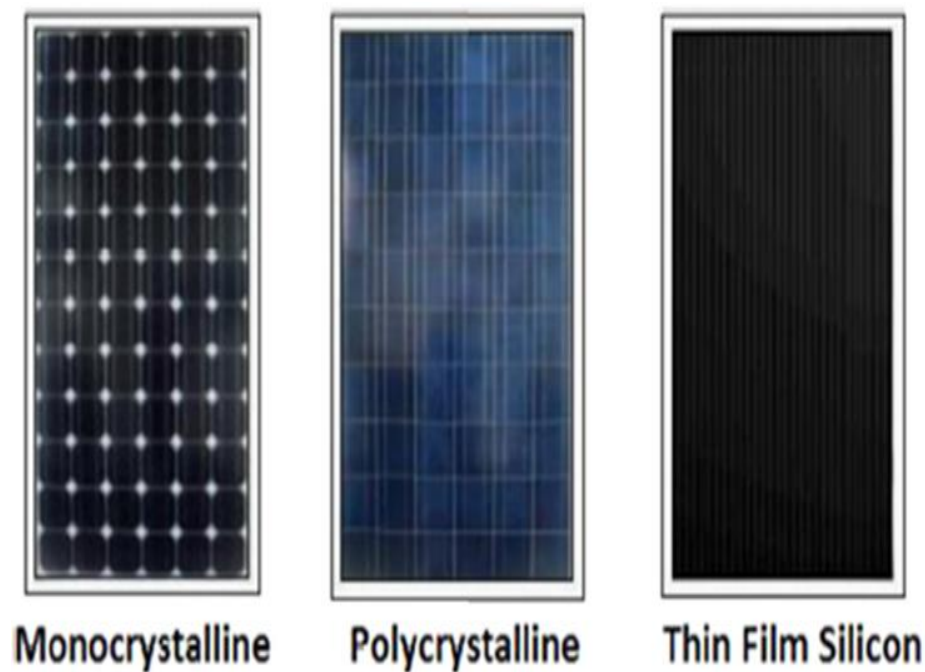
Figure 1.4. Main types of PV panels [6].

Photovoltaic cells are made up of various silicon crystals formed from an ingot. Additionally, they are cut and then engraved. Conversion efficiencies for polycrystalline cells are typically between (13-15)%, which are slightly lower than those of monocrystalline cells which are usually (16-18)%. Polycrystalline PV modules come with a 20-year guarantee from reputable manufacturers. The monocrystalline cells are the most developed modules available. Manufacturers of this unit offer warranties from 20 to 25 years.

Photosensitive materials are deposited in extremely thin layers onto a cheap substrate like glass, stainless steel, or plastic to create thin-film modules. Thin-film PV has not yet achieved field efficiencies of more than 10% [8].

Therefore, the monocrystalline type of photoelectric panels has been selected to conduct the tests for this thesis.

1.4. Components of PV system

One of the world's fastest-growing sectors is photovoltaic solar energy (PV). To maintain that pace, new advancements have been made in the usage of materials, the energy required to make those materials, the design of devices, production techniques, as well as novel ideas to improve the overall efficiency of cells. Through the use of some of the authors' common terminology for photovoltaic systems, including solar radiation, generation, conversion, and electricity, we may understand an appropriate idea of solar PV [9]. It converts direct sunlight into electricity using a single-diode junction (or several junctions) [10].

A photovoltaic system typically includes arrays of a Photovoltaic panel, a device that converts (DC to DC), a DC to AC converter, a power meter, a breaker, and depending on the system's size a battery or array of batteries Figure (1.5) [11].
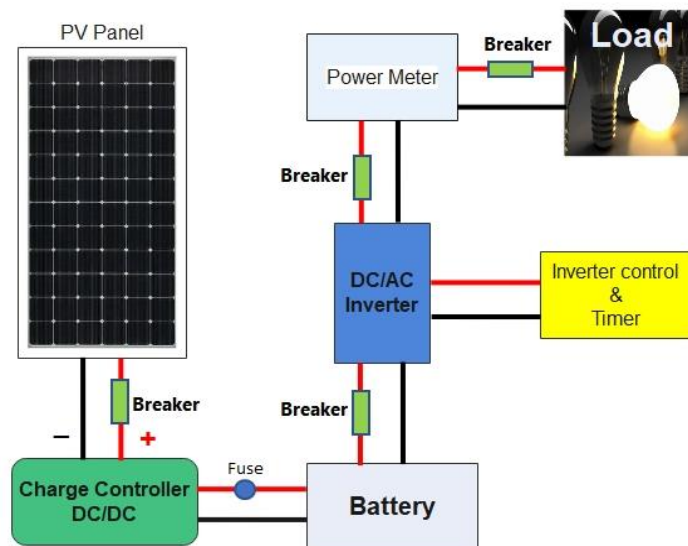
Figure 1.5. Components of the solar energy system[11]

1.5. Some factors affecting the efficiency of PV cells

The PV system becomes ever more comparable with traditional energy systems as its efficiency rises. The performance of PV systems increases significantly when the temperature is reduced, which encouraged many researchers to investigate various cooling methods for the PV system [12]. Passive and active cooling techniques have both been studied to determine the most effective way to cool photovoltaic panels[13].

A PV module's capacity to produce energy is primarily determined by the type, composition, and environmental elements, particularly temperature and solar irradiation [14]. Photovoltaic Cell temperature can be considered a crucial metric, which when it rises can generate thermal tensions that shorten the system's working, life and cause a drop in electrical efficiency. As a result, it is to properly research this parameter. The performance or efficiency of a photovoltaic module is defined as the ratio of its highest power production to the solar radiation incident on its surface at a given module surface temperature [15]. The electrical efficiency may be seen to be a linear function of module temperature. With an increase in PV module temperature, the electrical efficiency of the module decreases [16].

1.6. Problem statement

One of the main factors that can influence the performance of PV panels is their operating temperature. Which affects the voltage and current of the solar cells. A decline in electricity production efficiency is brought by rising temperatures.

Lowering the operating temperature of solar cells is crucial for optimal operation and to prevent damage to PV panels. So, that should use the quickest and easiest means possible for heat transfer and disposal to lower cell surface temperature.

It is important to use the air ducts with heat sinks to reduce the temperature of photovoltaic cells, because the high operating temperature of the cell reduces the open-circuit voltage and thus reduces the power generated. By taking care of improving the PV cooling module, the photovoltaic panels can operate at lower temperatures. It results in improved system performance and energy production.

1.7. Objectives of this study

The study aims to achieve the following objectives:

1- Constructing a new simulation model to determine the performance of the cooling model proposed for photovoltaic panels. Verification of the proposed model was also carried out by changing the number of ribs of the porous metal to improve the unit design.

2- Improving the performance of photovoltaic panels by reducing their operating temperature by using an effective cooling method.

3- Reducing the temperature of photovoltaic panels using an effective cooling method to improve their performance and increase energy production.

4- Finding experimental results for the performance of the PV panels cooling module and comparing them with the numerical results for the same unit.

5- Finding the appropriate air speed to dissipate the largest amount of PV panels heat.

Chapter Two: Literature Review

2.1. Introduction

The high working temperature of photovoltaic panels, accumulation of dust on the surface of panels, and low absorption of solar radiation caused by the scattering of sunlight are factors affecting performance [17]. With increasing temperature, the efficiency of the photovoltaic cells typically falls about 0.5 percent for each one-degree rise in the cell temperature, for example, silicon solar cells at 1000 W/m^2 and 25 °C are characterized as the ideal temperature of the panel, keeping the temperature of the cell at 25°C can maintain the optimum efficiency of the photovoltaic cells [18].

Solar cell temperature reduction is crucial for photovoltaic applications. In previous studies and applications, many cooling techniques were studied and developed to be used in cooling solar cells. One of the most common cooling methods is to improve convective heat transfer between solar panels and the surrounding environment with additional media (eg, ambient air and water), and this method can be divided into two classifications: the first classification transfers heat to the media and then dissipates it to the surrounding environment. One application that adopts this method is forced airflow [19]. For example, **Teo et al.** [16] designed a hybrid solar system to effectively cool solar cells providing it with a parallel set of channels that distribute air uniformly in the rear side of the photovoltaic cell. This causes a significant lowering of the temperature and increases performance of 12% to 14%. The second one includes utilizing waste heat from solar cells for another use, which is known as the photovoltaic/thermal system [20]. For example, **Min Yu et al.** [21] proposed a new design for micro-channel heat pipes to collect heat energy and cool solar cells at the same time. A higher-than-current thermal collector

efficiency was measured at 17.2%, which ranged from 25.2% to 62.6% during the test period, and an electrical efficiency of 19%. The researchers worked to develop cooling systems categorized as active cooling systems that required external power inputs with a heat sink. The addition of a heat sink made of a thermally conductive material to the bottom of the photovoltaic cell increases the surface area of heat exchange between the photovoltaic cell and the surrounding medium. Heat sinks, despite being very simple and inexpensive to construct, offer a high potential for reducing the heat of solar panels and need to be improved substantially [22].

This chapter discussed several air-cooling techniques for photovoltaic panels to get more information and to understand the scientific methods used to improve the performance of solar panels.

2.2. Methods for air cooling systems

There are several studies and investigations that used air to cool photovoltaic panels with heat sinks, and others used forced air cooling without heat sinks.

2.2.1. Active air-cooling techniques

An active cooling system uses additional energy to reduce excess heat from solar panels and distribute it elsewhere. Therefore, the energy that is circulated must be used for a cooling medium like water or air [23]. There are two methods for using air to reduce heat in the panels; reducing the temperature on the upside and cooling the back side of PV panel [26]. Where it is used a fan on either the front or the back of the solar panels when using air to cool them; both techniques help to lower the operating temperature of the panels [24]. To increase electrical efficiency, surplus heat is removed in a technique that incorporates the unit with a heat exchanger that uses a stream of fluids like air [25].

Teo et al. [16] demonstrated a distinct impact of active cooling. When the blower was employed to cool the solar cell, the PV unit's operational temperature decreased from 68 degrees Celsius to 38 degrees Celsius. Thus, the efficiency rose from 8.6% to 12.5%.

Nabil A.S.Elminshawya et al. [27] conducted a research on a new active PV panels cooling system by pushing precooled air over the rear of the panel, in Port Said, Egypt to enhance the solar panel's performance. They succeeded in lowering the Photovoltaic unit temperature from 55 to 42 degrees Celsius at a flow velocity of 0.0288 m3/s, increasing the photovoltaic panel's power by 18.90 % and electrical efficiency by 22.98%. **Soudabeh Golzari et al**. [28] investigated how to enhance thermoelectric heat transfer using electrodynamics in a single-pass by the air-cooled system. The results revealed a 65% improvement in the heat transfer coefficient and electrical efficiency of roughly 28.9% when they employed a voltage of 11 KV. The relation between cell temperature and electrical efficiency is depicted in Figure (2.1).
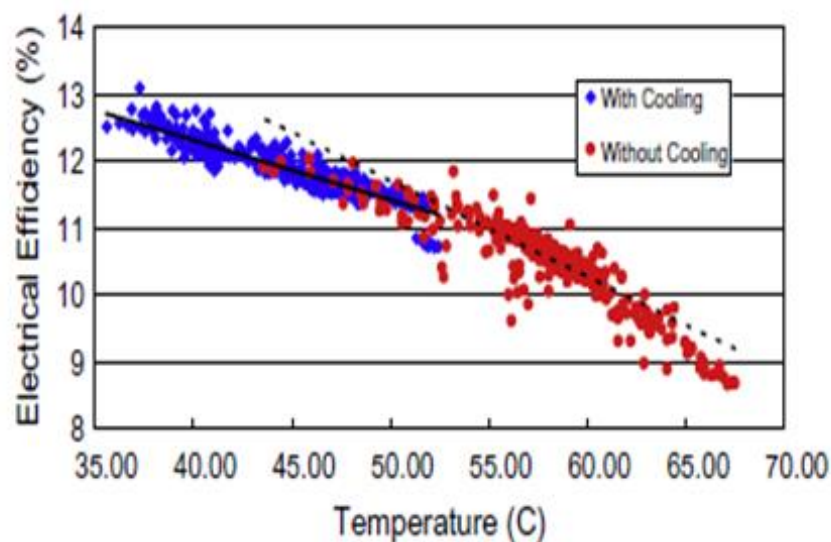

Figure 2.1. Correlation between cell temperature and electrical efficiency [16]

2.2.2. Cooling techniques with heat sink

A heat sink is a type of exchanger used to dissipate heat to the environment efficiently. Many applications that call for efficient heat transmission use heat sinks. There are numerous methods for enhancing the heat sink's performance, including increased fin surface area, thermal conductivity, or heat transfer coefficient. Figure (2.2) shows one of the simplest, most dependable, and least expensive fin types frequently utilized in convection cooling systems are rectangular fins[29].
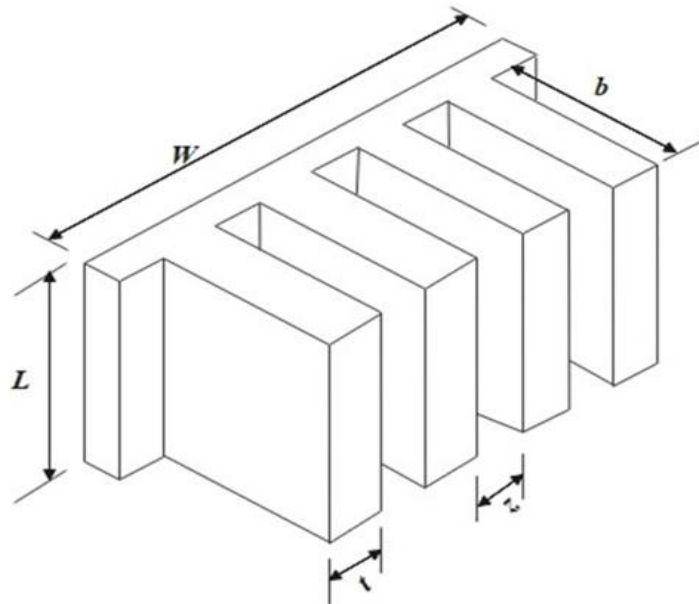
Figure 2.2. Heat sink for rectangular fins with dimensions as (Z) distance between fin, (t) a thickness, (b) length, (L) base length, and (W) base width[29]

There are several studies of various methods that used heat sinks. **A.M. Elbreki et al.** [30] carried out an experiment examination to determine how well the PV module Polycrystalline with an area of 1.7 m² is cooled. For the redesigned fin heat sinks, they used two alternative designs. Figure (2.3) is longitudinal and

winding. The experiment was performed at an ambient temperature of 33 °C and an average sun irradiance of 1000W/m^2. With winding fins, the best results were obtained. Where the average photovoltaic system temperature is 24.6 °C lower than the reference photovoltaic unit. An electrical efficiency of 10.68% and a power of 37.1W was achieved. **Fatih Bayraka et al.** [31] showed that fins positioned beneath the photovoltaic panels which are aluminum fins that act as an effective heat sink. In their study, they used aluminum fins with 10 different configurations designed as a 70 x 200 mm array. Considering the results of the pilot research, the design showed an improvement in efficiency with the highest efficiency values being 11.55% and energy for the panels at 10.91%. The PV panel used has dimensions of 770 mm x 670 mm, polycrystalline type.
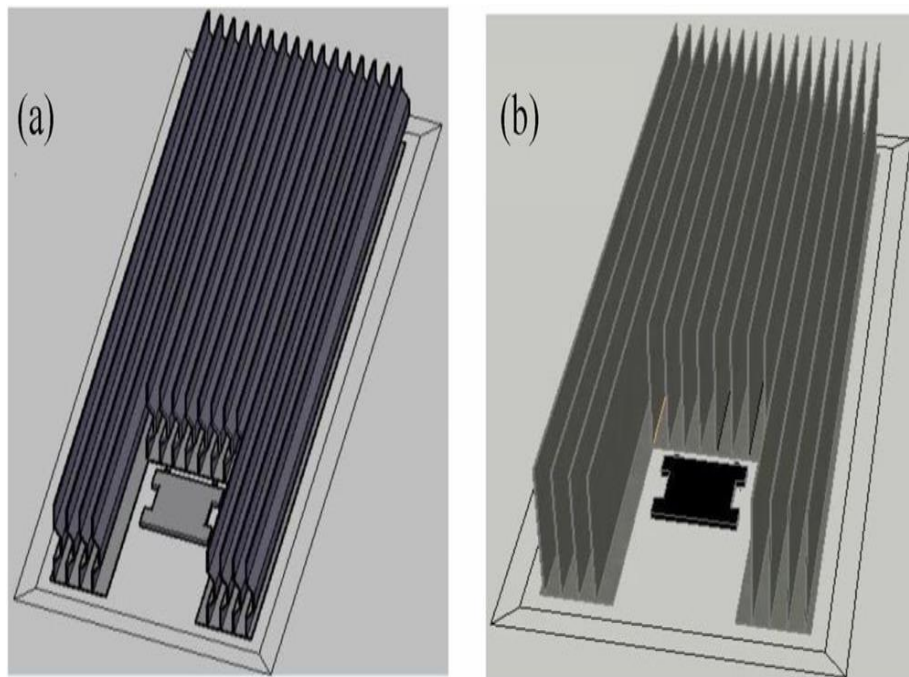

Figure 2.3. (a) Heatsink with winding fin (b) Longitudinal fin for heat sink [30].

Ayman Abdel-raheimAmra et al. [32] studied how a cell's high operating temperature affects the PV module's power output. They investigated heat transport in PV modules with and without fins. The findings revealed that when the fins' height, number, and airflow velocity rose, the unit temperature decreased and electrical performance rose. The recorded values are that the output power at 1.5 m/s is 182.7 with fins and 175W without fins, while at 3 m/s it was 185 and 178 W.

Ahmad El Maysa et al. [33] studied the optimal heat sink design used to cool photovoltaic (PV) panels. Figure (2.4) Heat from the solar cells is effectively dispersed via a heat sink and keeps the temperature of photovoltaic cells below the allowable temperature. The built system delivered an average electrical efficiency improvement of 1.77% and an average output power of 1.86 watts. The frontal temperature dropped by an average of 6.1 °C.
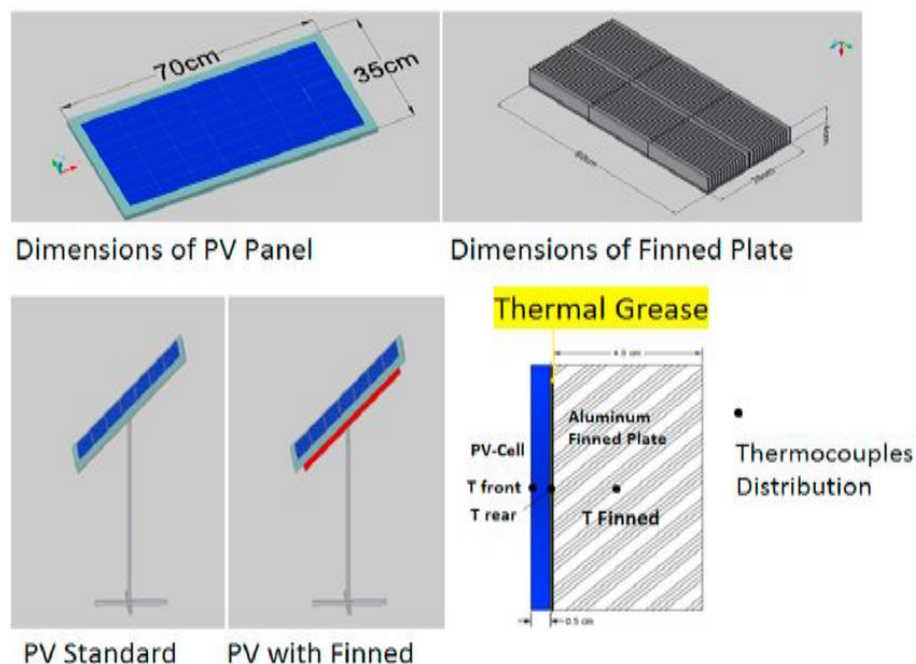

Figure 2.4. Schematic model showing one of the types of heat sinks with a photovoltaic panel [33].

Wei Pang et al. [34] created a hybrid PV/T system to assess the associated thermal behaviors and cooling effectiveness when TE units and heat sink units are joined. It was found that the most effective structure involves integrating the heat sink and the TE unit, which reduces heat by cooling the cell by 8°C and Improved cooling by 27% in addition to its function as an energy generator.

Xiaoling Yu et al. [35] studied a novel style of the heat sink with fins (P P F H S) Figure (2.5), which consists of placing a few vertical screws in between the plate fins. To compare the thermal performance of two different kinds of heat sinks, some experiments were carried out. According to experimental findings, the resistance thermal of Plate pin fin heat sink (P P F H S) is 30% less than the resistance of Plate fin heat sink (P F H S) that was utilized to create it with the same blowing speed, and the gain percentage is roughly 20 percent greater than the latter while having equivalent pumping power.

J.K. Tonui and Y. Tripanagnostopoulos [36] implemented two low-cost designes to enhance heat recovery in the PV / T system duct in order to increase heat output and (PV) cooling and maintain an acceptable level of electrical efficiency. They used thin and flat metal plates placed in the center of the back wall as well as duct fins used in a photovoltaic thermal system, which includes two systems, one is glass (GL) and one is non-glass (UNGL). When a standard system includes a simple duct, it is called a REF, and for modified systems which means modifying the ducts, thin metal plates are suspended (called TMS) in the center or by affixing rectangle-shaped fins (called FIN) to the ducts' corresponding back wall. The results of the experiments and theoretic analyses showed that the improvements enhanced PV/ T performance. Additionally, it was determined that the glazed kinds with rear wall fins (FIN) exhibit a sufficient enhancement in efficiency thermal over the standard system (REF). The outcomes further support the notion that the FIN system is the efficiency increased by about 11%.
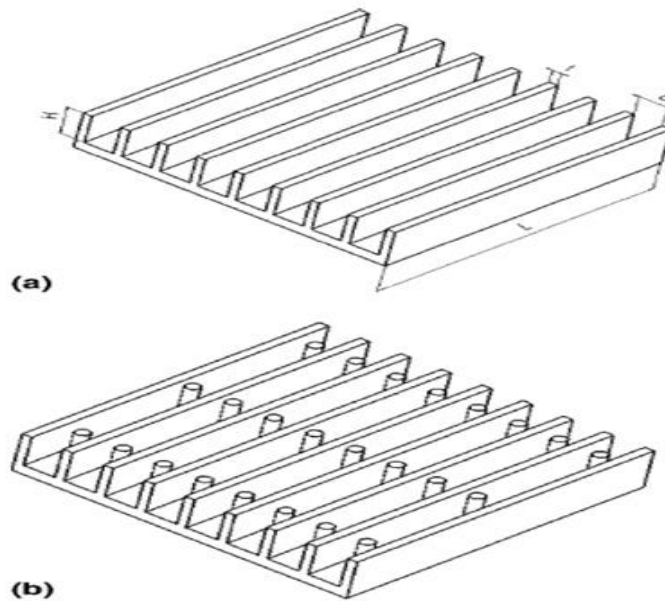
Figure 2.5. models PV/T air collection (Perpendicular flow) [36].

Y. Tripanagnostopoulos and P. Themelis [37] studied improving the electrical performance of photovoltaic installations in buildings by cooling photovoltaic panels with natural airflow. They used a prototype based on three silicon PV modules placed in series. The air passes through a 3 m long channel on the PV panels' reverse side and the area of the aperture is 1.2 square meters. The rectangular channel was designed with a depth of 0.15 m and they used insulating panels 0.05 m thick to construct the box. The possibility of increasing heat exchange from the photovoltaic panel to diffused air has been studied by adding a thin metal plate (T M S) in the air duct's center or metal fins (FIN) along the duct's length. There are two advantages to having the suspended TMS in the middle of the airway. The first is to improve heat extraction in the air duct, while the second is to protect the system's rear wall, which serves as overheating protection. They also made another low-cost modification, a fin in the rear wall of the system (FIN) intended to enhance the cooling of the PV modules as shown in Figure (2.6). They studied device operation with the airway tightly closed to avoid air circulation and airway opening

(REF) using thin plate metal (TMS) and finned metal (FIN). The outcomes demonstrated that the FIN systems can perform better than the TMS system, the efficiency was about 10.2% and 9.8%, respectively.
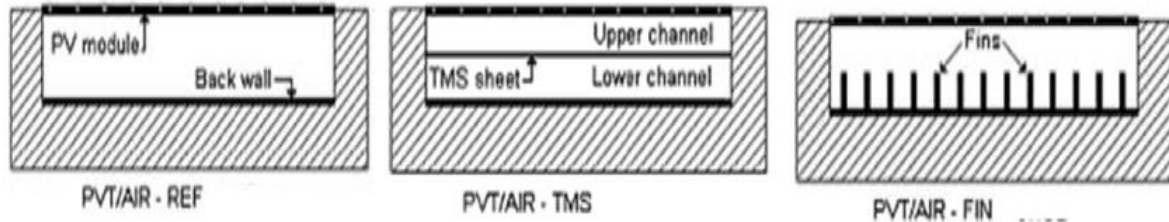

Figure 2.6. The three types of tests PVT/AIR [37].

Heat sinks with perforated fins or porous materials are used in numerous investigations, for example, **Karim Egab et al.** [38] studied the cooling efficiency of the numerous heat sink configurations. It was discovered that adding more fins and holes causes the board's temperature to drop. As a result, the temperature of the finned panel was 50% lower than that of the panel finless. Thus, the number of fins and the spacing between the holes were altered Figure (2.7). The computational model was created by using the Ansys program with an ambient temperature of between 25-35 °C.
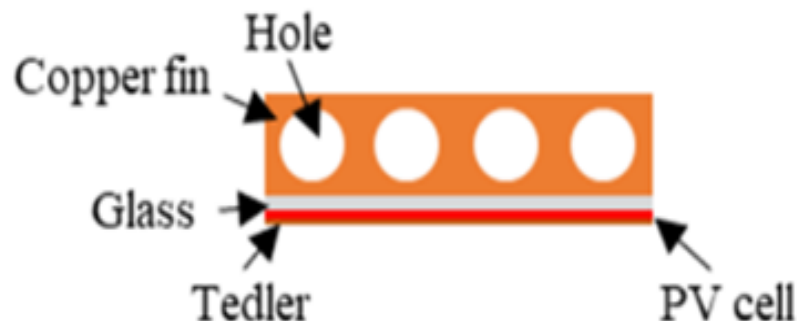
Figure 2.7. PV panel have holes and fins [38].

Zainal Arefin et al. [22] used numerical and empirical analysis to significantly reduce the solar panels' working temperature. They created a heat sink by the arrangement of a plate of aluminum with perforated fins affixed to the PV panel's back. The photovoltaic cell's temperature dropped from 85.3 to 72.8 °C. Its electrical performance improved with airflow of 1.5 m/s at 35 °C under a heat flux of 1000 W/m2. The improvement percentage of the maximum power point (P M P P) and PV voltages for the open circuit reached 10% and 18.67%, respectively, and the electrical efficiency reached 11.11% as a result of the decrease in temperature. **Cătălin George Popovicia et al.** [39] This study used air cooling with heat sink to reduce the solar panels' temperature Figure (2.8). In this instance, the photovoltaic panel's working temperature is approximately 56 °C, and the maximum power generated is 86% of the asset value. The photovoltaic panel's average temperature decreases when a heat sink is utilized. The maximum output was established above 90% of the nominal capacity, which is inferior to the value obtained in the base case by at least 10 °C. For the investigated arrangement, the highest increase in PV panel power generation above the base case varies from 6.97% to 7.55% for rib angles 90° and 45° respectively.

Sebastian Valeriu Hudis et al. [40]: This study concentrated on heat sinks with fin with holes that were distributed both vertically and horizontally. A comparison was made with the non-perforated fins. Simulations for CFD were performed in real wind conditions. The perforated fin heat sink achieved the best cooling performance of 88.74%, confirming an increase of 6.49% in power generation, While the basic case maximum power output percentage was 83.33%.
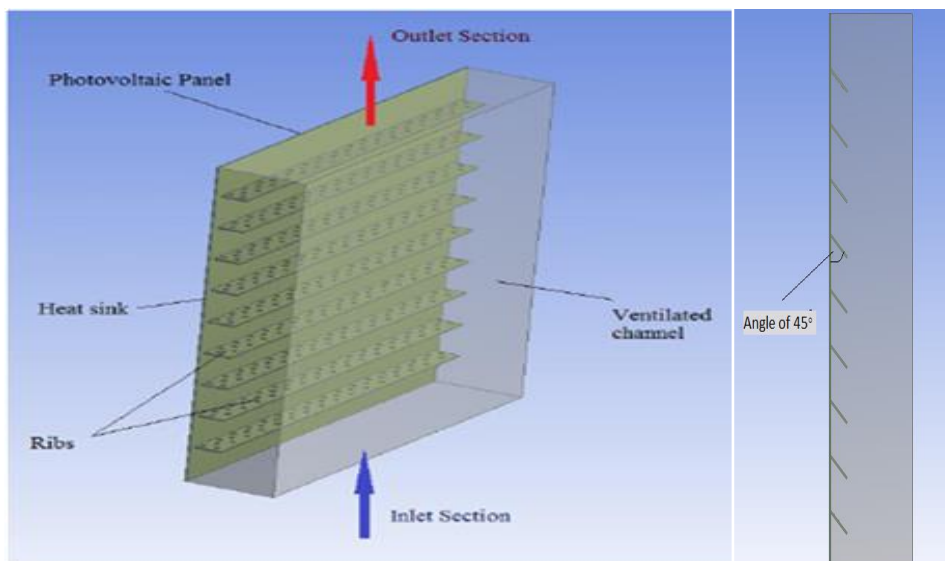
Figure 2.8. Model under study's geometry [39].

Yusron Abudllah et al. [41] studied heat transfer of the PV model numerically by made into four variations of base and fins, namely: AL-AL, Cu-Al, Al-Cu, and Cu-Cu Placed on the back surface of the PV panel. Using the ANSYS-Fluent software, the simulation's findings of the photovoltaic cell with 4 alternative shapes of the heat sink are compared to assess the solar panel's effectiveness. It was discovered that the greatest power that may be generated can reach 91.94% of nominal power when using an Al-Cu heat sink, which achieves the biggest temperature drop at an irradiance intensity of 1100 W/m^2 of 22.82 ° C in the case of Al.- Cu. Power can be produced at an intensity of irradiance without heat sink1100 Watts per meter square at the rate of 82.81% of the nominal power.

Additionally, it was discovered that increasing fin perforations have an effect on how airflow through the heat sink. There are studies that used just one perforated fin. such as **Filip Grubi si c- Caboa et al.** [42] proposed a method for cooling photovoltaic (Si-poly) panels Figure (2.9). They employed two different designs of aluminum fins attached to the rear side of the photovoltaic cell by using conductive epoxy adhesive (they used 50W). The measurements were taken in November for a specific area in

split, which is on Croatia's coast. Aluminum fins were in two different configurations. The first of which had parallel L-shaped fins without perforations while the second one had L-shaped perforations. The first type was not further examined because it was less effective than the second. the findings revealed that (the second configuration of the randomly perforated L – section) response is better performance, with an average efficiency improvement of 2%.
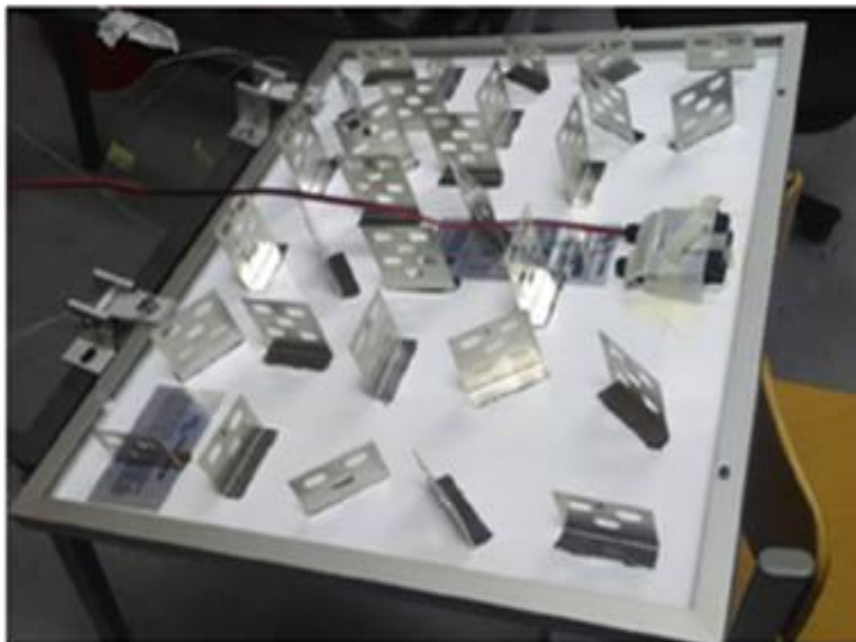

Figure 2.9. . Perforated L-shaped aluminum fins [42]**.**

To cool solar panels, many researchers have employed porous metals. **Maha Shata et al.** [43] found that it is possible to reduce the solar panels' temperature by utilizing a porous substance Figure (2.10) where they researched the impact of cooling solar panels by using a porous substance on their electrical performance. There are twenty-eight points where the solar panel's front surface temperature is measured, both with and without cooling. The results were a maximum temperature reduction of 9.8 %. Additionally, when it cools, the PV's electric current rises. The maximum measured voltage gain is 16.4 % at a given voltage, 19.6 V, and the

maximum power output gain is about 15%. **Jaemin Kim et al.** [44] suggested used grids made of iron and aluminum for cooling and examined cooling performance through internal experiments utilizing a solar simulator. The testing findings showed that the iron and aluminum grids significantly lowered the PV unit temperature by 6.56 and 4.35 degrees Celsius, respectively. Computational analyses utilizing CFD software were done to compare cooling fins and grilles. If the adhesion is increased, grids rather than cooling fins will likely be used in PV systems, where the average temperature of the units with iron and aluminum grids was 48.4 °C and 46.2 °C, respectively, whereas the mean photovoltaic module's temp without cooling was 52.7 °C. The aluminum grid led to a higher increase in solar efficiency 1.44% more than the iron grid, although the aluminum grid was less thick than the iron grid by 1 mm Opposite by 4.5 mm. As a result, the aluminum grids reduced the temperature of the photovoltaic panel by approximately 6.56 degrees Celsius, while the iron grids reduced the temperature by 4.35 degrees.

Figure 2.10. PV cell porous material (c) The porous material [43].

Rohan Kansara et al. [45] showed that the highest heat transfer occurred in porous media in contrast to fins and other geometric forms. They used a solar simulator to study how the flow rate of air mass and heat flow input affected rising temperature and the absorbed heat by the air. They also studied the distribution of fluid flow in the suggested arrangement. Moreover, the performance of the board was tested in relation to the number of fins, the porous material foam, and the porosity of the foam. The porous medium-containing composite produced results that were 16.17% better compared to the empty channel. **Fatih Selimefendigila et al.** [46] conducted an analytical and experimental study in Technology Faculty of Frat University, situated between latitudes 36° and 42°N in Elazig, Turkey to see the effectiveness of a solar PV unit that porous fins. As in Figure (2.11). They orient the PV module south and make its inclination angle 36°. they discovered that the photovoltaic module with porous fins had a greater output power of 6.7 watts at 11:00.
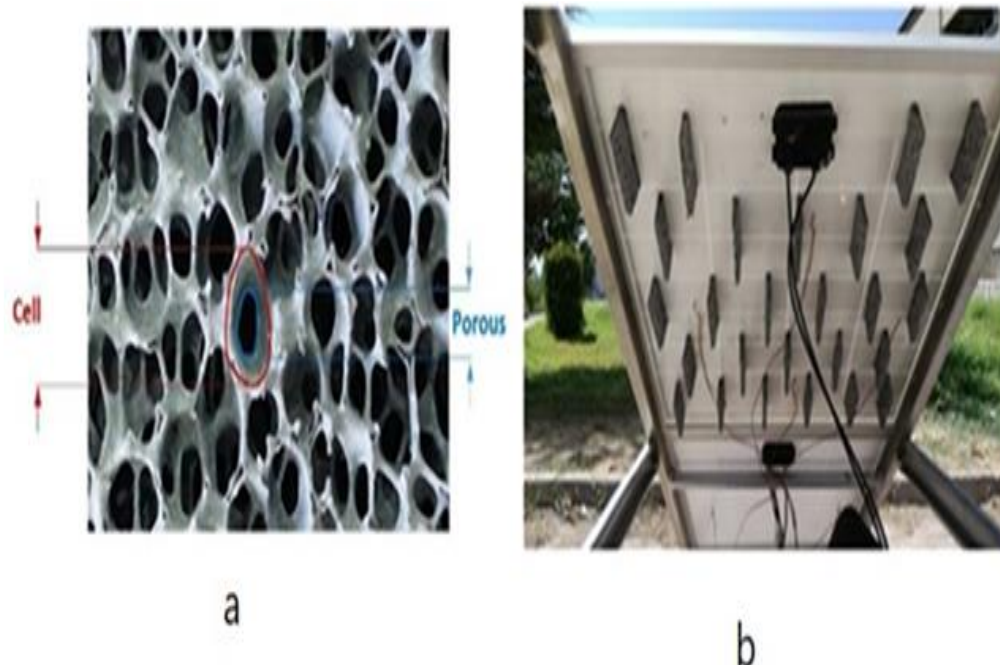
Figure 2.11. . a- demonstrates the usage of porous metals in the heat sink. b-Install the fins behind the photovoltaic panel [46]

Suhil M. Kiwana, and Ali M. Khlefat [47] proposed an efficient structuring approach that involves covering the back of the solar panel with a porous substance Figure (2-12). By conducting a numerical study using the ANSYS program, they examined the effect of convection coefficient λ, Darcy number Da, slope angle θ, pore the thickness of ratio Sp/S, and emissivity ϵ based on P.V unit conversion efficiency and the Nusselt number average in the Tedlar layer. 5 porous fins, 3 porous fins, and porous layer states were shown to have percentage increases in efficiency of 6.73%, 9.19%, and 8.34%, respectively, as compared to the net field.
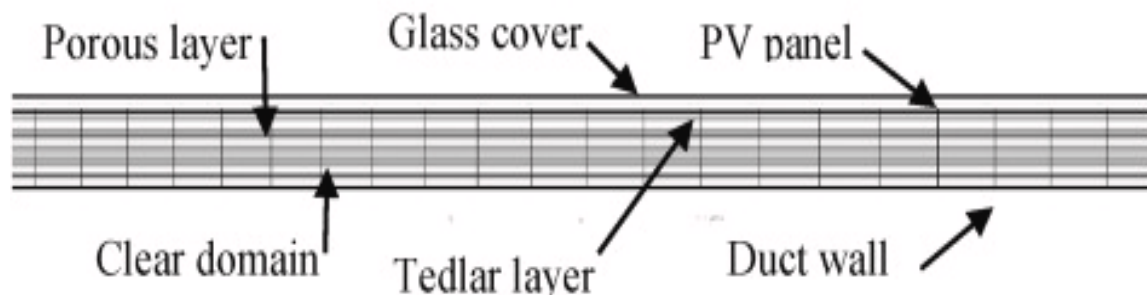
Figure 2.12. Diagram of the issue under discussion [47].

Duaa Jasim Hasan, and Ammar A. Farhan [48] developed A passive cooling technique was employed using open-cell copper metal foam fins to reduce the operating temperature of a photovoltaic panel, thereby enhancing its performance. Three polycrystalline photovoltaic panels were utilized in the study, which took place in Baghdad, through the 2nd, 3rd, and 4th months of 2019. Two of the panels had the proposed cooling mechanism installed, while the third was left unaltered for comparison. The average PV panel temperature was found to drop by roughly 8.4% with the addition of 10 longitudinal fins, where the average power output increased by 4.9%.

(a) Case I, four fins arrangement.

(b) Case II, six fins arrangement.

(c) Case III, eight fins arrangement.

(d) Case IV, ten fins arrangement.
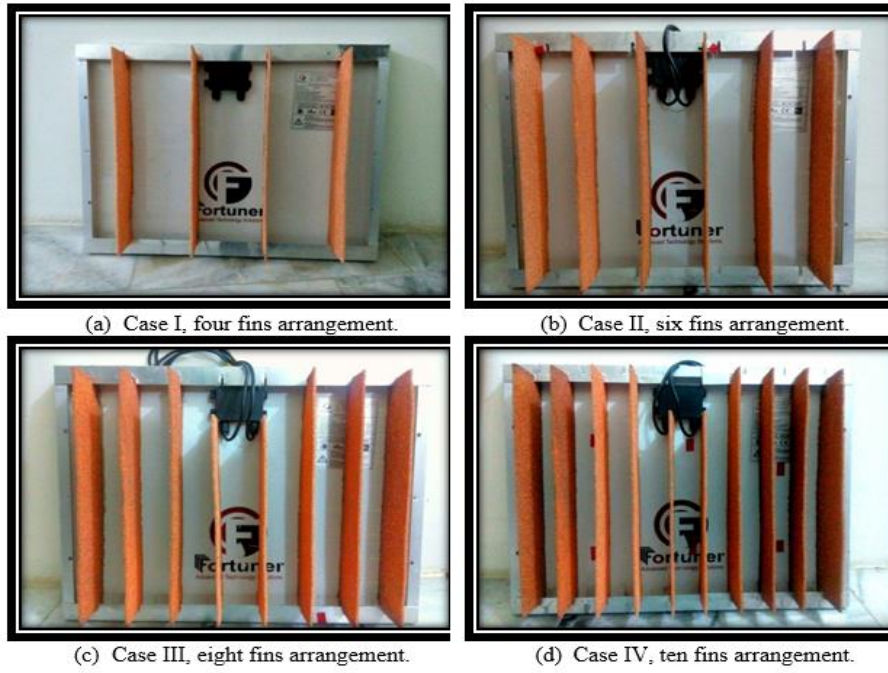
Figure 2.13. Arrangements for fins[48]

2.3. Summary of Prior Studies about Cooling Systems

In this part of the chapter, we note a summary of previous studies of air-cooling photovoltaic panels including the study's purpose, methodology, findings, and my personal viewpoint as shown in tables (2-1), (2-2), and (2-3).

Table 2-1. Summary of some previous studies.

Research Title	Authors	Aim of the study	Cooling approach	Finding	My opinion
An active cooling system for photovoltaic modules [16]	Teo et al.	By altering the airflow velocity inside the air duct, examined and compared the performance of PV panels with and without cooling. Additionally, a simulation model for monitoring the operational temperature of PV panels has been created.	They used an air duct uniformly on the lower side of the PV cell with effective cooling.	Working temperature decreased from 68°C to 38°C and performance increased by 12.5%.	Fins inside the air duct and attached to the back side of the photovoltaic panel might have increased the rate and amount of heat transfer, requiring less force to pump the air.

Numerical and experimental investigation of air cooling for photovoltaic panels using aluminum heat sinks [22]	Z. Arifin et al.	Know the effects of heat sink on the electrical properties of PV panels. While reducing the temperature and increasing the efficiency.	On back side of the P.V cell, an aluminum plate heat sink with perforated fins is mounted.	The temperature of photovoltaic panel's dropped from 85.3 to 72.8 degree Celsius. According to the results the maximum power grew by 18.67 %, while the open circuit photovoltaic (VOC) increased by 10 % and the electrical efficiency 11.11%.	The work was done at a constant air flow speed of 1.5 m / s. It was possible to work at different speeds to find out the appropriate speed to reduce the operating temperature faster
Performance of PV panel coupled with geothermal	N.A.S.Elmin shawy et al.	Improve the performance of the air-	In order to build a heat exchanger between the	The aid of precooled airflow at an ideal rate of	In this experimental

air-cooling system subjected to hot climatic [27]		cooled PV/T system which pre-cooled.	ground and air, the air is pre-cooled by burying tubes in the saturated wet ground before being applied to the back surface of the PV panels.	0.0288m3per second, the temperature of the P.V module was lowered from an average of 55°C to 42°C, improving its output power by 18.90% and electrical efficiency by roughly 22.98%.	work, the air was pumped from the bottom of the photovoltaic panel, so it needs a larger pump and more electrical energy than if the air was drawn from above.
Enhancing a solar panel cooling system using an air heat sink with different fin configurations [38]	K. Egab et al.	Know the effect of the size of the fins, the number of holes and the distance between them.	The fins number and spacing between orifices were changed to create a variety of heat sink configurations.	The finned panel's temperature dropped by 50% as a result, and the electrical efficiency 12%.	The diameter of the holes is not mentioned and was not studied in this experimental work. When using smaller diameter holes, more resistance is generated to the passage of air, thus increasing the heat transfer

					process and greater cooling of the solar cells.
Efficiency Improvement of Photovoltaic Panels by Using Air Cooled Heat Sinks [39]	C. G. Popovici et al.	The simulation may be used to discover a cost-effective solution and save energy, to know the right angle for the heat sink ribs.	The heat sink was created with a ribbed wall, perforated fins, and a high thermal conductivity material.	The output power was set at a maximum over 90% of the nominal power and the temperature was decreased by 10 °C. When the rib angles range from 90° to 45°, the highest increase in Power generated by the P.V cell is between 6.97% and 7.55% and the electrical efficiency 14.72% and 14.8% when comparison to the basic case.	The work can be done by changing the height of the ribs and the number of holes in addition to changing the angles of the ribs. This is because increasing the height of the ribs and the number of holes leads to faster cooling of the solar panels

Analysis of the Copper and Aluminum Heat Sinks Addition to the Performance of Photovoltaic Panels with CFD Modelling [41]	Y. Abudllah et al.	transfer by using copper and aluminum alloys in the heat sink.	the P.V cell, they used four different configurations: Al-Al, Cu-Al, copper, and Cu-Cu	demonstrated that for Al-Cu, the greatest energy that could be created was at irradiance intensity of 1100 Watt per meter square at a temperature of 22.82 °C, or 91.94% of the nominal energy. The electrical efficiency about 15.1%	because of the limited heat transfer by conduction. it is required to increase the air speed by experimenting with various speeds, to better cool the PV panels.
Enhancing the efficiency of photovoltaic panel using open-cell copper metal foam fins [48]	D. J. Hasan and A. A. Farhan	studying the effect of adding metal foam fins to the back surface of PV modules.	For a (PV) panel, Coper foam metal fins open cell are used.	The addition of ten longitudinal fins increases the output power by mean of 4.9% and reduces the average PV panel temperature by 8.4%. The electrical	To achieve the best results of the cooling process, the effective air method is used within the air duct, in addition

				efficiency has reached limits 21.5%	to the use of fins with porous materials.
Analytical expression for electrical efficiency of PV/T hybrid air collector [57]	Swapnil Dubey et al.	An analytical study to develop or increase the efficiency of photovoltaic panels	They used a numerical study to analyze the performance of photovoltaic panels with and without cooling	An electrical efficiency of 11.5% was achieved.	It is possible to perform the simulation by adding a heat sink inside the air duct to improve heat transfer and ensure better cooling

2.4. Comparison of previous studies
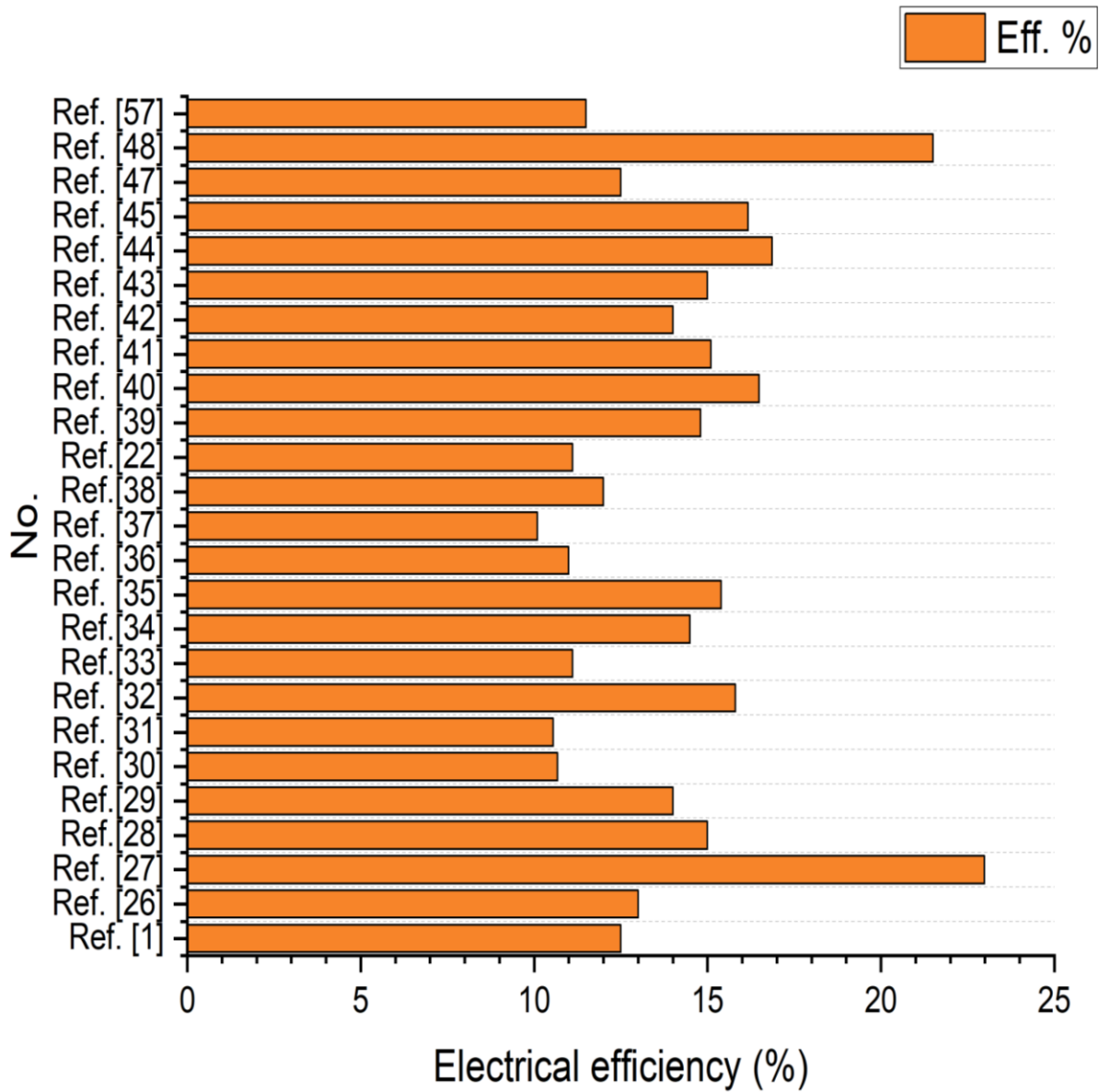
Figure 2.14. Compare the results of previous studies.

2.5. The important conclusions of previous studies

1. Photovoltaic panel air-cooling techniques are easy to install, and economical therefore are commonly used.

2. The use of forced air in PV panel cooling techniques gives higher cooling efficiency.

3. Using heat sinks attached to the base of the photovoltaic panels provides an increase in the heat transfer process between the PV panel and the air, thus, providing better cooling for the solar panel.

4. Porous metal media provides greater resistance to the passage of air through it, thus, the amount of heat transferred is greater.

5. Thermal photovoltaic systems PV/T combines solar systems that convert solar energy into electrical energy with a solar thermal system.

6. PV/T systems are more efficient than using solar PV and solar thermal systems alone.

In addition, the use of porous metal media installed inside the air duct in a winding manner connected to the back surface of the photoelectric plate with forced air by using the air pull fan of appropriate power in PV/T systems helps in the heat transfer process and achieves an improvement in thermal and electrical efficiencies. This was not found in previous studies.

Chapter three: Mathematical model

3.1. Introduction

Solar energy is an alternative energy source. Thermal or photovoltaic collectors can convert it into electrical energy [50]. There are many obstacles to increasing the efficiency of solar cells, such as increasing their temperature.[51]. Effective cooling methods increase performance, providing desired output outcomes [48]. Active cooling solutions might be helpful in hot climates where PV modules require efficient cooling performance [52].

This chapter describes the mathematical underpinnings of the actions taken to increase the power and efficiency of PV panels by reducing its temperature, and, how to estimate the size of the impact of this procedure. The electrical properties of the solar cell are also calculated and examined by using the numerical analysis of the PV/T system in the COMSOL Multiphysics 5.6. program.

3.2. The photovoltaic thermal PV/T components

The suggested photovoltaic thermal collector was tested numerically. The meant part of the collector is the PV module and the solar thermal collector. The PV panel consists of cells-type Perc monocrystalline TT375-72PM 375WP. The simulation work investigates the impact of a solar panel's working temperature on a sunny day on efficiency, the PV panel is placed regarded to the vertical solar radiation. The photovoltaic panel is connected to the air duct which consists of an air channel, porous media, and an air fan, as presented in Figure (3.1).

Figure 3.1. Characteristics of photovoltaic panel.

The PV/T collector was simulated on real wither conditions of Najaf city-Iraq (latitude 32°02', longitude 44°20'). In order to test the efficiency of the PV model, a two-dimensional PV with an air duct is investigated by using COMSOL Multiphysics 5.6. The module suggested for improving photovoltaic panel cooling by mounting a duct to the panel's rear with a heat sink made of porous metal. The PV panel utilized in this investigation has the following measurements: (length1903 mm), and (width of 951 mm). The photovoltaic panel's dimensions are taken into consideration when designing the duct, which has a 115 mm depth made of aluminum and is 0.7 mm thick.

The simulation model is 2-dimensional and completed for real weather conditions. The study type was a time-dependent study. The current two-dimensional

COMSOL model of a monocrystalline PV/T has been applied for the simulations. The numerical simulation is implemented on a laptop computer with a processor: Intel (R) Core (TM) i7-7820 HQ, CPU: 2.90GHz   2.90 GHz and Installed RAM: 16.0 GB.

The PV cell consists of different layers: back glass, thermoplastic material EVA (Ethyl Vinyl Acetate), Glass fiber, solar cells, EVA, and plastic back sheet layer TPT (Tedlar/ PET/ Tedlar). A photovoltaic thermal (PV/T) is an uncomplicated photovoltaic solar collector, as it is employed to convert solar radiation to electricity. The two dimensions geometry of photovoltaic thermal (PV/T) is illustrated in Figure (3.2).
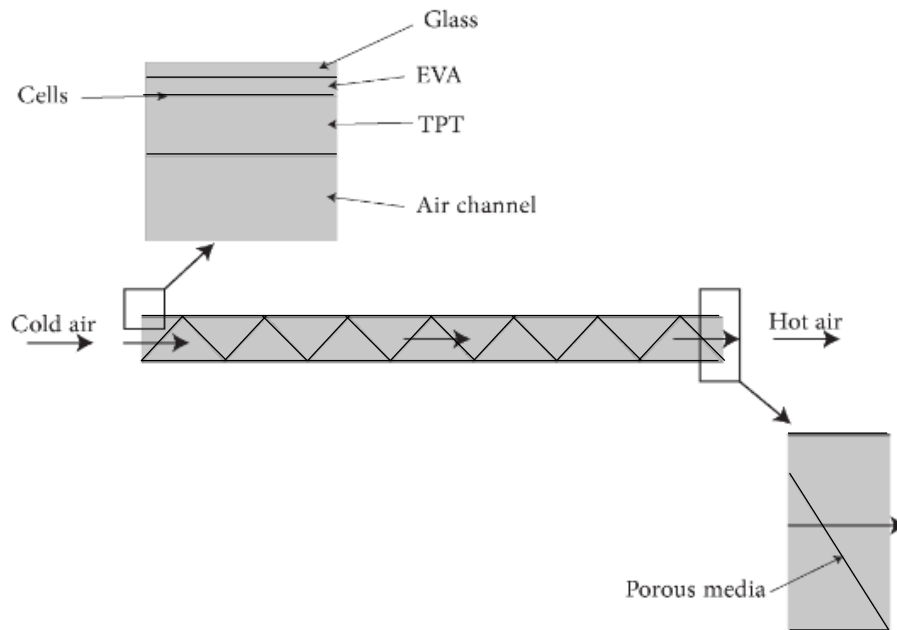
Figure 3.2. 2-D COMSOL model displays the main structure of PV/T.

3.3. Mathematical models

The real weather environment required for the COMSOL model of the PV/T has been used as input data. The meteorological data such as solar irradiance, outdoor

air temperature (ambient), and wind speed have been measured in 2020 in Najaf-Iraq and used as input data. The boundary heat source for the collector is at the surface cell equivalent to the heat rate from solar irradiance. Upon calculation of the Reynolds number, it has been determined that the flow is turbulent. The thermal parameters of the PV/T geometrical have been abbreviated in Table (3.1). The Reynolds number is given by [54];

$$Re = \frac{\rho V D_h}{\mu}$$ (3-1)

Wher Re is the Reynolds number, ρ air density, V air speed, D_h hydraulic diameter, and μ is the air viscosity.

$$D_h = \frac{2ab}{a+b}$$ (3-2)
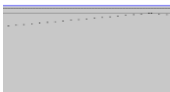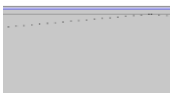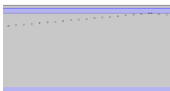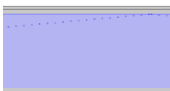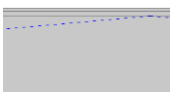
Wher a and b are the width and height of the air duct.

Different assumptions are made to implement this simulation as regards the PV panel and the solar air collector structures, the flow of working fluid, and other parameters that influence the PV/T thermal analysis.

1. The PV panel has homogeneous material properties in its layers.

2. The photovoltaic thermal panel works in unsteady-state conditions.

3. The solar radiations have been transported evenly to the layers surface of the PV panel.

4. Two-dimensional turbulent fluid flow and heat transfer are good approaches for this simulation.

5. The sky has been assumed as a blackbody. Because a black body is a body that absorbs all the radiation it receives, that is, it does not reflect any light, and does not allow any light to pass through it and exit from the other side.

6. The photovoltaic cover has a uniform temperature distribution over the PV cover.

Table 3.1. Geometrical and thermal properties used in simulation [COMSOL Multiphysics 5.6].

Part	Parameter	Value
Glass	Thermal conductivity	130 [W/(m.K)]
	Density	700 [kg/m^3]
	Heat capacity	2330 [J/(kg.K)]
Silicon Thermal	Thermal conductivity	1.9 [W/(m.K)]
	Density	2600 [kg/m^3]
	Heat capacity	700 [J/(kg.K)]
Aluminum	Thermal conductivity	k_solid _1(T)
	Density	C_solid_1(T)
	Heat capacity	rho_solid_1(T)
Air	Thermal conductivity	K(T) [W/(m.K)]
	Dynamic viscosity	eta(T) [Pa.s]
	Heat capacity	Cp(T) [J/(kg.K)]
Cast iron	Thermal conductivity	50 [W/(m.K)]
	Density	7000 [kg/m^3]
	Heat capacity	420 [J/(kg.K)]

3.4. Number of ribs of the porous metal media

The simulation was done using COMSOL Multiphysics software, where the air channel was analyzed to obtain the best heat exchange between the base of the photovoltaic panel and the air, by changing the number of porous metal ribs inside the air duct, where the simulation process is done depending on the number of

different ribs 10, 12 and 14, ribs as shown in Figure (3.3). The results show that the best design is using 14 ribs installed at an angle of 45°.
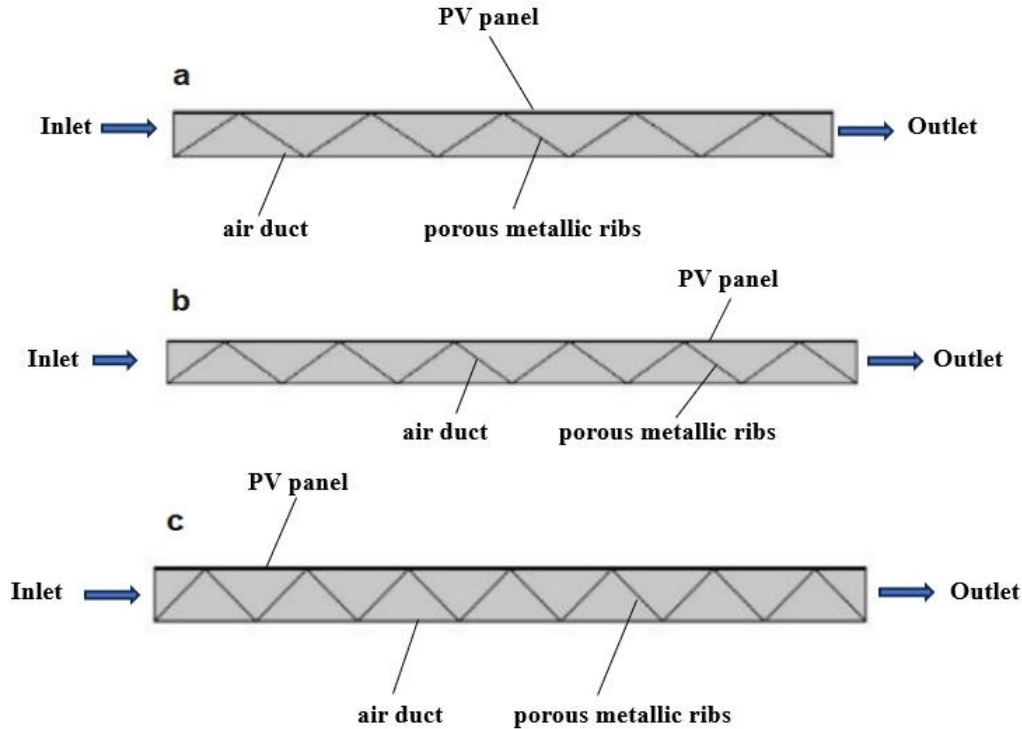
Figure 3.3. No. ribs of porous metallic a)10 ribs b)12 ribs c) 14 ribs.

3.5. The PV/T methodology

The weather variables are the main parameters that have affected the PV cell temperature (T_{PV}), the, like the solar irradiance (G), wind speed (V_w), and the temperature of ambient (T_{amb}). The maximum power PV model is given by [53];

$$P_m = I_m V_m = (FF)I_{sc}V_{oc} \tag{3-3}$$

Where; I_m and V_m refer to the maximum current and the maximum voltage, respectively. While FF is Fill factor, I_{sc} and V_{oc} are the open circuit voltage and short circuit current.

In a literature review, turns out the temperature has affected the output power of the PV. It showed the short circuit current was increased slightly with an increase in the temperature while the open circuit voltage decreases strongly with the temperature [54]. The influence of PV temperature on its PV efficiency can be computed by applying the equation [55].

$$\eta_{cel} = \eta_{T_{ref}}\left[1 - \beta_{ref}\left(T_{cel} - T_{ref}\right)\right] \tag{3-4}$$

where T_{ref} and T_{cel} are the PV model reference and cell temperatures, respectively. β_{ref} is the temperature coefficient (0.004K^{-1}), and $\eta_{T_{ref}}$ is the electrical efficiency of the PV at T_{ref}. The value of $\eta_{T_{ref}}$ and T_{ref} for the current PV panel are presented by its manufacturer, 0.15 and 25°C respectively.

The amount of the gained heat can be calculated through the following equation depending on the difference in incoming and outgoing temperatures and the mass flow rate of air [58].

$$Q_u = m^{\cdot}Cp(\Delta T) \tag{3-5}$$

The thermal and overall efficiency of the PV/T module is calculated by using the formulas[36].

$$\eta_{th} = \frac{m^{\cdot}Cp(\Delta T)}{GA} \tag{3-6}$$

$$\eta_O = \eta_{cel} + \eta_{th} \tag{3-7}$$

3.6. Initial and boundary conditions

The present COMSOL simulation shows the main governing equations of the PV/T simulation by predicting the temperature variation of the PV layers and velocity of the air flow. In the simulation model haven applied a set of governor equations, which are simulated together for all layers of the model. Applying the simulation model for the PV/T system, the natural convection in the working fluid has been

considered. The governing equations used in the simulation are momentum, energy, and continuity equations as presented below.

In x- momentum

$$\rho \left(\frac{\partial u}{\partial t} + u \frac{\partial u}{\partial x} + v \frac{\partial u}{\partial y} \right) = -\frac{\partial P}{\partial x} + \mu \left(\frac{\partial^2 u}{\partial x^2} + \frac{\partial^2 u}{\partial y^2} \right) \tag{3-8}$$

In y- momentum

$$\rho \left(\frac{\partial v}{\partial t} + u \frac{\partial v}{\partial x} + v \frac{\partial v}{\partial y} \right) = -\frac{\partial P}{\partial x} + \mu \left(\frac{\partial^2 v}{\partial x^2} + \frac{\partial^2 v}{\partial y^2} \right) \tag{3-9}$$

Mass conservation

$$\frac{\partial \rho}{\partial t} + \rho \left(\frac{\partial u}{\partial x} + \frac{\partial v}{\partial y} \right) = 0 \tag{3-10}$$

Energy equation

$$\frac{\partial T}{\partial t} + u \frac{\partial T}{\partial x} + v \frac{\partial T}{\partial y} = \alpha \left(\frac{\partial^2 T}{\partial x^2} + \frac{\partial^2 T}{\partial y^2} \right) \tag{3-11}$$

As an extension for the above equations, the electrical efficiency (η_{cel}) of the PV/T system has been calculated by [56].

$$\eta = \frac{(FF)(V_{oc})(I_{sc})}{(A_m)(G(t)} \tag{3-12}$$

where FF is the fill factor and is equal to 0.8, V_{oc} and I_{sc} are the open circuit voltage (V) and short circuit current (A) respectively.

3.7. Product of PV/T module and mesh geometry

The COMSOL simulation model is done by dividing the solar panel collector into the different isothermal areas: the front region is the PV glass cover, the photovoltaic cells, the EVA, and the back PV cover, and the screen heat absorber and the last region is the air duct. The main parts of PV/T geometry, functions, properties of the working fluid, PV panels layers, and screen were presented in COMSOL Multiphysics. The grid (mesh) of the geometry is generated by COMSOL also After

the PV/T collector has been modeled by COMSOL. The next step is to generate the model mesh. To solve the computational model implemented in this work, a small mesh size has been built. Because of the small dimensions of PV layers and the parts of the huge intersection. Different mesh types have been studied. There are three sizes predefined as normal, coarse, and fine. The PV/T is discrete into many parts, while finer mesh types for the layer of PV as shown in Figure(3.4). Where the number of domain elements was 109105 and boundary elements 20299. The main initial and boundary conditions for the simulation have been presented for the solid, fluid, inflow, outflow, PV/T walls, and heat surface transfer to ambient (sky) by radiation.
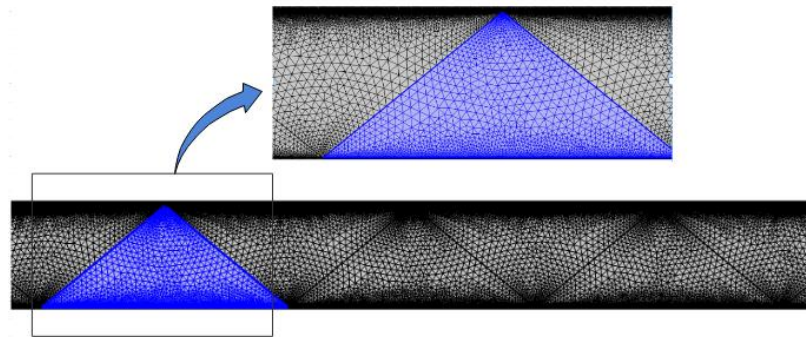
Figure 3.4. 2-D Front view of meshed PV/T system with porous.

3.8. Validation with literature

To confirm the COMSOL simulation model, it has been validated with previous studies. The predicted electrical efficiency for the present simulations is compared with those from Swapnil et al [56] in Figure (3.5). The expression of RMSE (root mean square error) has been applied to calculate the variance in the overall efficiency of the present study and previous study, by the following formal [57].

$$\text{RMSE} = \sqrt{\frac{\sum_{j=1}^{M}(\bar{\eta}_j - \eta_j)^2}{M}} \qquad (3\text{-}13)$$

Where M the total quantity of values for the efficiency. The root mean square error is 1.09.

It shows that a good validation of the model has been achieved. The accuracy has been achieved by using the same input in the verification process, the thermo-physical properties, boundary conditions, and initial conditions that have been utilized in the validation section are the same as in the ref [56].
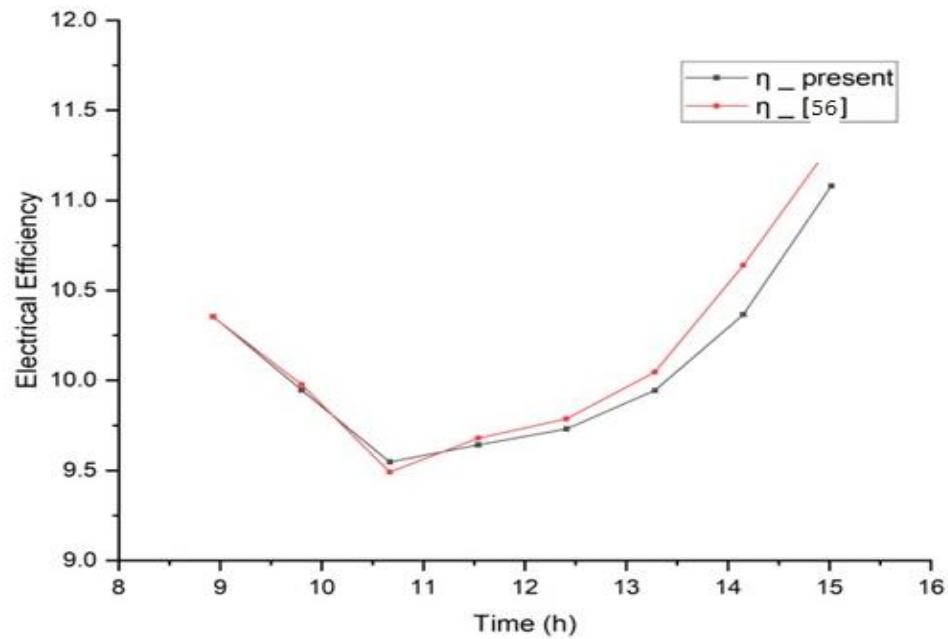
Figure 3.5. Validation of hourly change within a dayin the electrical efficiency of the PV/T Ref. [56].

Chapter Four: Experimental Work

4.1. Introduction

This section gives an overview of the experimental work conducted for this study. Additionally, all components of the system have been installed in AL-Rumaitha Technical Institute/AL-Furat AL-Awsat Technical University, Iraq. The geographical coordinates of Rumaitha city - Iraq is 31°42′ - 45°12′. Figure (4.1) shows the location of the experimental work.

Figure 4.1. The site of the experimental work.

4.2. Materials and procedures

The thermal photovoltaic PV/T system consists of several components. The photovoltaic unit is the system's first component, which is installed on the air duct. A porous metal is fixed inside the duct and works as a heat sink and is attached to the back side of photovoltaic panel.

The air intake fan used is an alternating (AC) current with variable speed to draw air from the outside and pass it through the porous metal media. So that the system was installed on a metal structure, and it was fixed according to the appropriate angle to benefit from the maximum solar radiation. The readings are taken by using a set of special devices and equipment. Figure (4.2) shows a detailed diagram of the system.

1. PV/T module
2. PV module
3. Air duct with DC fan
4. Inverter
5. Electrical box
6. Electrical Source (AC)
7. Battery
8. Electrical load
9. Arduino with sensors
10. Thermocouples
11. Wind speed sensor
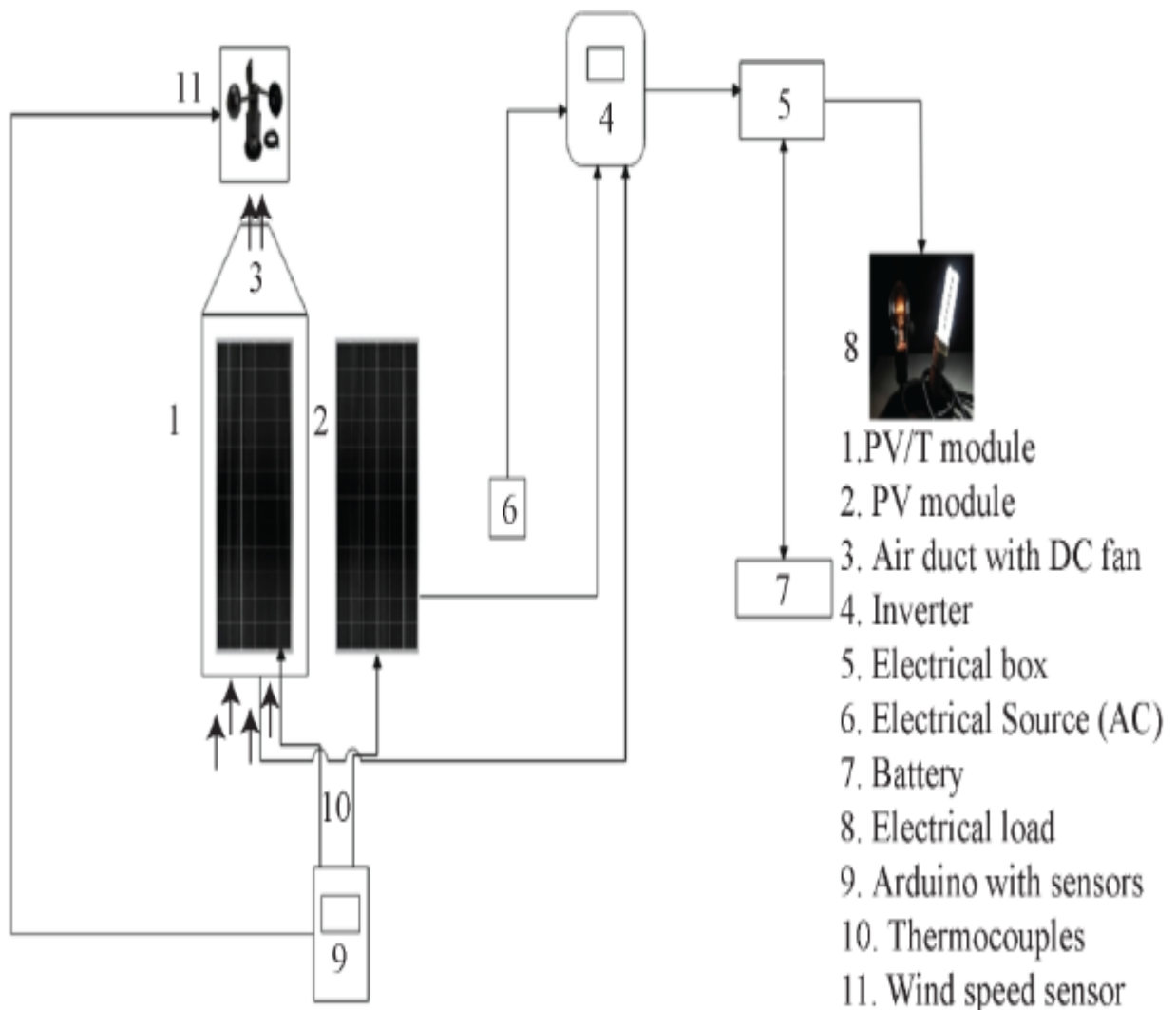
Figure 4.2. Schematic of the PV model integrated with and without air duct

4.2.1. Monocrystalline photovoltaic panel

The monocrystalline photovoltaic panels (TT375 72PM) in which the cells are of the type (PERC) are the panels that were used in the (PV/T) system. Which is made up of three layers: Glass, EVA, and Tedler, the thickness of the glass layer are 3.2 mm, and the frame material is aluminum alloy. The photovoltaic panel is the most important element in the system whose characteristics are shown in Table (4.1).

Two solar panels were used in the system that was installed in the city of Rumaitha , Iraq (31°42′ - 45°12). One of the panels is used in the module to compare its performance with the other solar panel under the same conditions. The solar panel used is displayed in Figure (4.3).

Table 4.1. Characteristics of PV panel [Tomma Tech datasheet].

Details	Characteristics
Type of Solar cell	Mono-crystalline silicon
Maximum Power (Pmax)	375 W
The voltage at maximum power (Vmpp)	40.14 V
Current at maximum power (Impp)	9.35 A
Open circuit voltage (Voc)	48.67 V
short circuit current (ISC)	9.94 A
Panel efficiency	19.75 %
Standard test conditions	Air mass 1.5, radiation 1000 W/m2, at 25 °C
Number of cells	72

Panel Dimensions (H/W/D)	1984x1007x40 mm
Weight	22.5 kg
Range of operating temperatures	-40-85 °C
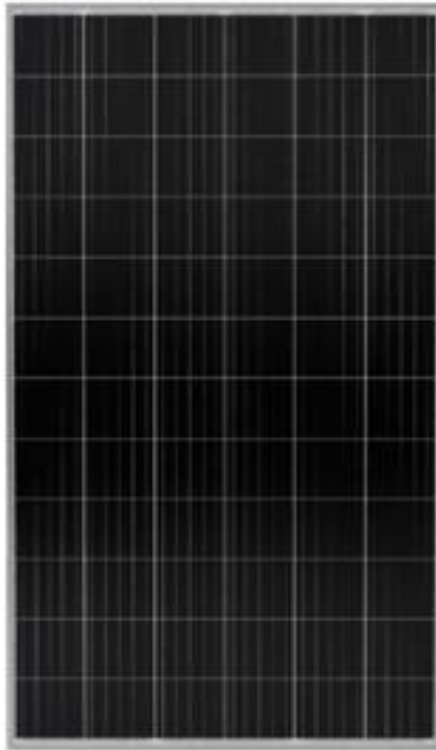
Figure 4.3. Monocrystalline photovoltaic panels.

4.2.2. Air duct of PV/T

The air duct is one of the main components of the thermal photovoltaic (PV/T). The back surface of the monocrystalline photovoltaic panel used in the system is attached directly to the air duct. The dimension of the air duct is chosen according to the dimensions of the solar panel that was employed. The length of the air duct is (1984 mm), Width is (1007 mm), height is (115), and thickness is (0.7). The air duct is constructed from heavy aluminum, and an insulating material was

used to cover the exterior surfaces to shield them from the effects of the environment. The inner surface of the solar panel is covered with a black thermochromic coating to absorb heat to prevent reflection onto the back cell surface.

Additionally, silicon is used to filling the gaps and prevent the air from leakage to the outside. The duct includes a porous metal (iron metal mesh) as shown in Figure (4.4).
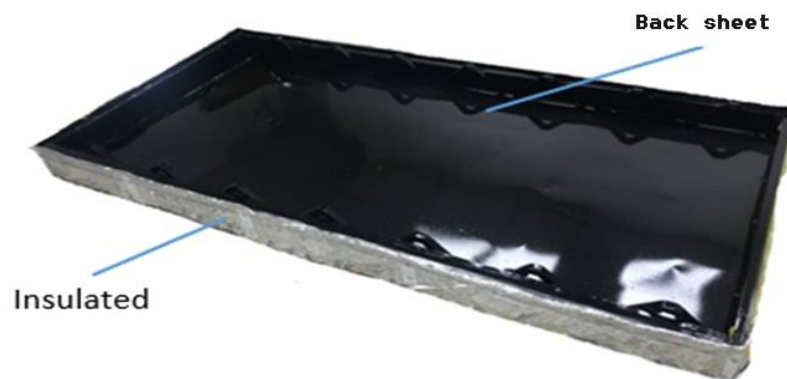
Figure 4.4. Air duct of the (PV/T) module.

4.2.3. Porous metal

Porous metal is a type of metal that combines the properties of metal with porousness by having tiny pores throughout. Depending on the substance and the pore shape, it is used for various purposes. In this experimental work, it is used as a heat sink that is installed inside the air duct with a length of 7m in the form of a zigzag at an angle of $4°$ to touch the back surface of the photovoltaic panel. The hole in the porous material has squared dimensions of (1x1 mm). Figure (4.5) shows the porous metal inside the air duct.
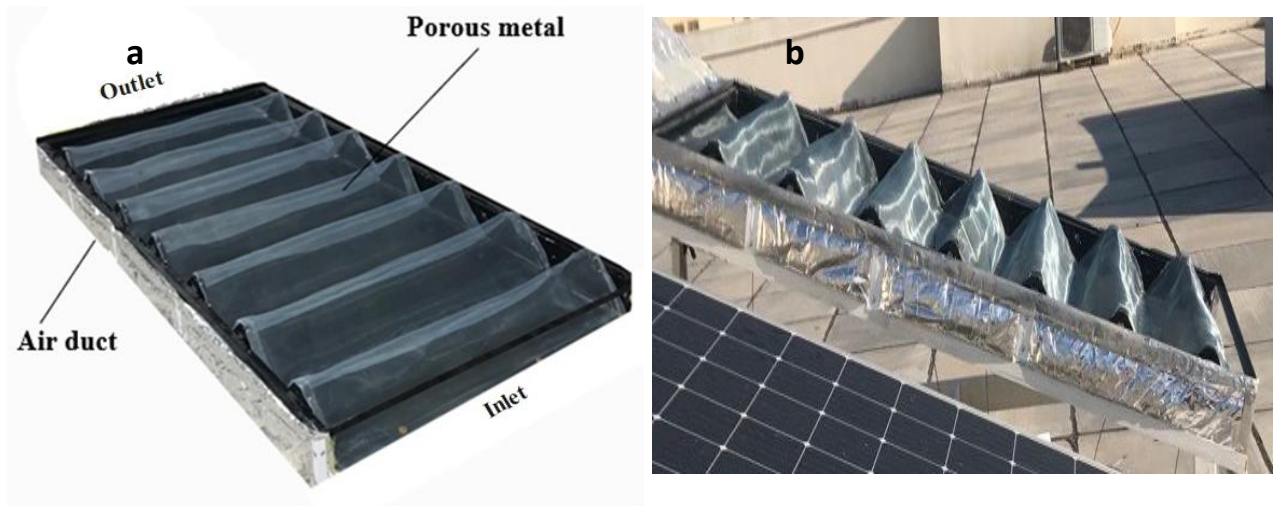
Figure 4.5. a) Porous metal inside the air duct b) side view of the air duct.

4.2.4. D-150 AG Air fan

The air fan is an essential component of the module. It is an AC 220-Volt fan with a varying speed and 75W power, and its speed is controlled by a speed regulator. Its purpose is to pull outside air into the air duct so that it can pass through the porous metal heat sink that is in contact with the back of the solar panel. The air fan has been installed on the air duct at the top of the system as shown in Figure (4.6).

Figure 4.6. D-150 AG air fan.

4.2.5. Structure of the system

The metal frame is one component of the system which is used to install the air duct and photovoltaic panel on it. It is made of thick iron that has been coated to prevent rust and corrosion as well as to resist environmental factors.   The metal frame has two parts: one is fixed and attached to the ground and the other is movable and carries the photovoltaic panel and is installed at an appropriate angle according to the geographical location of the city of Rumaitha (31°42′ - 45°12′). Two metal structures are used, the first is to install the T / PV system and the other is to install the PV reference unit as shown in Figure (4.7).
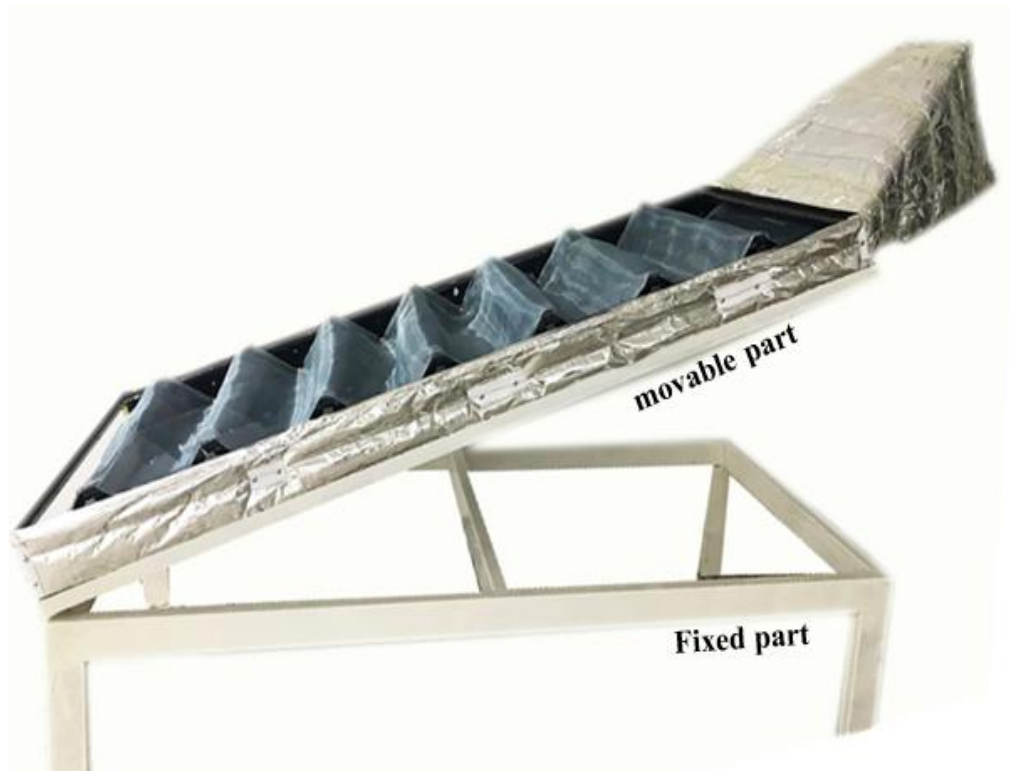
Figure 4.7. Structure of the system.

4.2.6. TOMMA TECH Inverter/Charger

The Inverter 1KVA-5KVA (PF=1) TOMMATECH German–based company. This Inverter/Charger combines the MPPT solar charger, battery charger, and inverter operations to provide an uninterruptible power supply in a small, portable package.Equipped with a wide LCD screen through which the user can view the commands he executes through the existing buttons, as well as see warnings, battery charging, and allowable input voltage based on various uses. The battery is also charged from the grid and gives priority to solar energy as shown in Figure (4.8). The characteristics of this Inverter are shown in Table (4-2).

Table 4-2. Characteristics of Inverter/Charger [User Manual].

Detail	Characteristics
Estimated power	1000VA/800W
Input voltage	230VAC
Frequency range	50Hz/60Hz (auto-sensing)
Regulation of AC Voltage (Battery Mode)	230VAC ± 5%
Standard efficiency	90%
Surge power	2000VA
Form the wave	Sine waves
Battery voltage	24VDC
Voltage for Floating Charge	27VDC
Protection from Overcharge	31VDC
Max. power of PV panel	600W
Consumption of Standby Power	2W
Dimension (mm) t x w x H	128 x 272 x 355
Weight (kg)	7.4
Humidity	5% - 95%

Work temp.	0°C – 55 °C
Temperature storage	-15°C – 60 °C

Figure 4.8. Inverter/Charger.

4.2.7. Store of DC Current (Batteries)

It is one of the Lead-acid batteries. The battery voltage is 12 volts, the number of cells inside the battery is 6 cells, the deep Cycle Gel, and the nominal capacity of the battery is 100 Ah Manufactured by NewMax. Two batteries are used to match with theuse of inverter Figure (4.9) and Table (4-3) shows its properties at 25 °C.

Figure 4.9. Store DC Current (NewMax Batteries)

Table 4-3. properties of Store DC Current at 25 °C [NewMax Manual].

Application	Charging voltage	Initial Current
Bilk	——	0.25c MAX.
Absorption	2.40 volts per cell	Final current / 0.005c max
Floating	2.28 volts per cell	——

4.3.   Measuring Equipment

To evaluate the performance of the PV/T module, the measurement equipment collects preliminary data that provides an impression of the system. Several measuring devices and appropriate sensors are used to record the readings according to the nature and working conditions to determine the results.

4.3.1. Solar Power Meter

During experimental work, this instrument is used to measure the sun's radiation intensity. The type of device used is SM206-Solar Manufactured by CEM. The Solar Power Meter can measure up to 1999 W/m^2 of radiation, has Rapid

responsiveness, high accuracy during the measurement, direct reading without any adjusting, and is easy to use. Table (4-4) displays the specifications of device. Figure (4.10) shows the Solar power meter device.

Table 4-4. Specifications of DT-1307 Solar Power Meter [User Manual].

Detail	Specification
Range	0.1-1999W/m^2
Accuracy	usually ±10W/m^2
Resolution	0.1W/m^2
Sampling time	About 2.5 t/s

1- Photosensitive window
2- LCD display
3-ON/OFF button
4- Units W/m2 and Btu/(ft^2-h) selection key
5- Value retention Key
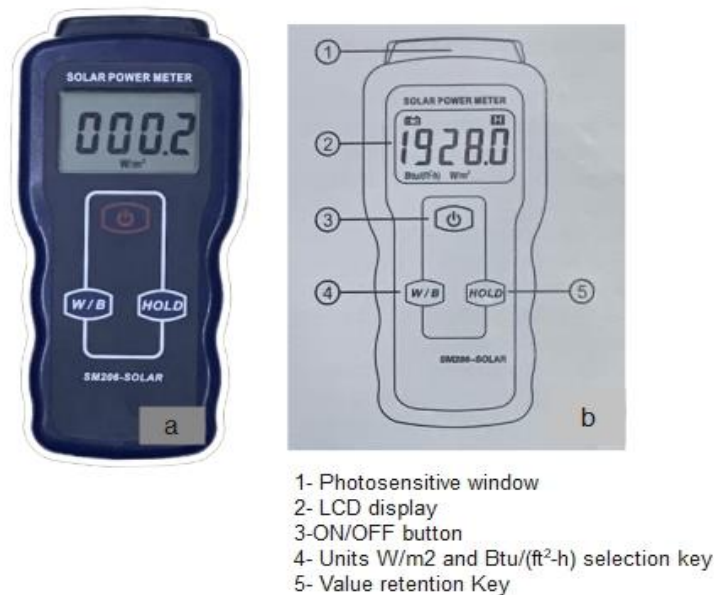
Figure 4.10. Solar Power meter b) Description of the keypad.

4.3.2. Arduino device

The Arduino device is used in the experimental work to record the necessary readings such as temperature, speed of air, and humidity through the use of numerous

sensors and connected electronic equipment. Figure (4.19) shows the Arduino device used. All parts of the Arduino will be presented in the next paragraphs.

The microcontroller board Arduino is the ideal board for those who want to learn more about code and electronics. This microelectronic board which has Multiple uses is equipped with an ATmega328P and an ATMega16U2 processors. It functions without difficulty when linked to a computer using a USB cable, an AC to DC adapter, or the battery to commence operation as shown in Figure (4.11). All the sensors of the experimental work are connected to this electronic board.

1.   USB B Connector   2. Rest   3. Power jack 2.1x5.5mm   4. USB cable

5. Regulator   6. ATMEGA328P Module   7. ATMEGA16U2 Module

8. Pin header connector (through hole 6)   9. Pin header connector (through hole 6)

10. Chip Capacitor, High Density
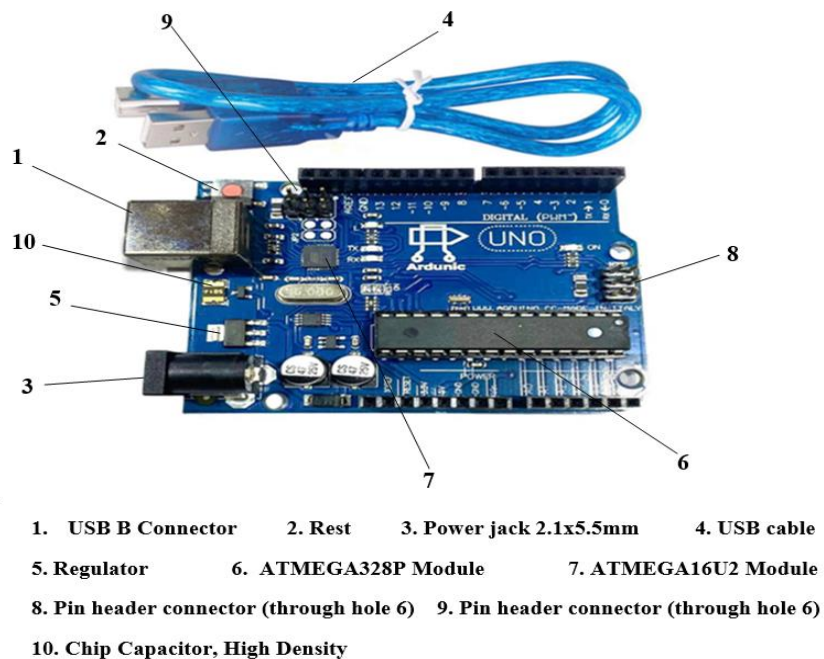
Figure 4.11 Arduino microcontroller board UNO R3.

The temperature sensor (MAX6675) can measure temperatures between -20°C and +80°C and has a resolution of 0.25°C. To report the measured temperature, it receives and amplifies the signal from the K-type thermocouple that it is connected with.

The temperature and Humidity Sensor DHT22 have a chip that converts analog data to digital data, producing a digital signal that includes temperature and humidity. The temperature ranges from -40 to 80 ℃ and the humidity ranges from 0 to 100%. Figure (4.12) shows the sensor used.

Figure 4.12. (a)Temperature Sensor (b)Ambient temperature and Humidity Sensor

The thermocouple used consists of two different wires that are welded together at one end and this is the place through which the temperature is measured. When the junction senses a temperature change, voltage is generated. The voltage is then translated and transformed into a direct reading by the specific sensors employed, shown on the Arduino device's screen, or saved in a RAM created for this reason. The thermocouple used is a K-type thermocouple that senses temperature between 0-1200°C and is equipped with an annular end as shown in Figure (4.13).

Figure 4.13. K-type Thermocouple.

Figure (4.14) shows the locations of where thermocouples are installed in the PV/T system.
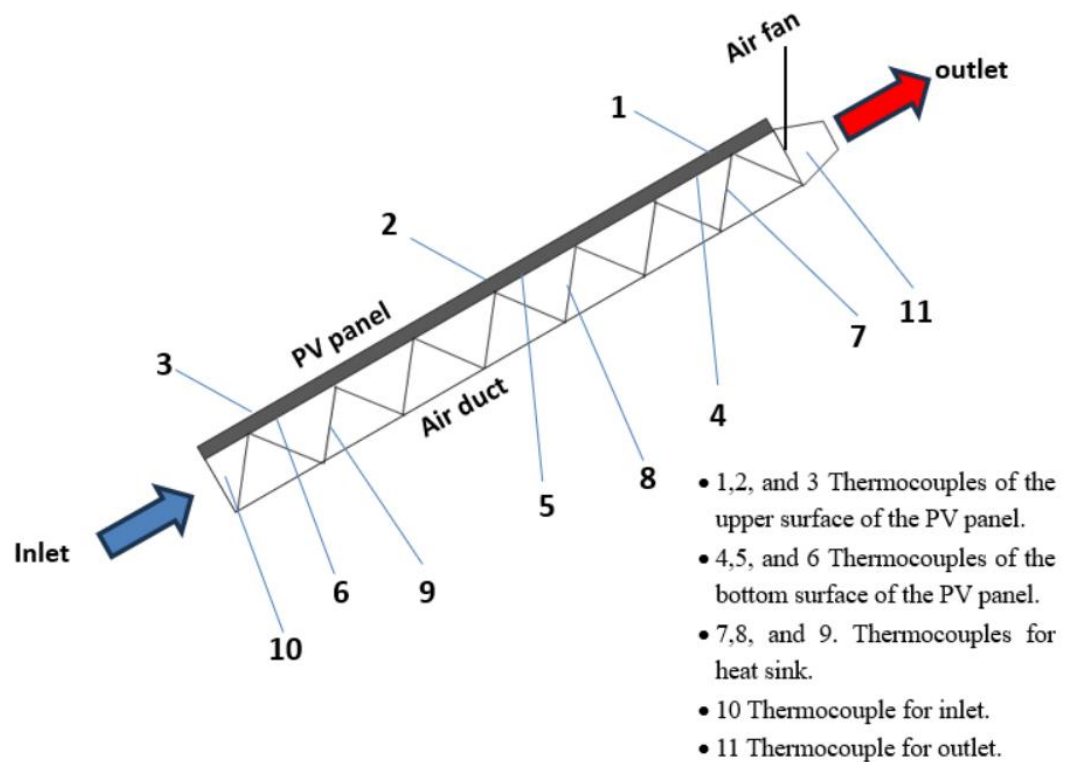
Figure 4.14. Places to install thermocouples in the PV/T system.

The air velocity in this experimental work can be measured by the Wind Speed Sensor (Anemometer) which is connected to the Arduino. Anemometers gauge the wind's speed instantaneously. The type used in this work is the rotating cup anemometer. Where the cups rotate according to the speed of the wind when you pass them. It is characterized by ease of use and stability even at high speeds, and it operates with a DC. The wind speed sensor has several technical specifications, the Input voltage range (7-24v DC), analog output voltage (0.4V - 2V), Testing Range of (0.5-50 meters/sec), measuring range (0-32.4 m/sec), when no wind (0.2 m/s), Resolution (0.1m/s), Accuracy (1 meter/s). Wind Speed Sensor Anemometer

construction consists of the shell, the wind cup, and the circuit module. The sensor is rugged, weather-resistant, and waterproof and we notice this in Figure (4.15).

Figure 4.15. Wind Speed Sensor.

The Solderless MB102 830 Bread board is used for experimenting with circuit designs in either a research and development laboratory or a university laboratory. The board is also used to make temporary circuits for testing or to try out an idea. No soldering is required, so, it is easy to change connections and replace parts. It also contains 380 connection pointins, as shown in Figure (4.16a).

Two types of connection wires are used in the Arduino: Male to Female and Male to Male cables. Male to Female connecting wires, 40 wires with a length of 200 mm used to connect parts. They are characterized by ease of connection and use. Male to Male an electrical wire or group of them in a cable with a connector or pins at each end, which is normally used for interconnecting the components of a breadboard or other prototype or test circuit, internally or with other equipment or components, without soldering as shown in Figure (4.16b).
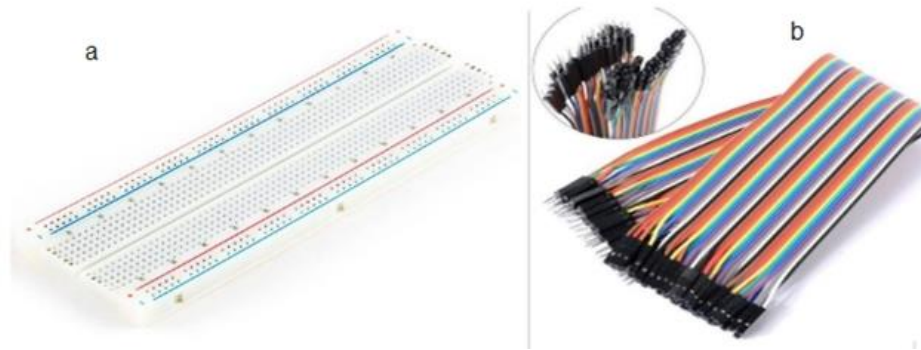
Figure 4.16. a) Breadboard 380P b) Connecting cables

The LCD screen display. It is used to display data in the Arduino device. The LCD screen is a 20*4 monochrome screen. 20 means that 20 characters can be displayed in four rows, so the number of characters that can be displayed on the screen is 80 characters. Figure (4.17) displays the LCD screen.

Figure 4.17. LCD display screen.

Micro SD is used to store the readings and provide the Arduino with the ability to communicate with the data storage unit, save it, and make a data logger in various projects as shown in Figure (4.18 a). The data and measurement results are saved in the Arduino device and transferred to the computer and used in the form of an Excel file. We use RAM for this purpose shown in the Figure (4.18b).
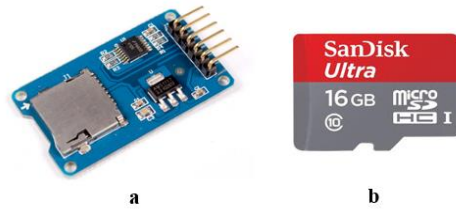
Figure 4.18. a) Micro SD Card driver model   b) Ram.

USP is the power unit needed to operate the Arduino. It provides stable DC output, long standby time, protection from overload and short circuits, protection from overcharging and over-discharging (Auto Cut), and (5v, 9v, 12v, 15v, and 24v) ports as shown in figure. See Figure c 4 in Appendix C for more details about the Arduino.

Figure 4.19. Final form of the Arduino device.

4.3.3. Solar module analyzer (PV Analyzer)

The photovoltaic module analyzer is used to analyze the characteristics of the photovoltaic module, such as the maximum output power and the maximum voltage, in addition to drawing the I-V and P-v relationship. The device used PROVA 210 type is shown in Figure (4.20) to analysis of the characteristics of the two photovoltaic panels with and without cooling to compare them. The device can measure voltage in the 0-60 V range with a resolution of 0.01 V and current in the 0.01-12 A range with a resolution of 10 mA and has an accuracy of $\pm 1\%$.

Figure 4.20. PV Analyzer device.

4.4. Procedures for experimental work

  The process of operating the thermal photovoltaic PV/T system in this experimental work shown in Figure (4-21) for cooling the photovoltaic units by using porous metal media. The experimental test was carried out under real weather conditions. The procedure have been included several steps:

1. Two photovoltaic modules with and without cooling are installed and readings are recorded at the same time to compare their performance.
2. The system is directed towards the south, and the complex is inclined at an angle of 31°, according to the geographical location of the city of Rumaitha.
3. The intensity of solar irradiance is measured every 10 minutes during the experimental period.
4. The data that is recorded such as the temperature of the photovoltaic panels, the system, the air speed, the humidity and the ambient temperature using a set of sensors in the Arduino.
5. The test was conducted according to the change in the mass flow rate of air (0.0.057 kg/s, 0.096 kg/s, 0.111kg/s)
6. Analyzing the characteristics of photovoltaic panels using the PV Analyzer every ten minutes throughout the experiment period.
7. The recorded readings have been analyzed according to equations, and then the results are presented and discussed.

For more information about the PV / T system, see Figures (1c - 5c) in Appendix (c) .
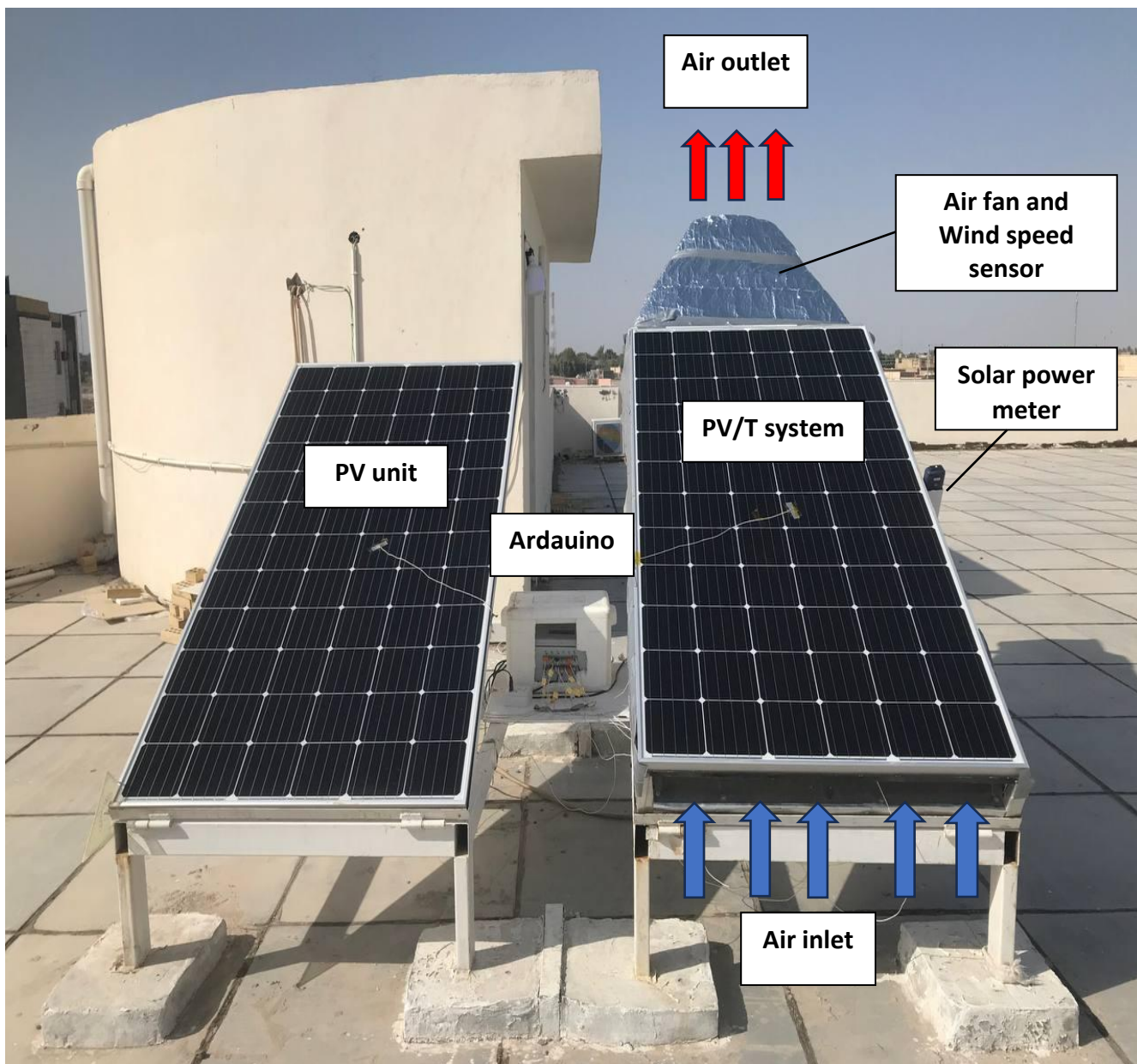
Figure 4.21. Experimental setup of the PV unit and PV/T system.
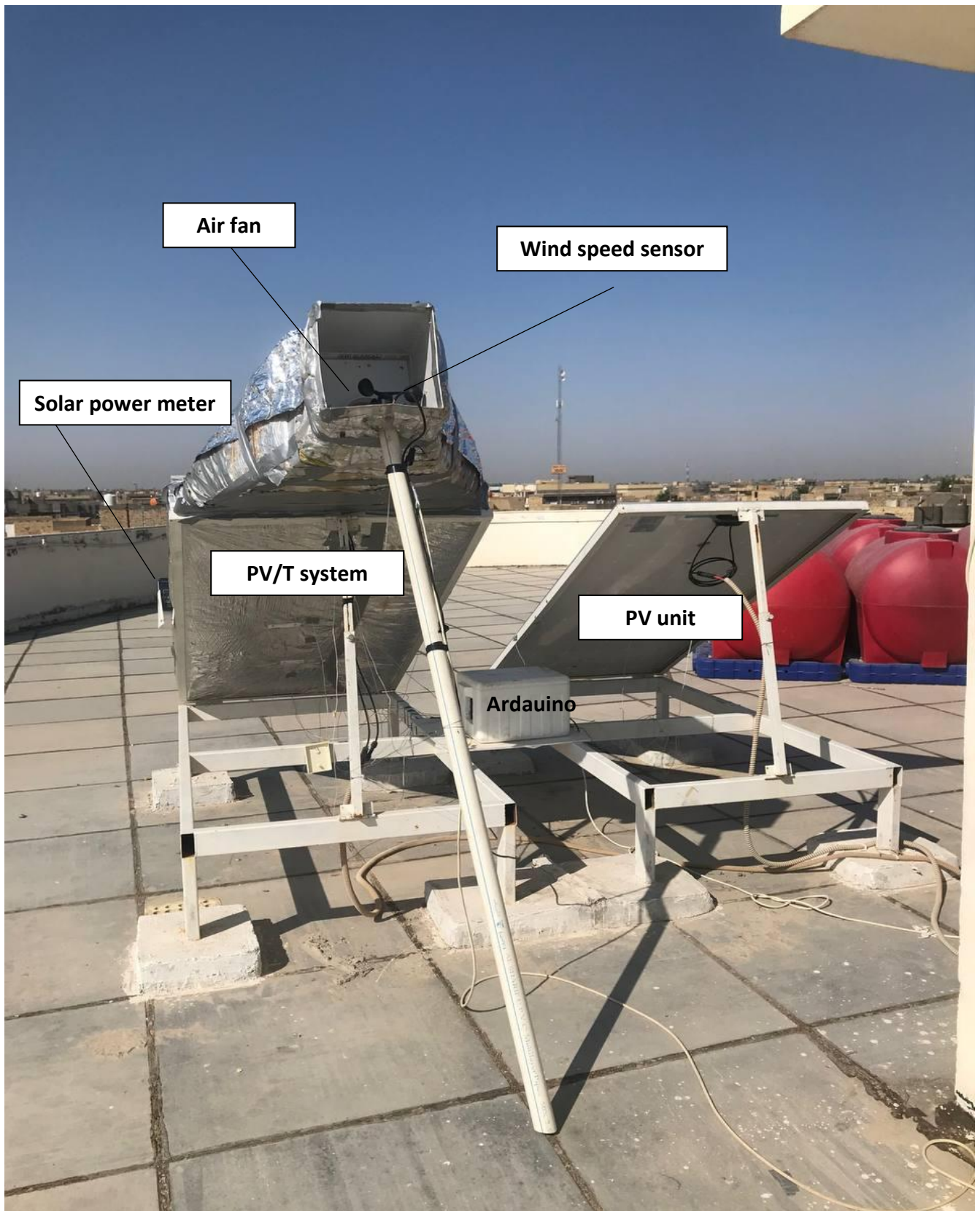
Figure 4.22. Rear view of the PV module and PV/T system.

Chapter Five: Results and Discussion

5.1. Introduction

This chapter discusses the numerical and experimental results obtained from the testing of PV panel cooling technology by using porous material. The simulation results will be discussed in the COMSOL program and the most suitable number of porous material ribs within the air duct are chosen. In addition to discussing the numerical and experimental results to improve photovoltaic panels' electrical and thermal efficiency. As will be the performance of the system discussed external factors such as the ambient temperature, Humidity, and the amount of solar irradiance. In addition, a discussion of the effect of air mass flow rate on the performance of PV panels.

5.2. Real weather condetions

The main input parameters that affect the performance of any solar system are the weather conditions. In PV/T systems, the solar irradiance and temperature of the ambient are important to them, they affect the output of the PV/T. Figure (5.1) presented the climatic parameters, the variations in solar intensity, and the ambient temperature for Iraq-Najaf (32°02',44°20') weather conditions that have been implemented for this study during different three days obtained from the Energy Research Unit at the Technical College of Engineering/Najaf. From the figure, we notice that the ambient temperature increases with the increase in the intensity of solar radiation. The highest data are recorded on 23th may 2020. From the figure, we notice that the ambient temperature increases with the increase in the intensity of

solar radiation. It reached 36.8 °C at 12 pm, so the maximum solar radiation reached 973 W/m^2.
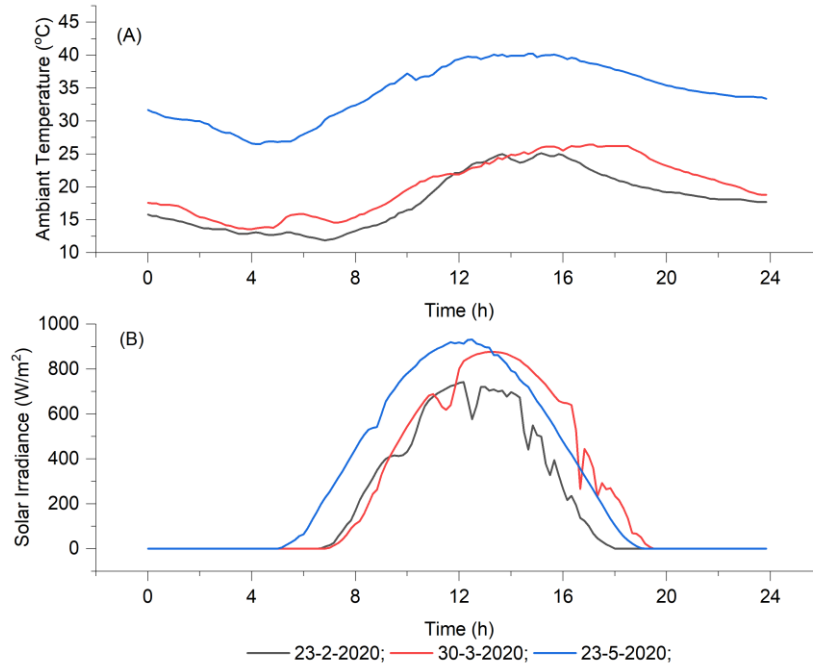
Figure 5.1. Hourly change of the, (A) ambient temperature and
(B) solar irradiance for three days.

5.3. Effect number of porous metal ribs inside the air duct

The change in the surface temperature of the photovoltaic panel during the cooling time it can be seen in the Figure (5.2). From the figure, it can be observed that the temperature increases over time as a result of the increase in the ambient temperature. At the end of time, the surface temperature of the photovoltaic panel decreases due to the decrease in the intensity of solar radiation and the ambient temperature. We also notice in the figure that the temperature of the photovoltaic panel varies according to the number of porous metal ribs. By increasing the number of ribs, the contact area of the porous metal with the solar panel increases, which

increases the heat transfer process, and thus the operating temperature becomes lower. This is what we see clearly in the figure below, so the average temperatures of the surface PV panel for the cases of 10 ribs, 12 ribs, and 14 ribs are 56.2°C, 53.9°C, and 49.7°C, respectively
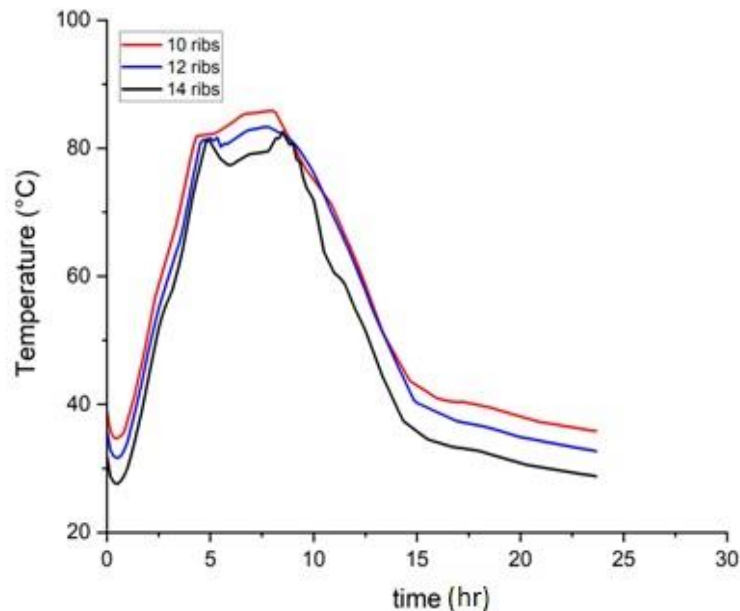
Figure 5.2. Effect number of ribs of a porous metal on the temperature of PV panels.

5.4. Internal temperature distribution

After defining the boundaries and initial conditions and performing a simulation process of the PV/T system using COMSOL Multiphysics to achieve the best design to improve the efficiency of photovoltaic panels, the results are obtained as shown in Figure (5.3). A side view of the PV/T system simulation is shown in the figure, where the temperature distribution can be observed in the proposed module. It is noted that the operating temperature of the photovoltaic module increases with the intensity of solar radiation until it reaches up to 82°C after 6.8 hours of cooling during the simulation. Due to the heat exchange between the photovoltaic panel, the

metal grid, and the air, it can be seen that the temperature inside the air duct increases in the direction of the airflow.
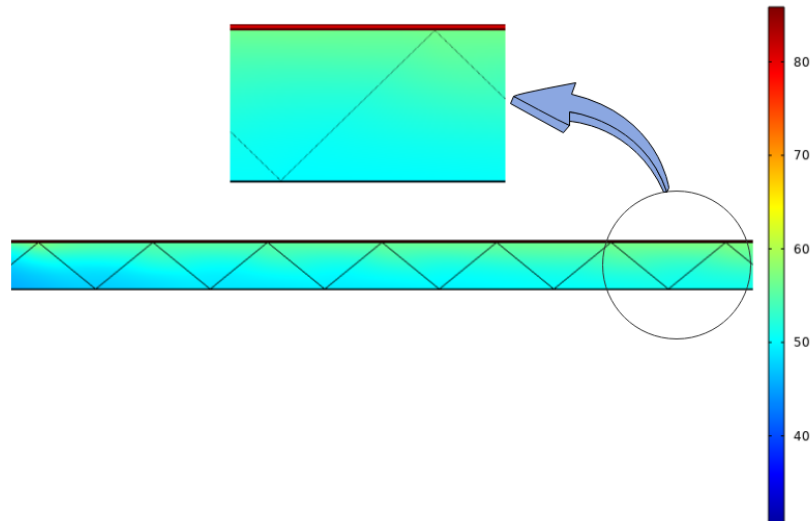
Figure 5.3. side view of the PV/T system simulation at time 8.6h.

The first function of this simulation involved the comparison of the PV/T temperatures. These are temperatures of the glass, cell and back the PV also inlet and outlet air temperatures. The simulation results for each intercomparison are presented in Figure (5.4). The temperature variation of the PV glass layer and the cell was the maximum value of others. Accordingly, in the simulation result, the cell temperature increased according to the increase in solar irradiances and ambient temperature The excessive temperature leads to a decrease in the performance of the PV and thus, the minimum PV output power.
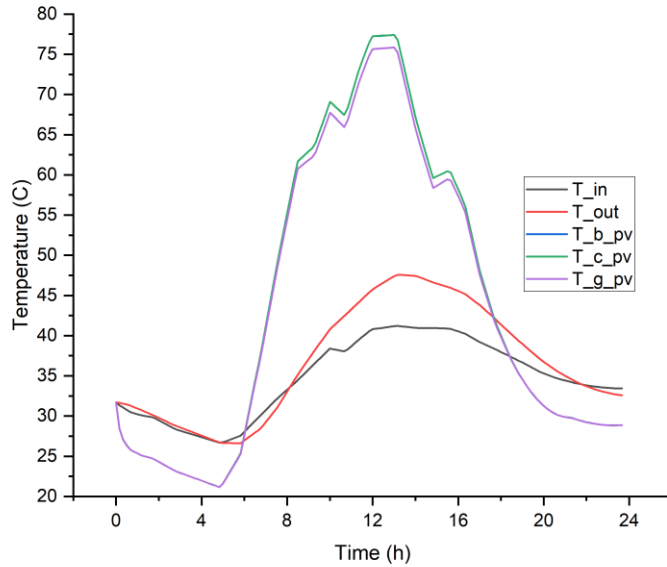
Figure 5.4. Simulated temperature comparison of air temperatures (inlet and outlet) and Layers of PV/T (23-5-2020).

The COMSOL Multiphysics 5.6 model is simulated to compute the streamline air velocity, temperature distribution, and pressure drop in the 2D of the PV/T system. Figure (5.5A) presents the streamline velocity of air flowing throw the triangular screen. the Turbulent Flow, k-ε physics has been used to test the air moving inside the air channel. The air temperature distribution inside the air duct for the PVT air collector has been illustrated in Figure (5.5B). The simulation result clarifies an increase in air temperature near the cell. The leaving air temperature has been increased from 319 K to 329 K by using porous metal. Figure (5.5C) illustrates the pressure distribution inside the air duct, it was the highest value in perforations.
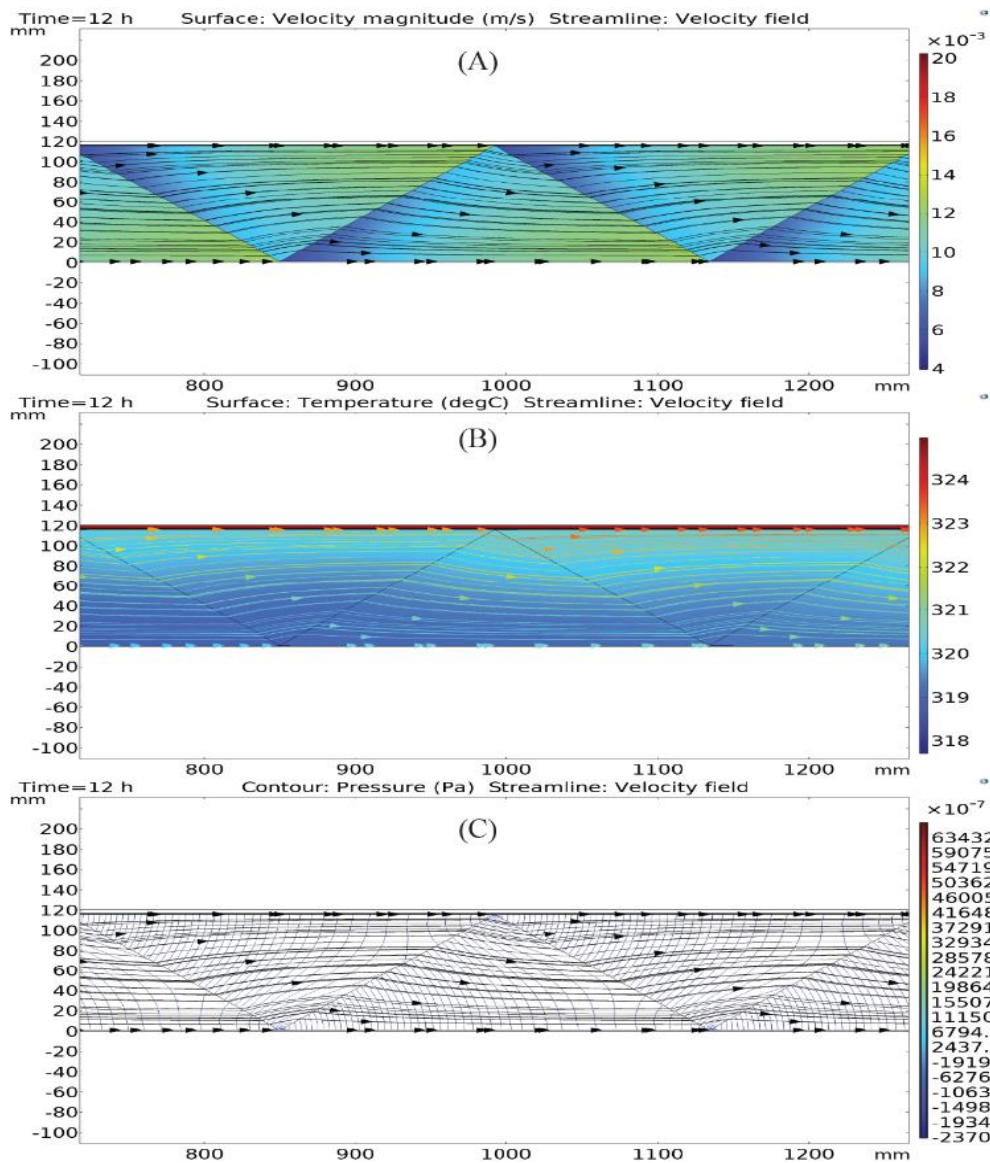
Figure 5.5. Evaluation of air inside the duct A) streamline velocity, B) Air temperature distribution, and C) Pressure drop.

The temperature of the air inside the air duct containing the porous metal increases due to the increased surface area for heat exchange which leads to an increase in the amount of heat gained. A comparison of the amount of thermal energy acquired by the air in the PV/T system for three different days is shown in Figure (5.6) as obtained from the simulation process. The amount of thermal energy

increases with the increase in solar radiation intensity and ambient temperature during the day. As we see in Figures (5.1A and B), the maximum value of solar irradiance and ambient temperature was on 23-5-2020. This working, the overall heat energy increases to the maximum value of 459W.
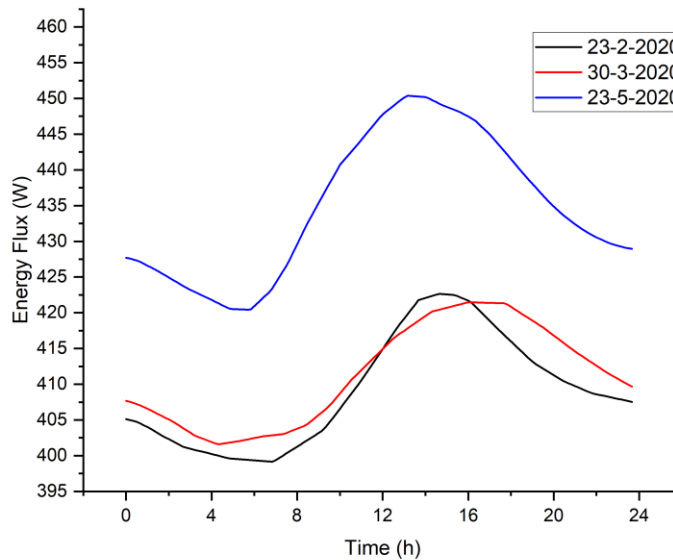
Figure 5.6. Hourly variation of input and output energy heat flux for the PV with air duct.

5.5. Efficiency of the PV/T Module

The efficiency of a photovoltaic panel is not constant over time. As solar radiation and ambient temperature increase, efficiency decreases, which can be seen in the simulation results in the two Figures (5.7) and (5.8) show the results. In Figure (5.7), it is evident that the electrical efficiency at the beginning, the efficiency has been at its peak due to the decrease in temperature, reaching 19.5%. However, it gradually declined and eventually hit its lowest point of 15% after 8 hours at the number of ribs 14 and a mass air flow rate of 0.111 kg/s.
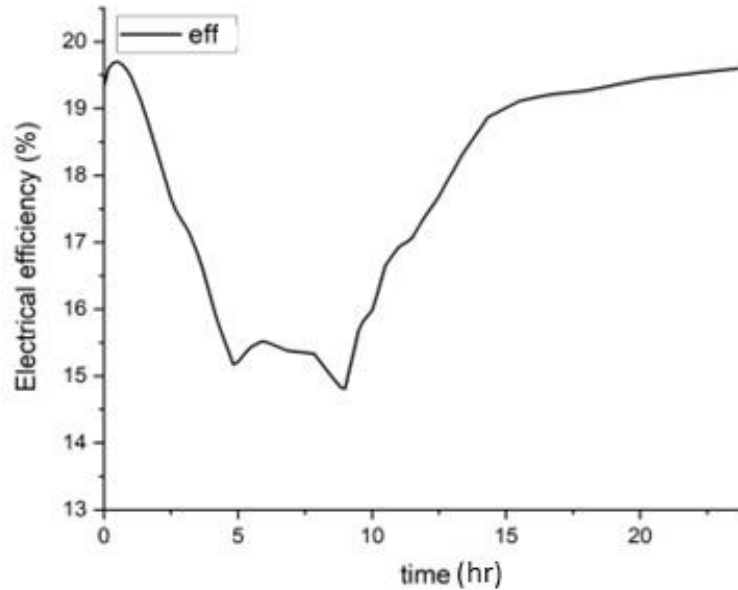
Figure 5.7. Simulation result for efficiency of PV/T system.

Note from Figure (5.8) that there is a substantial effect depending on how many ribs of the porous material are in contact with the PV panel's rear surface. By increasing the number of ribs, the surface area of the heat sink increases, and the contact area of the metal with the solar panel increases. seems that increasing the number of porous metal ribs inside the duct can greatly heat exchange and improve efficiency. Basically, the more ribs there are the better the heat transfer. Based on our findings, we observe that the efficiency rate varies depending on the number of ribs used. Specifically, we have found that using 10 ribs resulted in an efficiency rate of 16.6%, while using 12 ribs increased the rate to 17%, and using 14 ribs further improved the rate to 17.7%. This represents an overall rate of improvement of 4.2% in the case of 14 ribs.
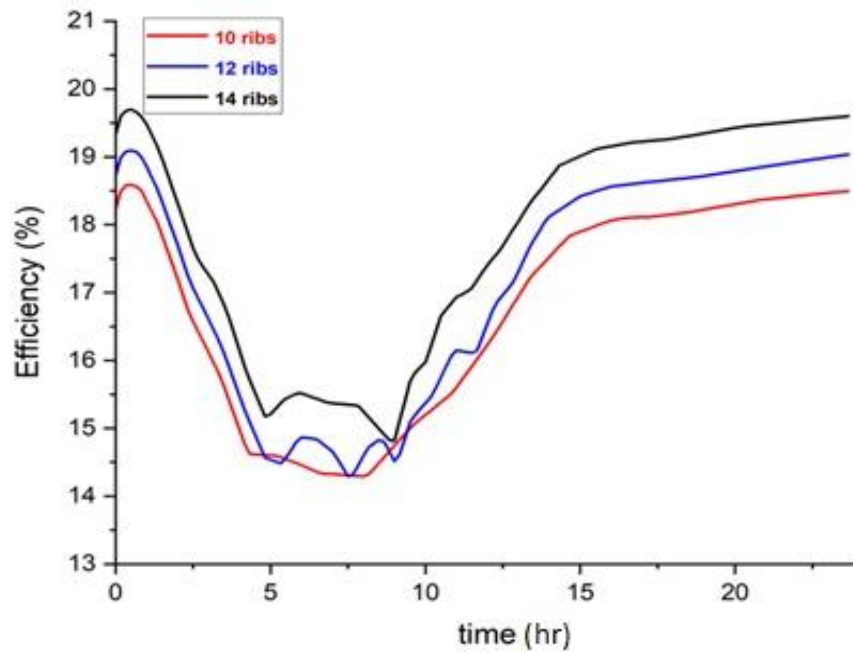
Figure 5.8. Efficiency PV/T with the number of porous metal ribs at 0.111kg/s.

5.6. Experiment results

This experiment is carried out at Al-Rumaitha Technical Institute/Al-Furat Al-Awsat Technical University. For several different days of the year 2023 with different weather conditions it is 24th June, 26th June, 2nd July, 5th July, and 7th July . Additionally, experiments have been implemented with different air mass flow rate (0.057, 0.069, and 0.111) kg/s.

5.6.1. Effects of weather characteristics

During the experimental work, tested the performance of the photovoltaic thermal system PV/T between 8 am and 4 pm. Tracked variations in weather, such as solar irradiance and ambient temperature, throughout the entire process in 2023. At the start of the experiment, it was observed that the ambient temperature was low due to decreased solar radiation, which continues to rise with increasing intensity of solar radiation. Figure (5.9) shows that the behavior of the ambient temperature is

directly related to the intensity of solar radiation. The highest data was recorded at 1:00 pm when the solar radiation reached 1192.14 W/m² and the ambient temperature reached 46.36.°C. For further reference, check the Figures (a 1 – a 3) in Appendix (a), which show weather characteristics for several days.
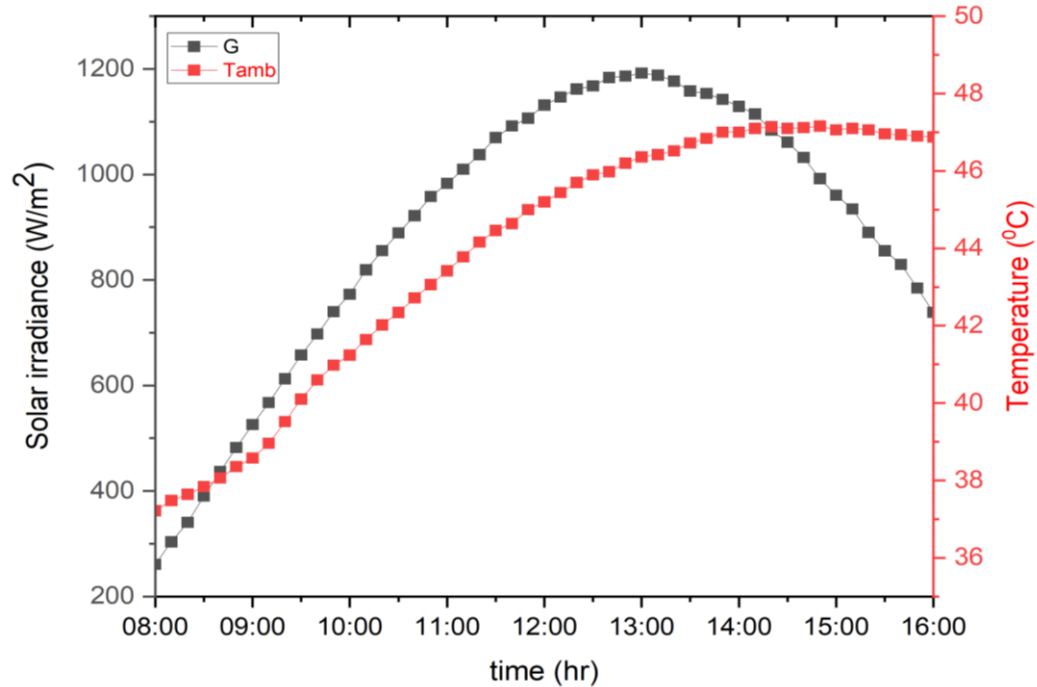
Figure 5.9. Variations in rates of ambient temperature and solar radiation to experimental workdays.

Based on Figure (5.10) which shows the rate of the ambient temperature and humidity level for the days of the experimental work, it appears that there is a correlation between humidity and ambient temperature. Specifically, observed that at the start of the experiment in the morning, humidity levels tended to be higher due to the lower temperature. As the temperature increases throughout the day, we can see a corresponding decrease in humidity levels. According to the findings, the initial hours of the experiment recorded the highest humidity level of 22.95% at an ambient temperature of 37.22 °C. Subsequently, the humidity levels exhibit a decreasing trend and reach about 14.68% as the ambient temperature rises to 46.36 °C. In order

to enhance the cooling mechanism for the solar cells, it's recommended to use pre-cooled air with water or spray water on the panels. For more information, see the figures (a 4) and (a 5) in Appendix (a).
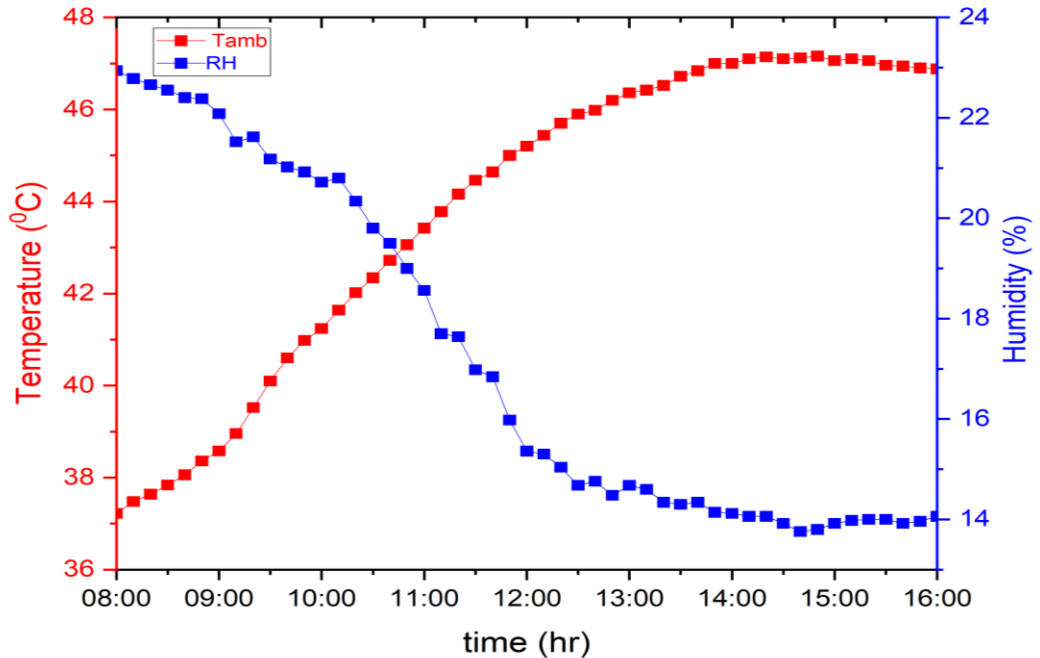
Figure 5.10. Average of relative humidity and ambient temperature for the experimental workdays.

With an increase in solar radiation comes a rise in ambient temperature, which leads to a higher operating temperature for photovoltaic panels as shown in Figure (5.11) which shows the rates of solar radiation and the temperature of the photovoltaic panel for the days of experimental work. Which reduces the performance of PV panels [5]. According to Figure, there is a correlation between the temperature of the photovoltaic panel and the intensity of solar radiation. As the solar radiation increases, the temperature of the panel also rises. This information can be useful in understanding the behavior of photovoltaic panels under different weather conditions and can aid in optimizing their efficiency.

Through the data that was recorded it was observed that at the lowest intensity of solar radiation, which is 261.08 W/m², the temperature of the photovoltaic cell reached 46.1⁰C. However, as the solar radiation increased and reached the maximum level of 1192.14 W/m², the temperature of the solar cell also increased and reached 67.7 ⁰C. It is important to monitor and regulate the temperature of the solar cell to ensure its optimal performance and longevity. For more information, see the Figures (a6 - a8) in Appendix(a).
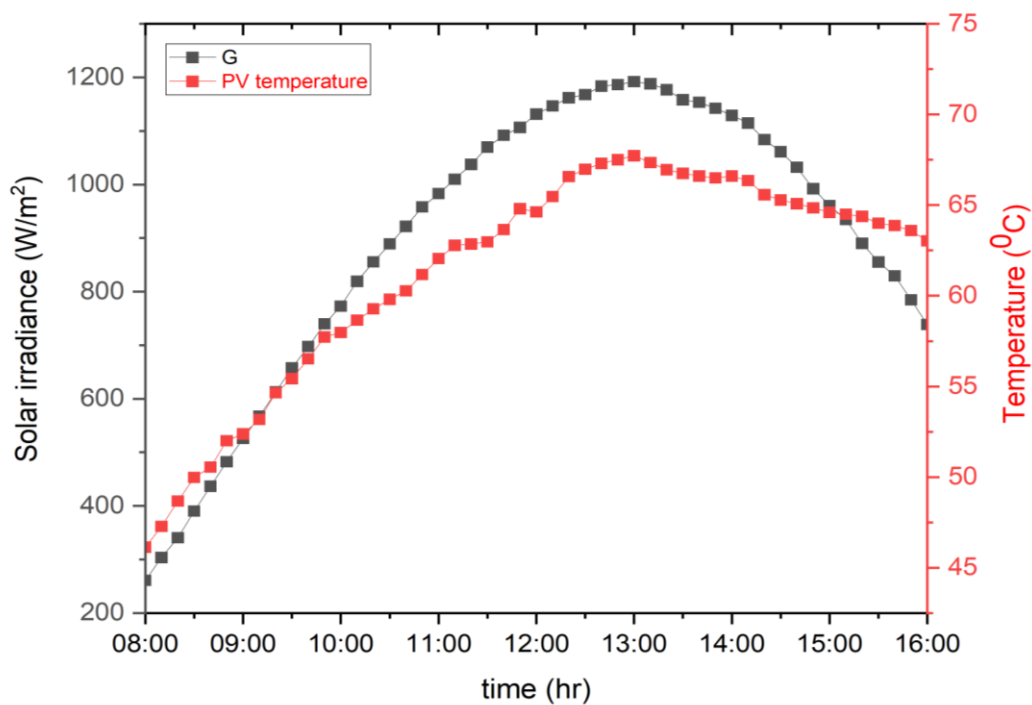
Figure 5.11. panel temperature and solar radiation for the experimental workdays.

5.6.2. Effect of mass flow rate on a PV/T module's performance

To determine the impact on the operating temperature of the PV panels, the thermal photovoltaic system PV/T is evaluated in this section using three mass flow rates of 0.057 kg/s, 0.096 kg/s, and 0.111 kg/s. Along with understanding how it affects solar panels.

Figure (5.12), shows the temperature of the solar cell depending on the mass flow rate of air inside the channel. Here, as noted previously, we see that the temperature of the photovoltaic panels rises over time as a result of an increase in solar radiation. Additionally, it can be seen that the operating temperature of the PV panels can be further decreased by raising the mass flow rate. The findings revealed that the average temperatures for the flow rates of 0.057 kg/s, 0.096 kg/s, and 0.111 kg/s were, respectively, 55.6 °C, 51.3 °C, and 49.4 °C. Therefore, increasing the flow rate in the proposed cooling technology affects the temperature of the solar cells during the testing period.
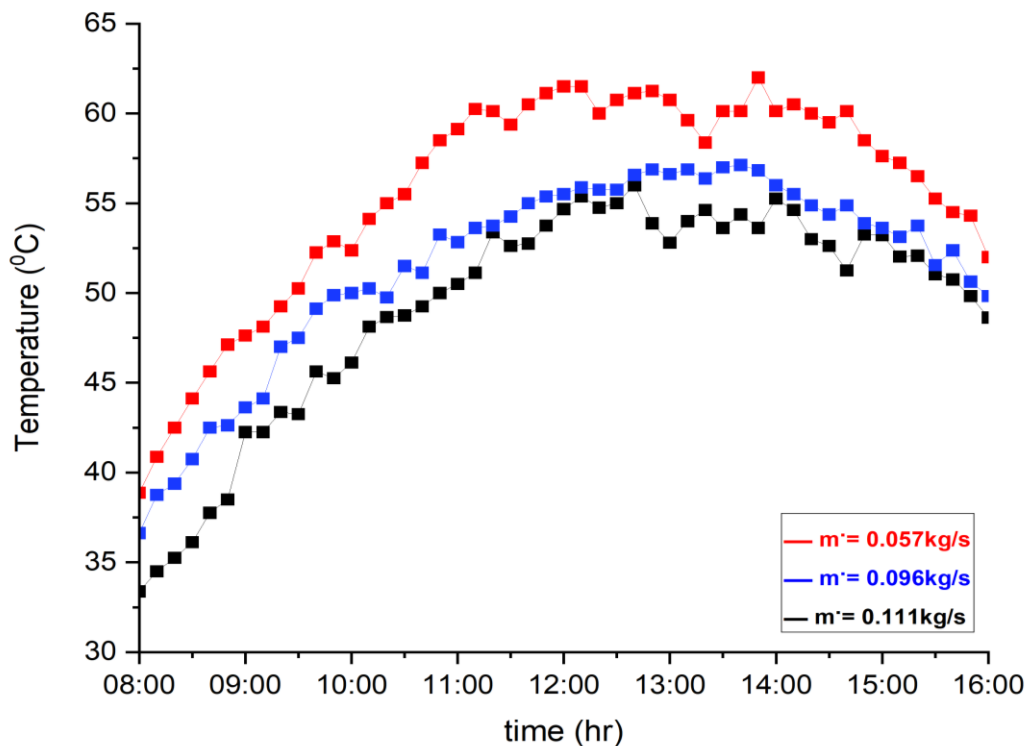
Figure 5.12. PV/T temperature with various mass flow rates.

5.6.2.1. Efficiency with mass flow rate

Increasing the mass flow rate positively affects the current and voltage generated, leading to increased output power, and improving electrical efficiency. Through results, the maximum output power for the three cases of 0.057 kJ/s, 0.096

kJ/s, and 0.111 kJ/s was recorded as 297.16 W, 313.39 W, and 330.79 W, respectively as shown in Figure (5.13).

The effect of increasing the flow rate is noted in the electrical efficiency of the PV panels in Figure (5.14). The results indicated that increasing the air mass flow rate improves the electrical efficiency of the PV panel. The results recorded for the average efficiency to cases 0.057 kg/s, 0.096 kg/s, and 0.111 kg/s are 16.17%, 17.06%, and 17.43% with an improvement rate of 2.3%, 2.9%, and 4.13%, respectively.
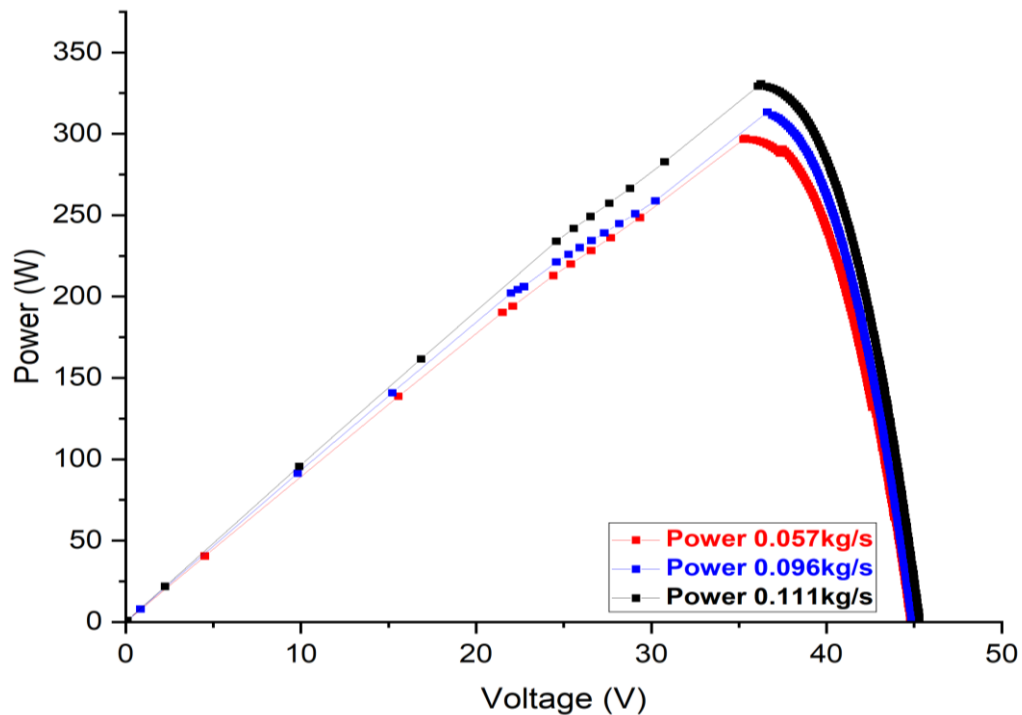
Figure 5.13. P-V curve for PV/T unit with various mass flow rates

.
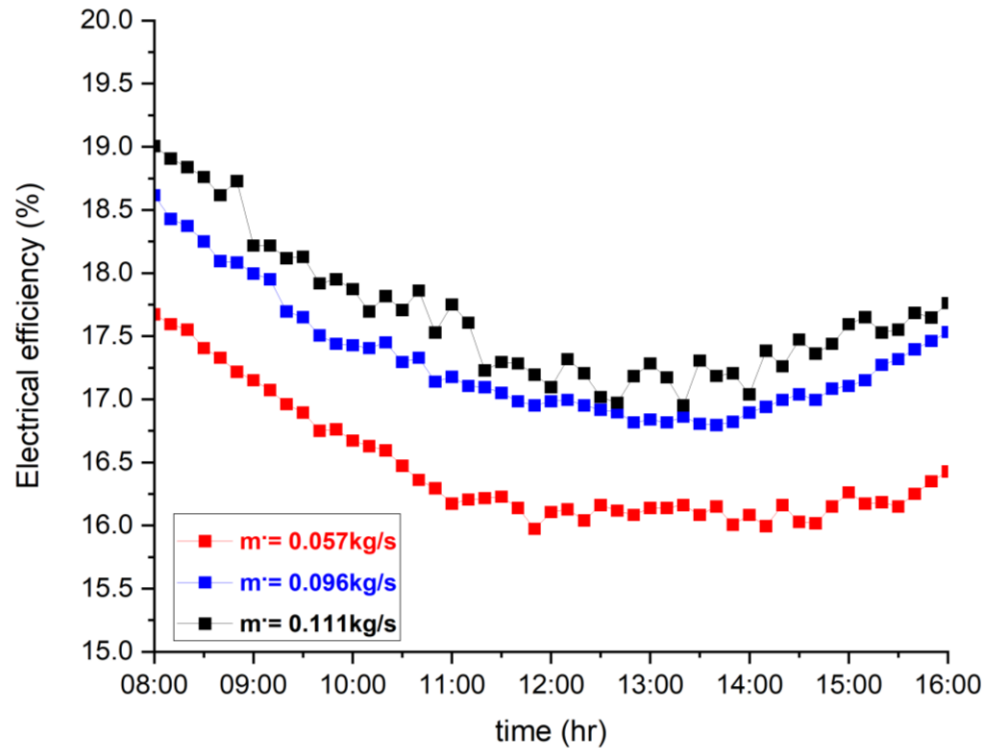
Figure 5.14. Electrical efficiency for PV/T unit with various mass flow rates.

5.6.2.2. Heat gain with mass flow rate

Figure (5.15) shows the effect of the change in the mass flow rate on the amount of heat gained. Increasing the air mass flow rate increases the amount of heat gained from the thermal photovoltaic system. The findings show that the biggest quantity of heat gain, at a rate of 484 W, could be obtained at the highest flow rate of 0.111 kg/s in comparison with the other two cases, 0.057 kg/s, and 0.096 kg/s, the results are 260.7 W and 414.4 W.

78
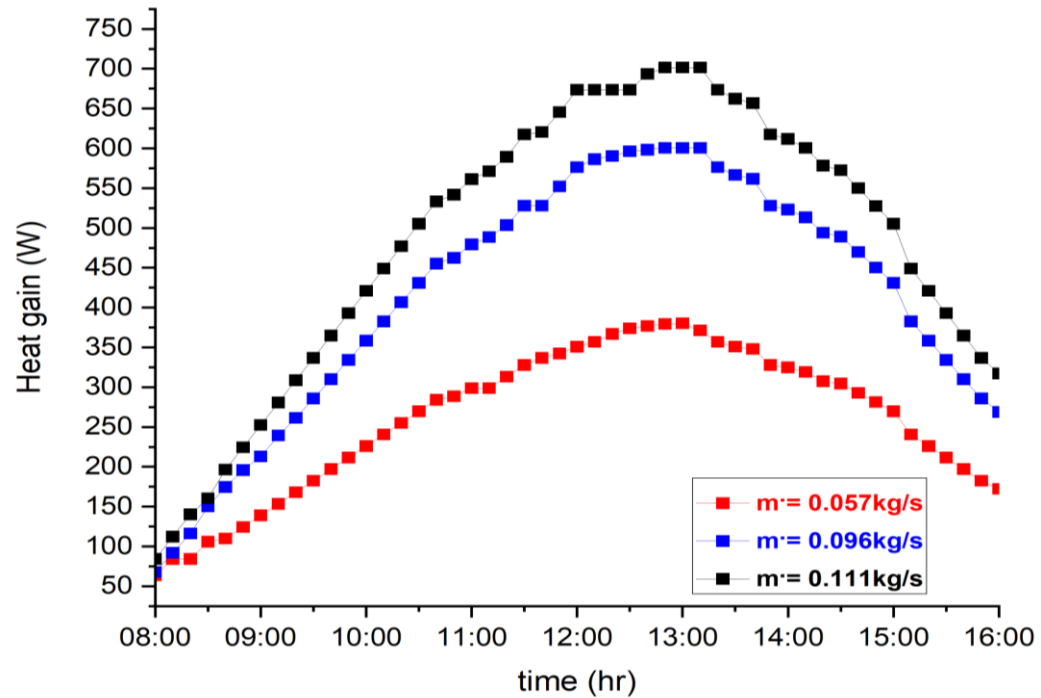
Figure 5.15. Heat gain with various mass flow rates.

5.6.2.3.   Thermal efficiency with mass flow rate

The thermal efficiency increases with an increase in the air mass flow rate. Figure (5.16) shows a comparison between the three cases. We can see from the figure that the highest rate of thermal efficiency obtained is 4.25% from a mass flow rate of 0.111kg /s compared to the other two cases 0.057 kg/s and 0.096 kg/s, the average thermal efficiency is 17% and 22.2%, respectively.
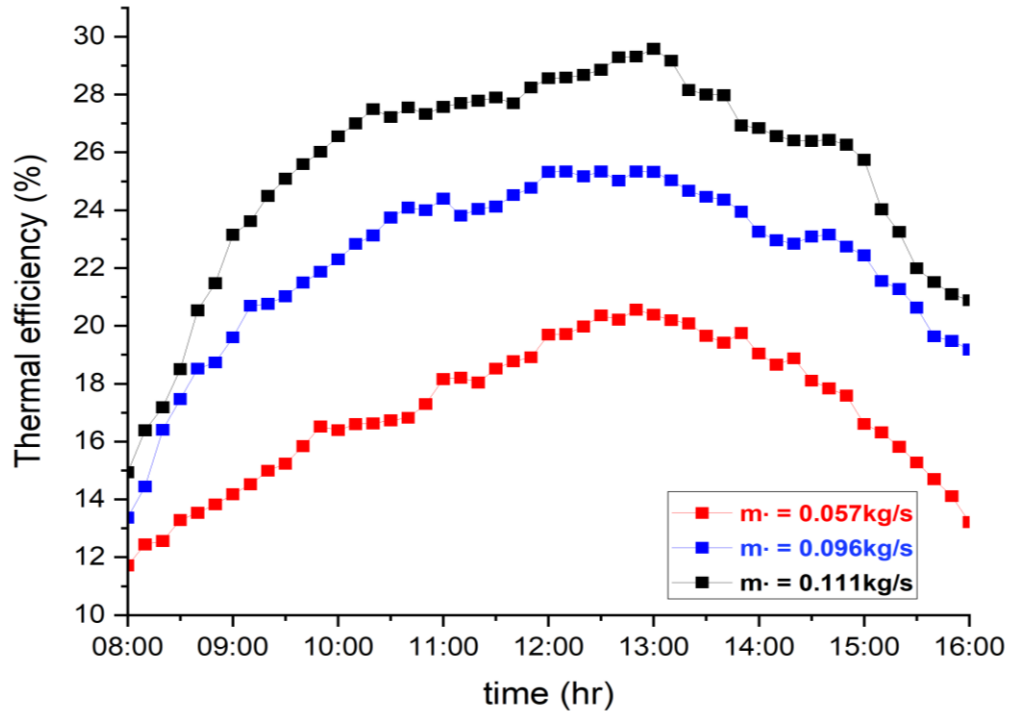
Figure 5.16. Thermal efficiency with various mass flow rates.

5.6.2.4. Total efficiency with mass flow rate

Figure (5.17) shows the comparison of the total efficiencies between three cases of 0.057 kg/s, 0.096 kg/s, and 0.111 kg/s for the PV/T system. As a result of increasing the electrical and thermal efficiency of the proposed system in response to the increase in flow rates, the overall efficiency of the system increases. The results show that the maximum total efficiency for the three cases is 36.8%, 42.4%, and 46.8%, respectively.
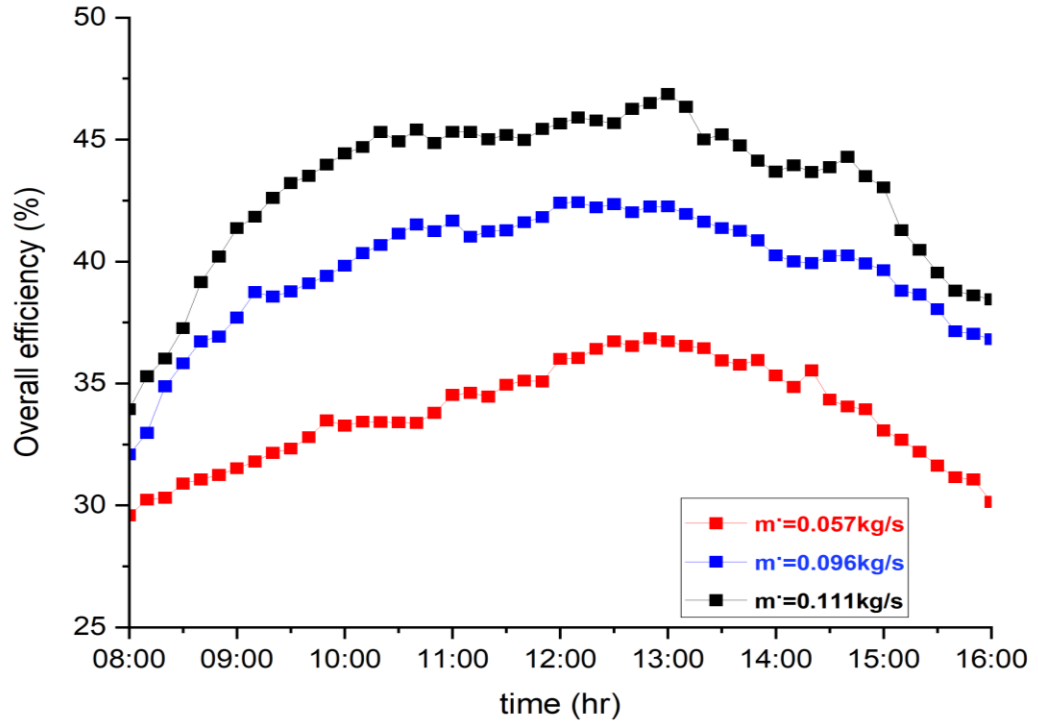
Figure 5.17. Overal efficiency with various mass flow rate.

5.6.3. Effect of cooling on PV panels' temperature

After conducting an experimental test according to changing the mass flow rate, the results showed that the best air mass flow rate is 0.111 kg/s. Figure (5.18) shows the average temperatures of photovoltaic cells are compared with and without a cooling system. The results clearly show that the PV panel with cooling experienced significantly lower temperatures compared to the PV panel without cooling at an air mass flow rate of 0.111kg/s. The maximum temperatures of the two PV panels with and without cooling, at 1:00 pm, reaching 62.7 ^{0}C and 67.7 ^{0}C. This represents a temperature decrease at a rate of 7.9%. Additional temperature data for both panels can be found in Appendix (b), Figures (b 1), and (b 2), which show the temperatures for various days and different mass flow rates.
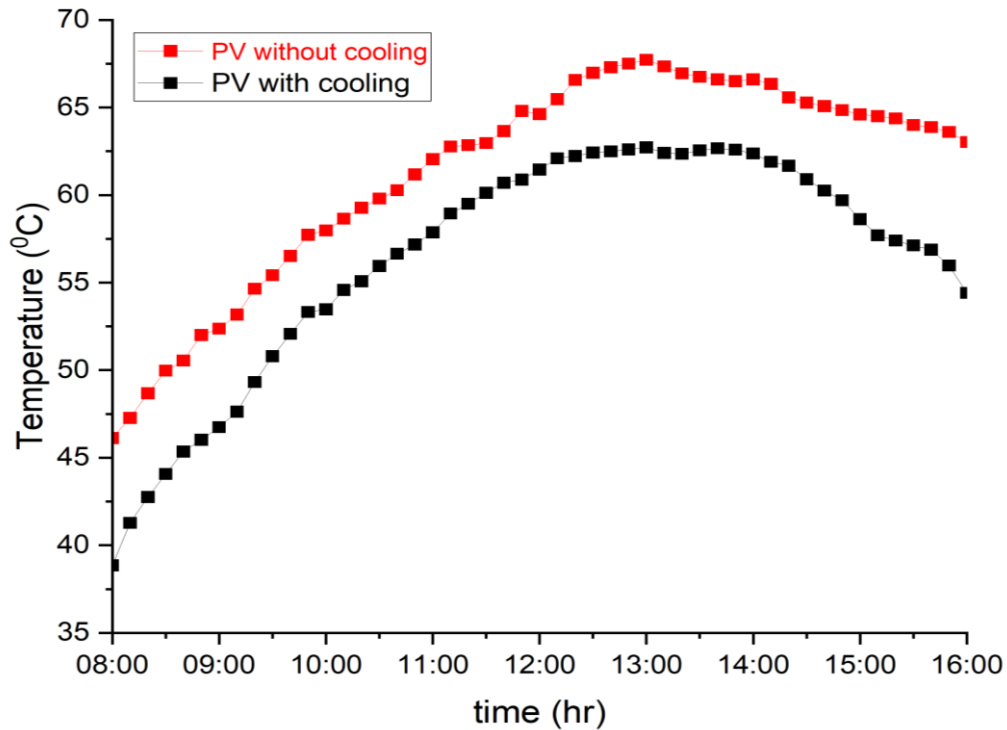
Figure 5.18. PV panels temperature with and without cooling at 0.111kg/s.

5.6.3.1. Power and efficiency of PV panels

Based on the data presented in Figure (5.19) which shows the comparison between the current rates of the two photovoltaic panels with and without cooling, where the average data was taken for the test days. It is found that the current difference between the two PV panels with and without cooling is very small and almost identical, and this usually happens in the case of current, with a recorded average difference of 0.07A an improvement of 0.7%. Both panels with and without cooling recorded a maximum current of 9.1A, and 8.6A, respectively. Figures (b 3) and (b 4) in Appendix (b), show the current difference over different days of the experiment.
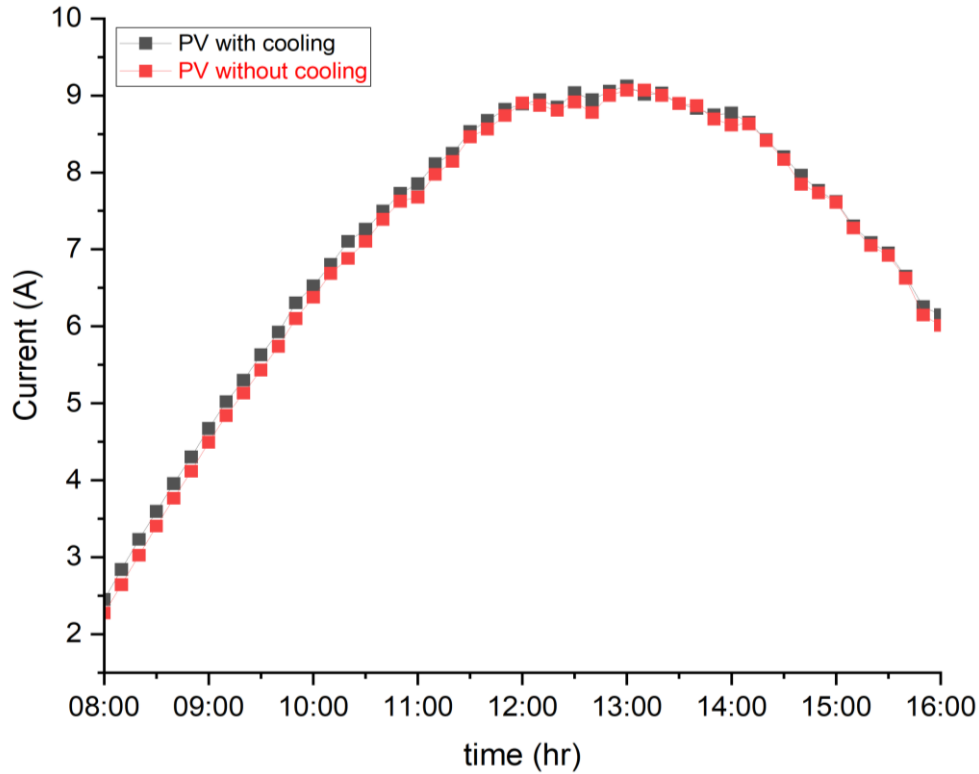
Figure 5.19. PV Current with and without cooling at 0.111kg/s.

As depicted in Figure (5.20), the voltage of both photovoltaic panels was high at the beginning of the test and decreased gradually over time due to the increase in solar radiation intensity and ambient temperature. However, by implementing cooling, the average voltage increased by 2.47V. The cooling mechanism helped in achieving an average voltage of 37.93V for the PV panel with cooling, while the reference panel only recorded an average voltage of 35.46V. This resulted in a 6.9% improvement in the voltage level. The maximum amount of voltage recorded at the beginning of the test was 39.3 V with cooling and 38.4 V for the panel without cooling.For further details on the voltage comparison between the two photovoltaic panels, please refer to Appendix B, Figures 5(b) and 6(b).
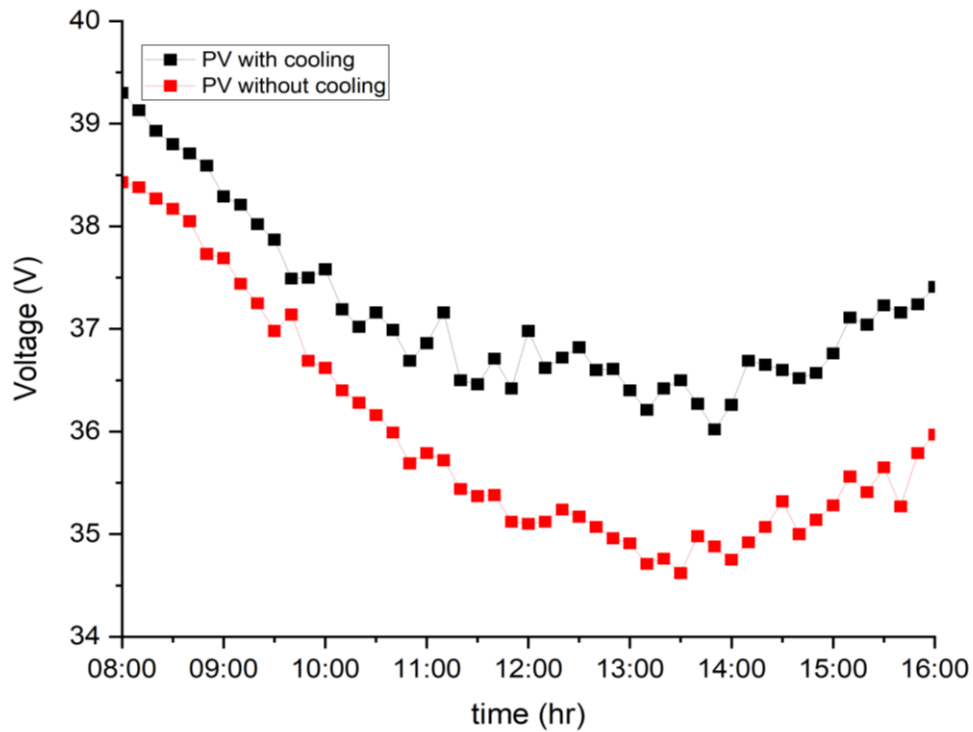
Figure 5.20. PV voltage with and without cooling at 0.111kg/s.

In Figure (5.21), a comparison of the rate power output of the two PV panels with and without cooling can be observed. The findings indicate that at 1:00 PM, the two panels had the highest output power, the PV panel with cooling producing 326.7W and the unit without cooling producing 314.5W. This confirms the effectiveness of the cooling technique, as the unit with cooling consistently produced higher output power throughout the experiment. It is worth noting that the output power showed an improvement rate of approximately 5%, which is expected as it depends on factors such as airspeed and surrounding temperature. Appendix (b) further compares the power output for different days, as shown in Figures (b 7) and (b 8).
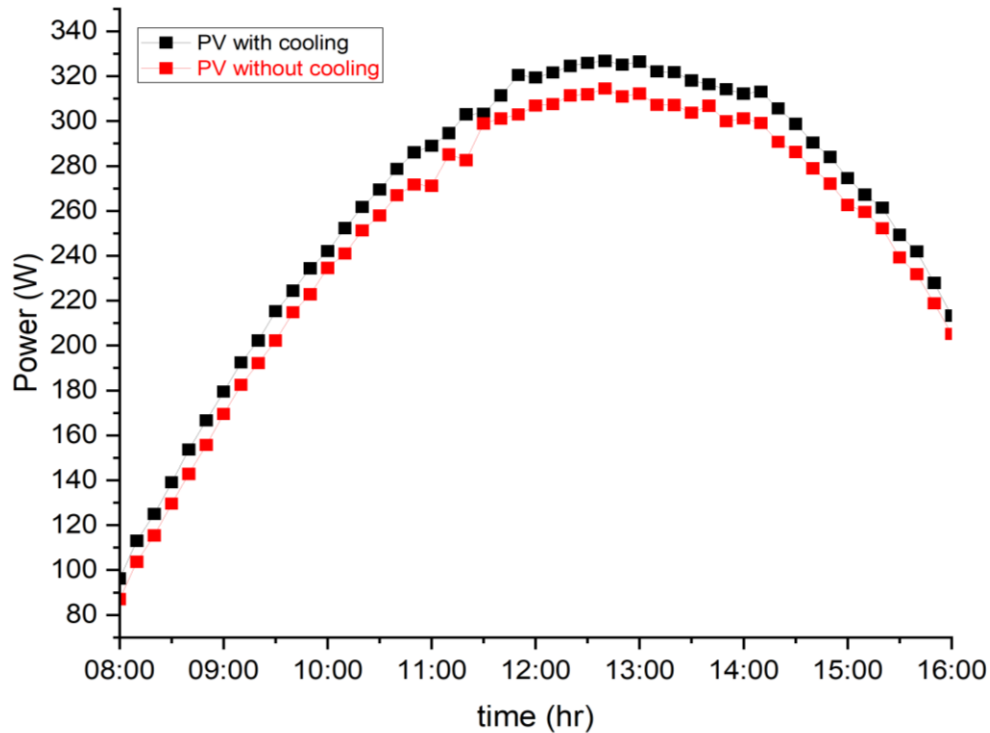
Figure 5.21. PV Power with and without cooling at 0.111kg/s.

A PV analyzer is used to compare the performance of photovoltaic panels with and without cooling as shown in Figure (5.22). The results are plotted in a graph, which showes the correlation between current, output power, and voltage. It is interesting to see how the addition of cooling affected the panels' performance and output. The data gathered from this experiment are useful in determining the best methods for optimizing solar energy production. See Figures (a 9-a 11) for more information.

Date Time : 2023-07-05 12:10:08
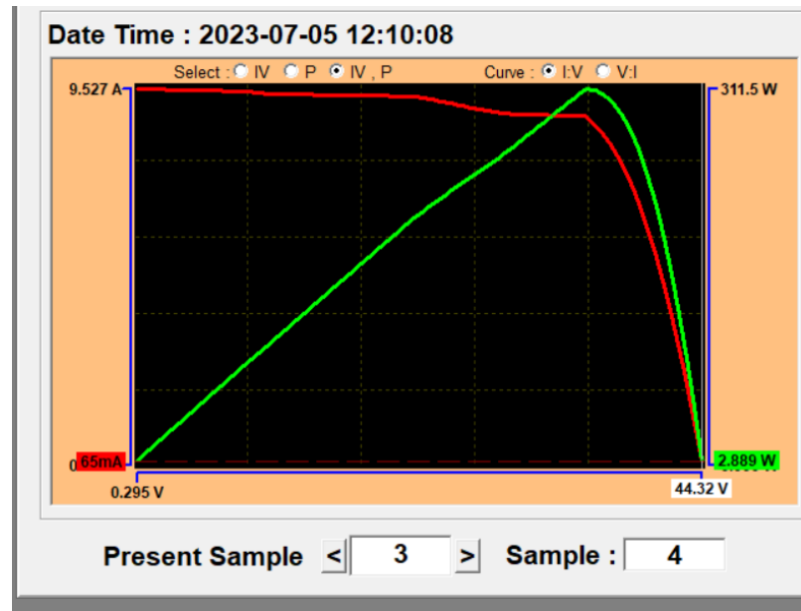
Figure 5.22. IV, P curve for PV analyzer.

In this study, the electrical efficiency of a photovoltaic panel is compared with and without cooling over a period of time as shown in Figure (5.23). The results showed that as temperatures increased due to higher solar radiation intensity, the performance of the panel decreased. Specifically, for every 10 °C increase in temperature, the electrical efficiency decreased by 0.8%. However, we have found that by implementing a cooling technique, the efficiency of the panel increased by 6.9% compared to the reference panel. The average electrical efficiency for panels with and without cooling is 17.63% and 16.9%, respectively. So, the maximum electrical efficiency of the photovoltaic panel with cooling is approximately 19%, gradually decreasing as the temperature increases over time. Despite this, the panel with cooling recorded a higher efficiency than the reference cell throughout the entire experimental period. This can be observed in the figure provided. These findings suggest that cooling can be an effective way to improve the efficiency of photovoltaic panels. You can also see Figures (b 15-b 17) in Appendix (b) for more information.
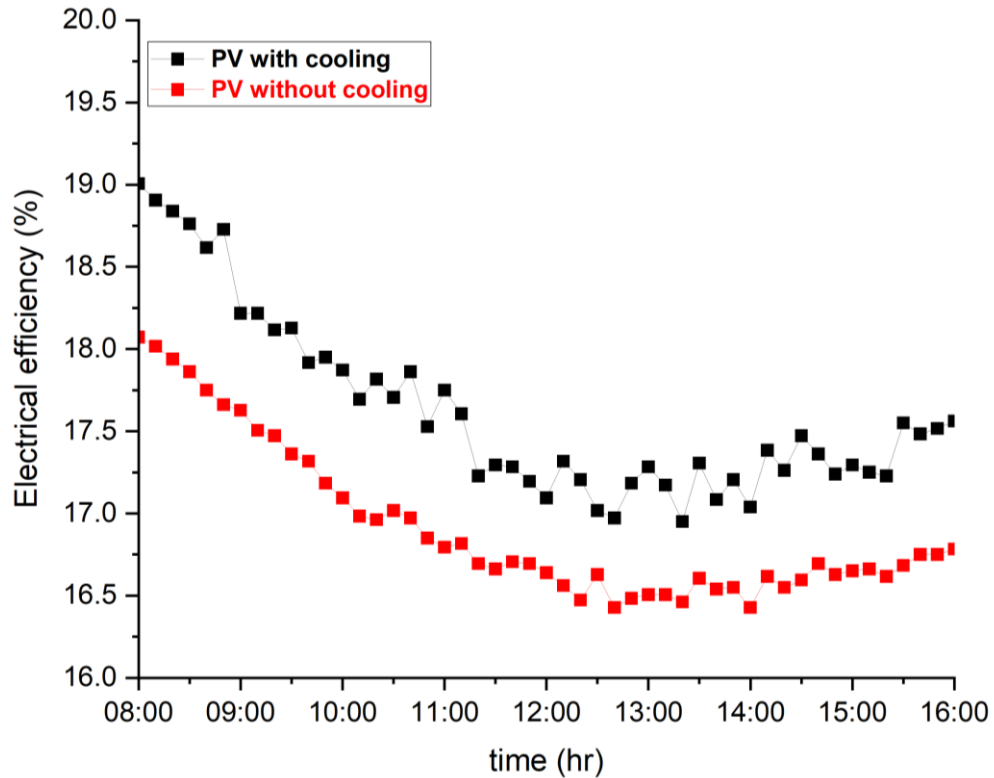
Figure 5.23. Electrical efficiency with and without cooling at 0.111kg/s.

5.6.3.2.   **Heat gain of PV/T system**

Figure (5.24) depicts the relationship between the change in heat gain and the change in solar radiation. Whereas the decrease in solar radiation causes a drop in temperature, where noted in the figure that the amount of thermal energy or heat gain is low. As noted at the beginning of the experiment, 61.9 W of heat is gained with a sun irradiance of 270.2 W/m2. It keeps rising as solar radiation intensity rises until it reaches its maximum of 378.6 W at 1192.14 W/m2 of solar radiation.
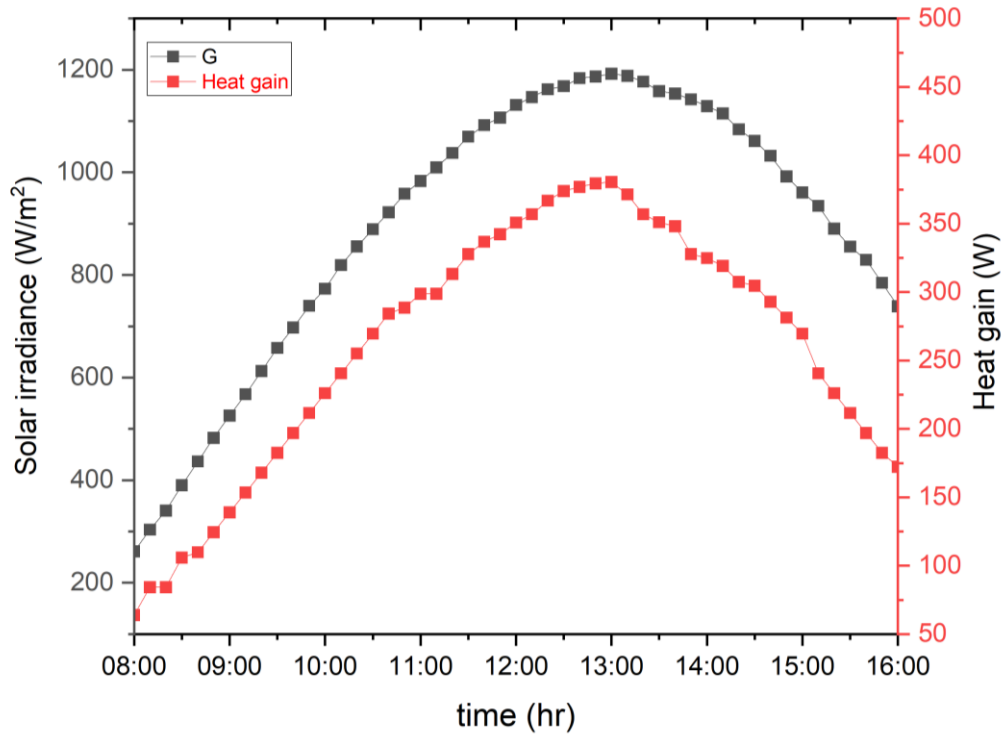
Figure 5.24. Heat gain and solar radiation at 0.111kg/s.

5.6.3.3. Thermal efficiency of PV/T

The thermal efficiency of the PV/T system can be seen in Figure (5.25). Where we can notice the change in heat efficiency with the change in the intensity of solar radiation. The results recorded throughout the experimental work show that with increasing solar radiation and ambient temperature, the temperature of the photovoltaic collector or panel increased. Thus, the thermal efficiency of the PV/T module increases, where the efficiency reaches a maximum rate of 20.6% at solar radiation of 1192.14 W/m^2. The thermal efficiency reached 29.57% at maximum radiation intensity of 1200 W/m^2. This information is displayed in Figure (a13) in Appendix (a).
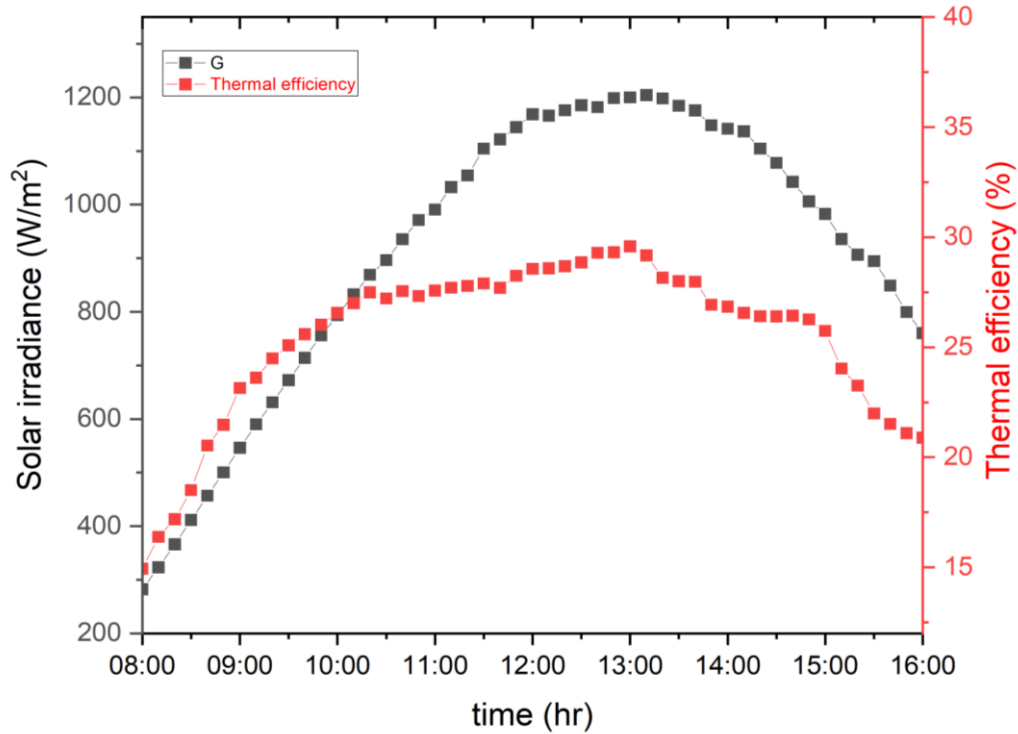
Figure 5.25. Thermal efficiency and solar radiation at 0.1111kg/s.

5.6.3.4.   Overall efficiency of PV/T

The overall efficiency of the PV/T module is depicted as time passes in Figure (5.26). The result that can be seen from the figure is that the overall efficiency rate is low at the beginning of the experimental work, reached 33.9%, and it continues to increase until it reaches its highest value at 1:00 pm 46.8%. At the end of the experiment, total efficiency declines due to reduced solar radiation and ambient temperature, resulting in lower electrical and thermal efficiency as the total efficiency results from these two efficiencies. Figures (a 14) and (a 15) in Appendix (a) display the total efficiency for several days of experimental work.
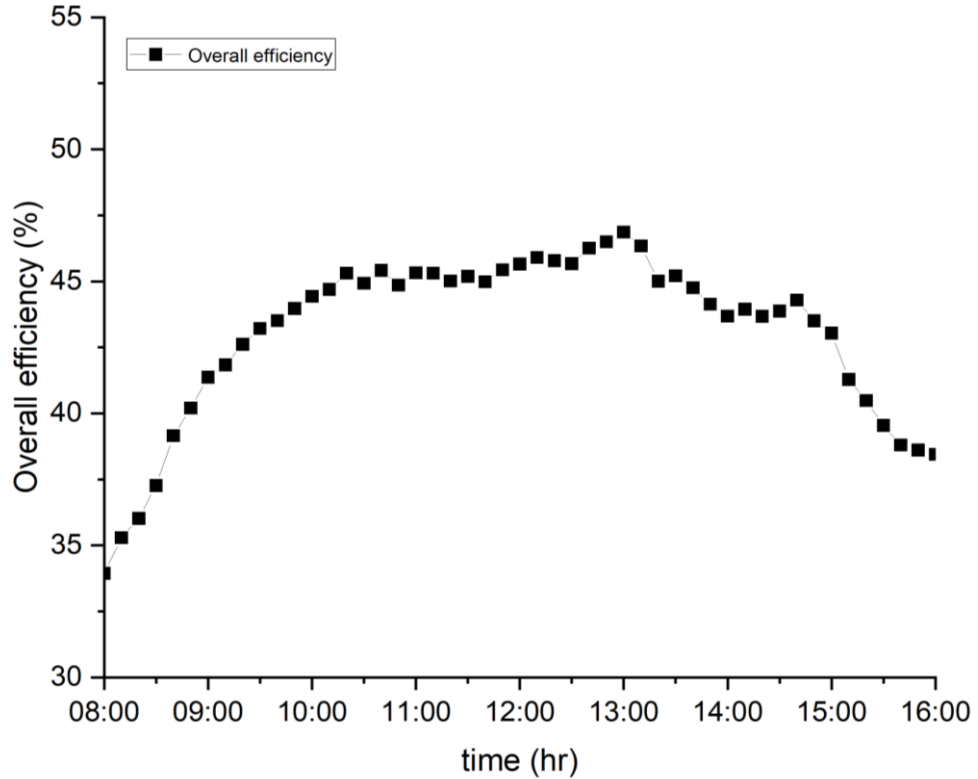
Figure 5.26. Overall efficiency of PV/T system at 0.111kg/s.

5.6.4. Experimental and Numerical Validation

It is very necessary to compare the results obtained through simulation with the results of experimental work to ensure the accuracy of the outcomes. Figure (5.27) shows a comparison of the electrical efficiency in the numerical analysis and the experimental work, where the efficiency rate in the simulation process was 17.53% and the electrical efficiency in the experimental work was 16.68%. The percentage difference between the experimental and numerical results is (4.8%). The maximum efficiency was initially reached by 19.4% and 18.5% respectively.
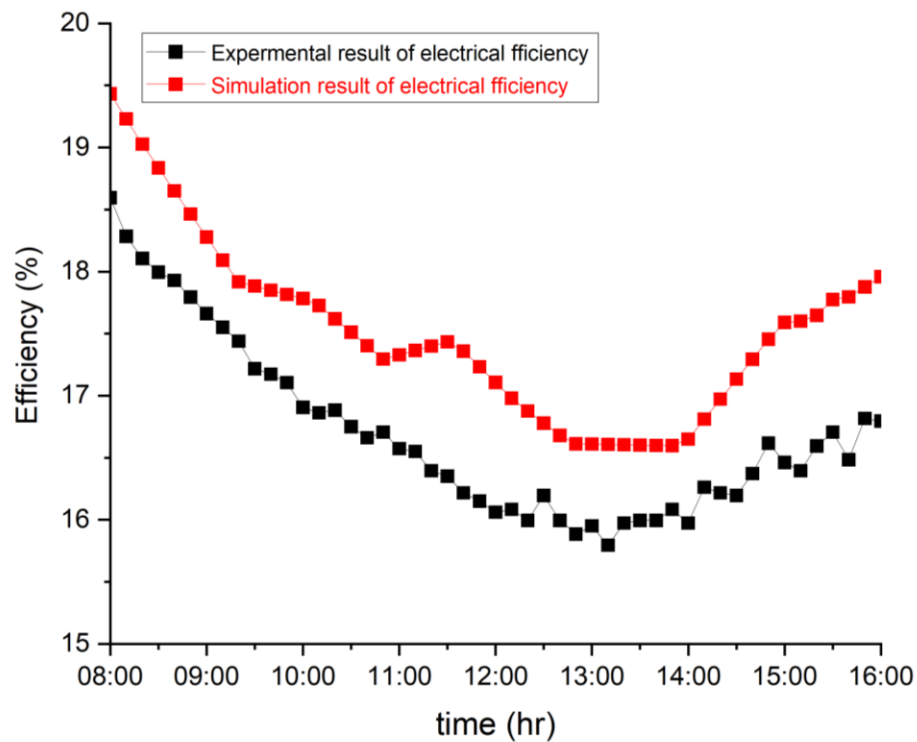
Figure 5.27. Comparison of electrical efficiency between simulation and

experimental work

5.6.5. Comparison of experimental results with a previous study

The findings were compared to one of the previous studies (41), as illustrated in Figure (5.28). The graph demonstrates a comparison between the electrical efficiency of the previous study and the current study, as well as its response to solar radiation. The results were so good, as the percentage difference between them was only 5.57%.
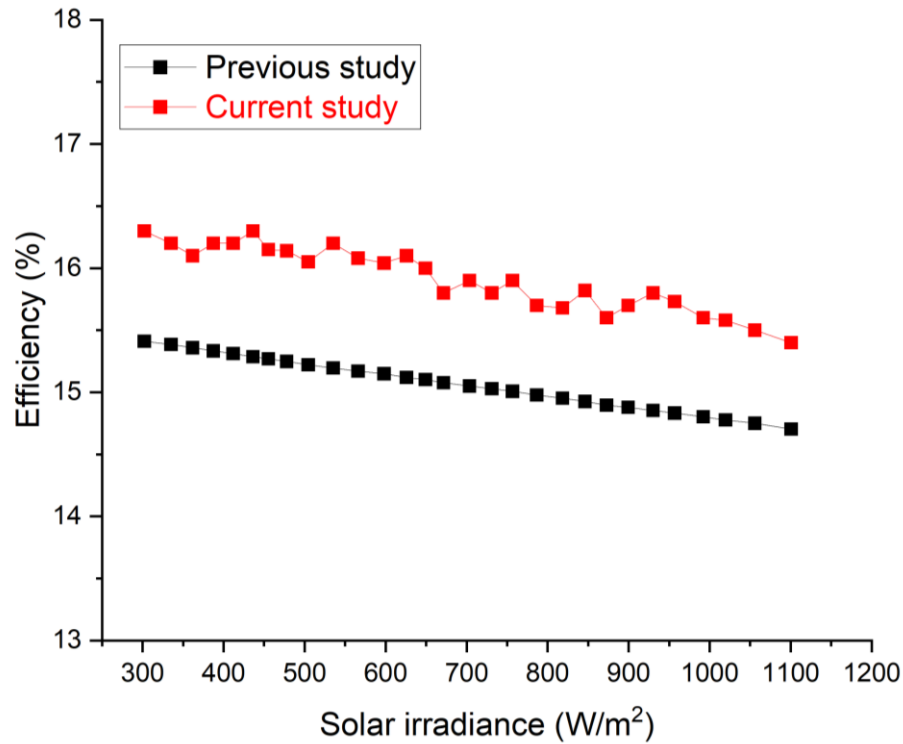
Figure 5.28. Comparison the efficiency with previous studies.

5.6.6. Power consumption of air fan

The operating temperature of photovoltaic panels decreases significantly by visiting the air conditioner. As a result of increased heat transfer between the base of the photovoltaic panel and the air passing through the porous medium inside the air duct. An increase in air speed means an increase in the power consumption required by the air intake fan, as in the Figure (5.29) . The amount of power consumed by the air fan with the air mass flow rate of the air, where at the highest air mass flow rate, 48.4 watts of power was consumed.
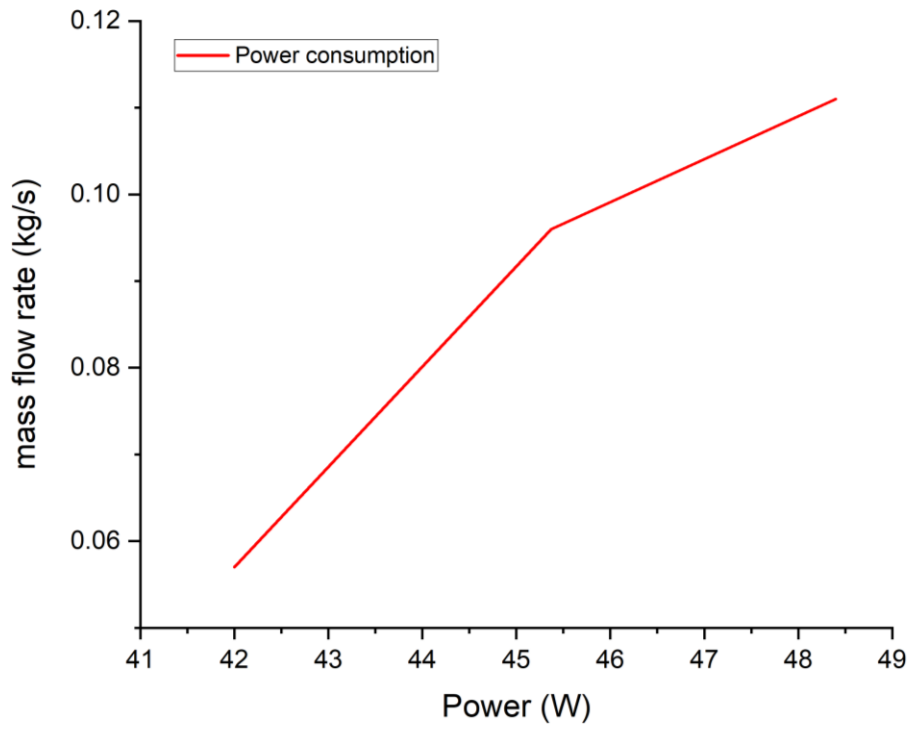
Figure 5.29. Power consumption of intake air fan.

CHAPTER SIX: CONCLUSIONS AND RECOMMENDATIONS

6.1.   INTRODUCTION

This study demonstrate the performance of the proposed PV panel cooling technique through the results of the theoretical and practical work that are obtained. The purpose of this study is to use porous metal media that contact with the base of the PV panel inside the air duct to increase the electrical and thermal efficiency of a Solar PV/T system. Experiments that proved that it is possible to reduce the working temperature of the photovoltaic module and improve its electrical and thermal performance are conducted at Al-Rumaitha Technical Institute / Al-Furat Al-Awsat Technical University/ Iraq (31°42′ - 45°12′).

6.2.   Conclusions

The conclusions of this study can be summarized according to the results obtained as follows:

1. Good agreement is obtained for the module simulation with previous studies, making it eligible for testing new PV module designs. Where the best results were obtained when using 14 ribs of porous metal.
2. Controlling the air mass flow rate is essential for enhancing the performance of the photovoltaic module and increasing its thermal and electrical efficiency. The optimal flow rate of 0.111 kg/s yielded the highest results.

3. The base temperature of the photovoltaic panel decreased by 17%, with the average temperature dropping from 56.9 °C to 49 °C at the highest air mass flow rate. This leads to a significant increase in electrical efficiency and output power.

4. After the cooling process, the PV/T system has an average electrical efficiency of 17.63%, with a maximum efficiency of 19% (compared to the nominal efficiency of the photovoltaic panel, which is 19.75%). This represents an improvement rate of 6.9%.

5. The maximum output power of the PV/T system after cooling is 330.7W, compared to 314W for the PV module without cooling. This translates to a net gain of 16 W and an improvement rate in output power of 5%.

6. The maximum heat gain from the PV/T system for several different days of the year, for example 701.6 W for 27th June, 2023 at the highest air mass flow rate 0.111kg/s , 380.35 W for 24th June 2023 at the mass flow rate 0.057kg/s and 414.45 W for 26th June 2023 at the mass flow rate 0.096.

7. The PV/T system achieved a maximum thermal efficiency of 29.57% by using porous metal media inside the air duct. This was due to the temperature difference of 6.25 between the air entering and leaving the airway.

6.3. Recommendations

The current study deals with enhancing the electrical and thermal efficiency of photovoltaic panels for a PV/T system using porous metal media placed inside the air duct and connected to the base of the photovoltaic panel. In addition, there are many future recommendations for this study:

1. The hot air generated from the PV/T module can be drawn and utilized in various applications.

2. Controlling the air fan speed by using a temperature sensor to reduce and increase the fan speed and turn it off when the photovoltaic module reaches a certain temperature to reduce energy consumption.

3. The air can be pre-cooled by using water and applied to the back surface of the PV panel to ensure better cooling results.

4. In addition to cooling the back surface of the photovoltaic panel with air, spraying water droplets on the front surface of the PV cell can ensure better cooling and clean the surface from dust.

5. Use a suitable phase change material to extract heat from the back surface of the photovoltaic cell.

REFERENCE

[1]   M. Guermoui, F. Melgani, and C. Danilo, "Multi-step ahead forecasting of daily global and direct solar radiation: A review and case study of Ghardaia region," *J. Clean. Prod.*, vol. 201, pp. 716–734, 2018, doi: 10.1016/j.jclepro.2018.08.006.

[2]   S. Siah Chehreh Ghadikolaei, "Solar photovoltaic cells performance improvement by cooling technology: An overall review," *Int. J. Hydrogen Energy*, vol. 46, no. 18, pp. 10939–10972, 2021, doi: 10.1016/j.ijhydene.2020.12.164.

[3]   I. Ahmed Hasan, I. Saleh kareem, and D. Adil Attar, "Effect of Evaporative Cooling Combined with Heat Sink on PV Module Performance," *J. Univ. Babylon Eng. Sci.*, vol. 27, no. 2, pp. 252–264, 2019, doi: 10.29196/jubes.v27i2.2345.

[4]   K. Yang and C. Zuo, "A novel multi-layer manifold microchannel cooling system for concentrating photovoltaic cells," *Energy Convers. Manag.*, vol. 89, pp. 214–221, 2015, doi: 10.1016/j.enconman.2014.09.046.

[5]   P. Mohanty, T. Muneer, E. J. Gago, and Y. Kotak, *Solar radiation fundamentals and PV system components*, vol. 196. 2016. doi: 10.1007/978-3-319-14663-8_2.

[6]   S. Yilmaz, H. R. Ozcalik, S. Kesler, F. Dincer, and B. Yelmen, "The analysis of different PV power systems for the determination of optimal PV panels and system installation - A case study in Kahramanmaras, Turkey," *Renew. Sustain. Energy Rev.*, vol. 52, pp. 1015–1024, 2015, doi: 10.1016/j.rser.2015.07.146.

[7]   A. H. A. A. H. A. Kazem, *Photovoltaic / Thermal (PV / T) Systems*.

[8]   N. Sebastian, "Limiting approach to generalized gamma bessel model via fractional calculus and its applications in various disciplines," *Axioms*, vol. 4, no. 3, pp. 385–399, 2015, doi: 10.3390/axioms4030385.

[9]   P. Gonçalves, V. Sampaio, M. Orestes, and A. González, "Photovoltaic solar energy : Conceptual framework," vol. 74, no. February, pp. 590–601, 2017, doi: 10.1016/j.rser.2017.02.081.

[10]   A. A. Rockett, "The future of energy – Photovoltaics," vol. 14, pp. 117–122, 2010, doi: 10.1016/j.cossms.2010.09.003.

[11]   Malek Kamal Hussien Rabaia, Mohammad Ali Abdelkareem, Enas Taha Sayed, Khaled Elsaid, Kyu-Jung Chae, Tabbi Wilberforce, A.G. Olabi,

"Science of the Total Environment Environmental impacts of solar energy systems : A review," *Sci. Total Environ.*, vol. 754, p. 141989, 2021, doi: 10.1016/j.scitotenv.2020.141989.

[12] S. A. Nada, D. H. El-nagar, and H. M. S. Hussein, "Improving the thermal regulation and e ffi ciency enhancement of PCM- Integrated PV modules using nano particles," *Energy Convers. Manag.*, vol. 166, no. April, pp. 735–743, 2018, doi: 10.1016/j.enconman.2018.04.035.

[13] H. Najafi and K. A. Woodbury, "Optimization of a cooling system based on Peltier effect for photovoltaic cells," *Sol. Energy*, vol. 91, pp. 152–160, 2013, doi: 10.1016/j.solener.2013.01.026.

[14] J. G. Hernandez-Perez, J. G. Carrillo, A. Bassam, M. Flota-Banuelos, and L. D. Patino-Lopez, "A new passive PV heatsink design to reduce efficiency losses: A computational and experimental evaluation," *Renew. Energy*, vol. 147, pp. 1209–1220, 2020, doi: 10.1016/j.renene.2019.09.088.

[15] M. Tahmasbi, M. Siavashi, and A. Mohammad, "Thermal and electrical ef fi ciencies enhancement of a solar photovoltaic- thermal / air system (PVT / air) using metal foams," *J. Taiwan Inst. Chem. Eng.*, vol. 000, pp. 1–14, 2021, doi: 10.1016/j.jtice.2021.03.045.

[16] H. G. Teo, P. S. Lee, and M. N. A. Hawlader, "An active cooling system for photovoltaic modules," *Appl. Energy*, vol. 90, no. 1, pp. 309–315, 2012, doi: 10.1016/j.apenergy.2011.01.017.

[17] M. S. Abd-Elhady, M. M. Fouad, and T. Khalil, "Improving the efficiency of photovoltaic (PV) panels by oil coating," *Energy Convers. Manag.*, vol. 115, pp. 1–7, May 2016, doi: 10.1016/j.enconman.2016.02.040.

[18] T. Nehari, M. Benlakam, and D. Nehari, "Effect of the fins length for the passive cooling of the photovoltaic panels," *Period. Polytech. Mech. Eng.*, vol. 60, no. 2, pp. 89–95, 2016, doi: 10.3311/PPme.8571.

[19] B. Zhao, M. Hu, X. Ao, Q. Xuan, and G. Pei, "Spectrally selective approaches for passive cooling of solar cells: A review," *Appl. Energy*, vol. 262, no. October 2019, p. 114548, 2020, doi: 10.1016/j.apenergy.2020.114548.

[20] Xiao Ren, Jing Li, Mingke Hu, Gang Pei, Dongsheng Jiao, Xudong Zhao, Jie Ji, "Feasibility of an innovative amorphous silicon photovoltaic/thermal system for medium temperature applications," *Appl. Energy*, vol. 252, no. May, p. 113427, 2019, doi: 10.1016/j.apenergy.2019.113427.

[21] Min Yu, Fucheng Chen, Siming Zheng, Jinzhi Zhou, Xudong Zhao,

Zhangyuan Wang, Guiqiang Li, Jing Li, Yi Fan, Jie Ji, Theirno M.O. Diallo, David Hardy, "Experimental Investigation of a Novel Solar Micro-Channel Loop-Heat-Pipe Photovoltaic/Thermal (MC-LHP-PV/T) System for Heat and Power Generation," *Appl. Energy*, vol. 256, no. April, p. 113929, 2019, doi: 10.1016/j.apenergy.2019.113929.

[22] Z. Arifin, D. D. D. P. Tjahjana, S. Hadi, R. A. Rachmanto, G. Setyohandoko, and B. Sutanto, "Numerical and experimental investigation of air cooling for photovoltaic panels using aluminum heat sinks," *Int. J. Photoenergy*, vol. 2020, 2020, doi: 10.1155/2020/1574274.

[23] K. K. Dixit, I. Yadav, G. K. Gupta, and S. K. Maurya, "A Review on Cooling Techniques Used for Photovoltaic Panels," *2020 Int. Conf. Power Electron. IoT Appl. Renew. Energy its Control. PARC 2020*, pp. 360–364, 2020, doi: 10.1109/PARC49193.2020.236626.

[24] Y. S. Bijjargi, S. S. Kale, and K. A. Shaikh, "Cooling techniques for photovoltaic module for improving its conversion efficiency: A review," *Int. J. Mech. Eng. Technol.*, vol. 7, no. 4, pp. 22–28, 2016.

[25] H. Bahaidarah, A. Subhan, P. Gandhidasan, and S. Rehman, "Performance evaluation of a PV (photovoltaic) module by back surface water cooling for hot climatic conditions," *Energy*, vol. 59, pp. 445–453, 2013, doi: 10.1016/j.energy.2013.07.050.

[26] U. Sajjad, M. Amer, H. M. Ali, A. Dahiya, and N. Abbas, "Cost effective cooling of photovoltaic modules to improve efficiency," *Case Stud. Therm. Eng.*, vol. 14, no. January, p. 100420, 2019, doi: 10.1016/j.csite.2019.100420.

[27] R. Mazón-Hernández, J. R. García-Cascales, F. Vera-García, A. S. Káiser, and B. Zamora, "Improving the electrical parameters of a photovoltaic panel by means of an induced or forced air stream," *Int. J. Photoenergy*, vol. 2013, 2013, doi: 10.1155/2013/830968.

[28] S. Golzari, A. Kasaeian, M. Amidpour, S. Nasirivatan, and S. Mousavi, "Experimental investigation of the effects of corona wind on the performance of an air-cooled PV/T," *Renew. Energy*, vol. 127, pp. 284–297, 2018, doi: 10.1016/j.renene.2018.04.029.

[29] W. K. Hussam, A. Alfeeli, and G. J. Sheard, "Efficiency Enhancement of Photovoltaic Panels Using an Optimised Air Cooled Heat Sink," *Int. J. Energy Power Eng.*, vol. 14, no. 7, pp. 196–202, 2020.

[30] A. M. Elbreki, A. F. Muftah, K. Sopian, H. Jarimi, A. Fazlizan, and A. Ibrahim, "Experimental and economic analysis of passive cooling PV module

using fins and planar reflector," *Case Stud. Therm. Eng.*, vol. 23, no. December 2020, p. 100801, 2021, doi: 10.1016/j.csite.2020.100801.

[31] F. Bayrak, H. F. Oztop, and F. Selimefendigil, "Effects of different fin parameters on temperature and efficiency for cooling of photovoltaic panels under natural convection," *Sol. Energy*, vol. 188, no. June, pp. 484–494, 2019, doi: 10.1016/j.solener.2019.06.036.

[32] A. A. raheim Amr, A. A. M. Hassan, M. Abdel-Salam, and A. H. M. El-Sayed, "Enhancement of photovoltaic system performance via passive cooling: Theory versus experiment," *Renew. Energy*, vol. 140, pp. 88–103, 2019, doi: 10.1016/j.renene.2019.03.048.

[33] Ahmad El Mays, Rami Ammar, Mohamad Hawa, Mohamad Abou Akroush, Farouk Hachem, Mahmoud Khaled, and Mohamad Ramadan, "Improving Photovoltaic Panel Using Finned Plate of Aluminum," *Energy Procedia*, vol. 119, pp. 812–817, 2017, doi: 10.1016/j.egypro.2017.07.103.

[34] W. Pang, Y. Liu, S. Shao, and X. Gao, "Empirical study on thermal performance through separating impacts from a hybrid PV/TE system design integrating heat sink," *Int. Commun. Heat Mass Transf.*, vol. 60, pp. 9–12, 2015, doi: 10.1016/j.icheatmasstransfer.2014.11.004.

[35] X. Yu, J. Feng, Q. Feng, and Q. Wang, "Development of a plate-pin fin heat sink and its performance comparisons with a plate fin heat sink," *Appl. Therm. Eng.*, vol. 25, no. 2–3, pp. 173–182, 2005, doi: 10.1016/j.applthermaleng.2004.06.016.

[36] J. K. Tonui and Y. Tripanagnostopoulos, "Air-cooled PV/T solar collectors with low cost performance improvements," *Sol. Energy*, vol. 81, no. 4, pp. 498–511, 2007, doi: 10.1016/j.solener.2006.08.002.

[37] Y. Tripanagnostopoulos and P. Themelis, "Natural flow air cooled photovoltaics," *AIP Conf. Proc.*, vol. 1203, pp. 1013–1018, 2010, doi: 10.1063/1.3322300.

[38] K. Egab, A. Okab, H. S. Dywan, and S. K. Oudah, "Enhancing a solar panel cooling system using an air heat sink with different fin configurations," *IOP Conf. Ser. Mater. Sci. Eng.*, vol. 671, no. 1, 2020, doi: 10.1088/1757-899X/671/1/012133.

[39] C. G. Popovici, S. V. Hudişteanu, T. D. Mateescu, and N. C. Chereches, "Efficiency Improvement of Photovoltaic Panels by Using Air Cooled Heat Sinks," *Energy Procedia*, vol. 85, no. November 2015, pp. 425–432, 2016, doi: 10.1016/j.egypro.2015.12.223.

[40] S. V. Hudișteanu, F. E. Țurcanu, N. C. Chereches, C. G. Popovici, M. Verdeș, and I. Huditeanu, "Enhancement of pv panel power production by passive cooling using heat sinks with perforated fins," *Appl. Sci.*, vol. 11, no. 23, 2021, doi: 10.3390/app112311323.

[41] Y. Abudllah, Z. Arifin, D. Danardono Dwi Prija Tjahjana, S. Suyitno, and M. R. Aulia Putra, "Analysis of the Copper and Aluminum Heat Sinks Addition to the Performance of Photovoltaic Panels with CFD Modelling," *Proceeding - 1st Int. Conf. Inf. Technol. Adv. Mech. Electr. Eng. ICITAMEE 2020*, pp. 41–45, 2020, doi: 10.1109/ICITAMEE50454.2020.9398314.

[42] F. Grubišić-Čabo, S. Nižetić, D. Čoko, I. Marinić Kragić, and A. Papadopoulos, "Experimental investigation of the passive cooled free-standing photovoltaic panel with fixed aluminum fins on the backside surface," *J. Clean. Prod.*, vol. 176, pp. 119–129, 2018, doi: 10.1016/j.jclepro.2017.12.149.

[43] E. Scharifi, A. Danilenko, U. Weidig, and K. Steinhoff, "Influence of plastic deformation gradients at room temperature on precipitation kinetics and mechanical properties of high- strength aluminum alloys," *J. Eng. Res. Appl.*, vol. 9, no. 1, pp. 24–29, 2019, doi: 10.9790/9622.

[44] M. Shata, W. .Aboelsoud, and M. I. Marei, "Experimental Investigation of the Photovoltaic Performance Using Porous Media based Cooling System," *Eng. Res. J. - Fac. Eng.*, vol. 46, no. 1, pp. 39–42, 2020, doi: 10.21608/erjsh.2020.229908.

[45] J. Kim, S. Bae, Y. Yu, and Y. Nam, "Experimental and numerical study on the cooling performance of fins and metal mesh attached on a photovoltaic module," *Energies*, vol. 13, no. 1, pp. 1–12, 2019, doi: 10.3390/en13010085.

[46] R. Kansara, M. Pathak, and V. K. Patel, "Performance assessment of flat-plate solar collector with internal fins and porous media through an integrated approach of CFD and experimentation," *Int. J. Therm. Sci.*, vol. 165, no. March, p. 106932, 2021, doi: 10.1016/j.ijthermalsci.2021.106932.

[47] F. Selimefendigil, F. Bayrak, and H. F. Oztop, "Experimental analysis and dynamic modeling of a photovoltaic module with porous fins," *Renew. Energy*, vol. 125, pp. 193–205, 2018, doi: 10.1016/j.renene.2018.02.002.

[48] S. M. Kiwan and A. M. Khlefat, "Thermal cooling of photovoltaic panels using porous material," *Case Stud. Therm. Eng.*, vol. 24, no. October 2020, p. 100837, 2021, doi: 10.1016/j.csite.2020.100837.

[49] D. J. Hasan and A. A. Farhan, "Enhancing the efficiency of photovoltaic

panel using open-cell copper metal foam fins," *Int. J. Renew. Energy Res.*, vol. 9, no. 4, pp. 1849–1855, 2019, doi: 10.20508/ijrer.v9i4.10116.g7789.

[50] N. A. S. Elminshawy, A. M. I. Mohamed, K. Morad, Y. Elhenawy, and A. A. Alrobaian, "Performance of PV panel coupled with geothermal air cooling system subjected to hot climatic," *Appl. Therm. Eng.*, vol. 148, no. November 2018, pp. 1–9, 2019, doi: 10.1016/j.applthermaleng.2018.11.027.

[51] P. Dwivedi, K. Sudhakar, A. Soni, E. Solomin, and I. Kirpichnikova, "Advanced cooling techniques of P.V. modules: A state of art," *Case Stud. Therm. Eng.*, vol. 21, no. December 2019, p. 100674, 2020, doi: 10.1016/j.csite.2020.100674.

[52] J. Kim and Y. Nam, "Study on the cooling effect of attached fins on PV using CFD simulation," *Energies*, vol. 12, no. 4, 2019, doi: 10.3390/en12040758.

[53] E. Skoplaki and J. A. Palyvos, "On the temperature dependence of photovoltaic module electrical performance: A review of efficiency/power correlations," *Sol. Energy*, vol. 83, no. 5, pp. 614–624, 2009, doi: 10.1016/j.solener.2008.10.008.

[54] H. ZONDAG, "Flat-plate PV-Thermal collectors and systems: A review," *Renew. Sustain. Energy Rev.*, vol. 12, no. 4, pp. 891–959, 2008, doi: 10.1016/j.rser.2005.12.012.

[55] G. Notton, C. Cristofari, M. Mattei, and P. Poggi, "Modelling of a double-glass photovoltaic module using finite differences," *Appl. Therm. Eng.*, vol. 25, no. 17–18, pp. 2854–2877, 2005, doi: 10.1016/j.applthermaleng.2005.02.008.

[56] S. Dubey, G. S. Sandhu, and G. N. Tiwari, "Analytical expression for electrical efficiency of PV/T hybrid air collector," *Appl. Energy*, vol. 86, no. 5, pp. 697–705, 2009, doi: 10.1016/j.apenergy.2008.09.003.

[57] Y. W. Koholé and G. Tchuen, "Experimental and numerical investigation of a thermosyphon solar water heater," *Int. J. Ambient Energy*, vol. 41, no. 4, pp. 384–394, 2020, doi: 10.1080/01430750.2018.1472641.

APPENDIXES

Apendix (a): Thermal and electrical characteristic diagrams for PV and PV/T
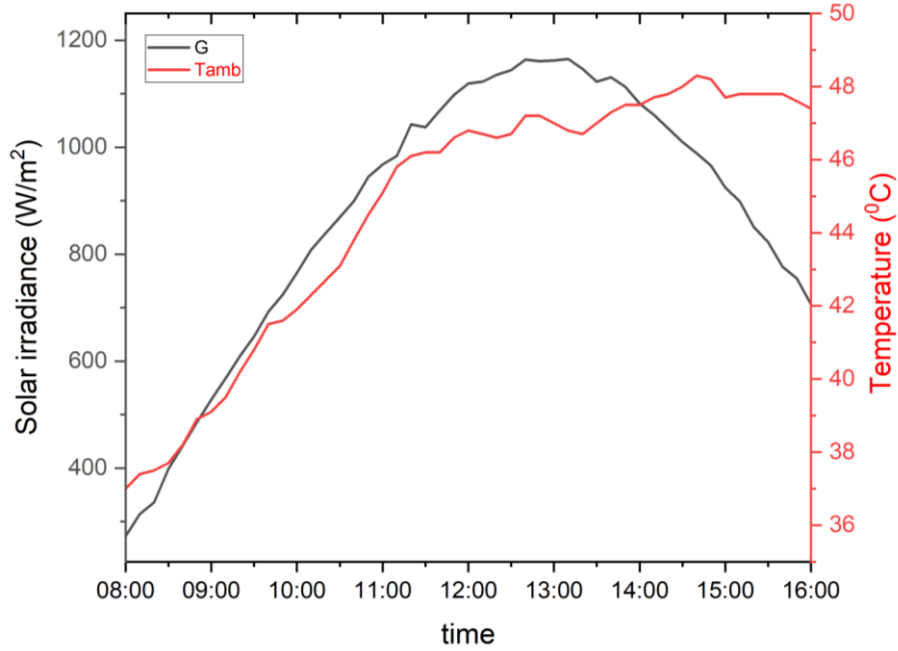
Figure a 1. Variations ambient temperature and solar radiation 24th June 2023.
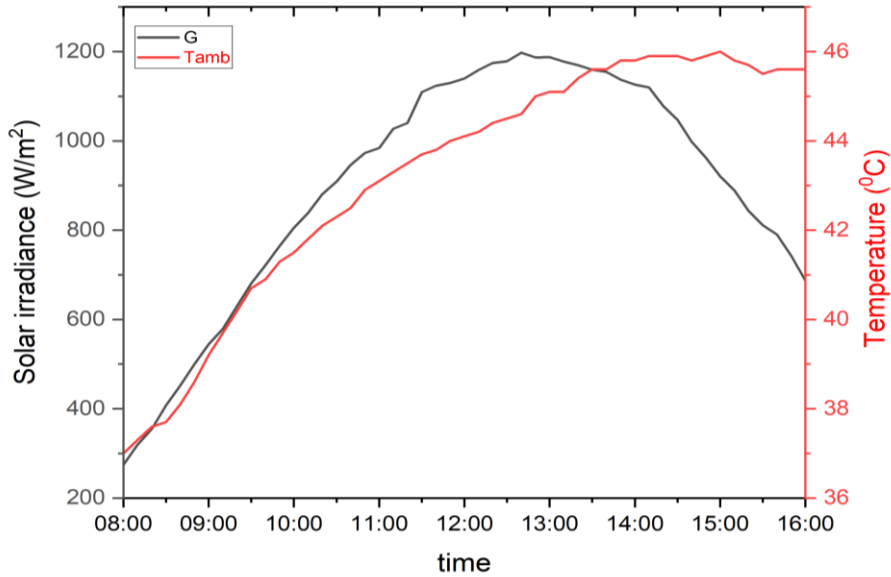
Figure a 2. Variations ambient temperature and solar radiation 26th June 2023.
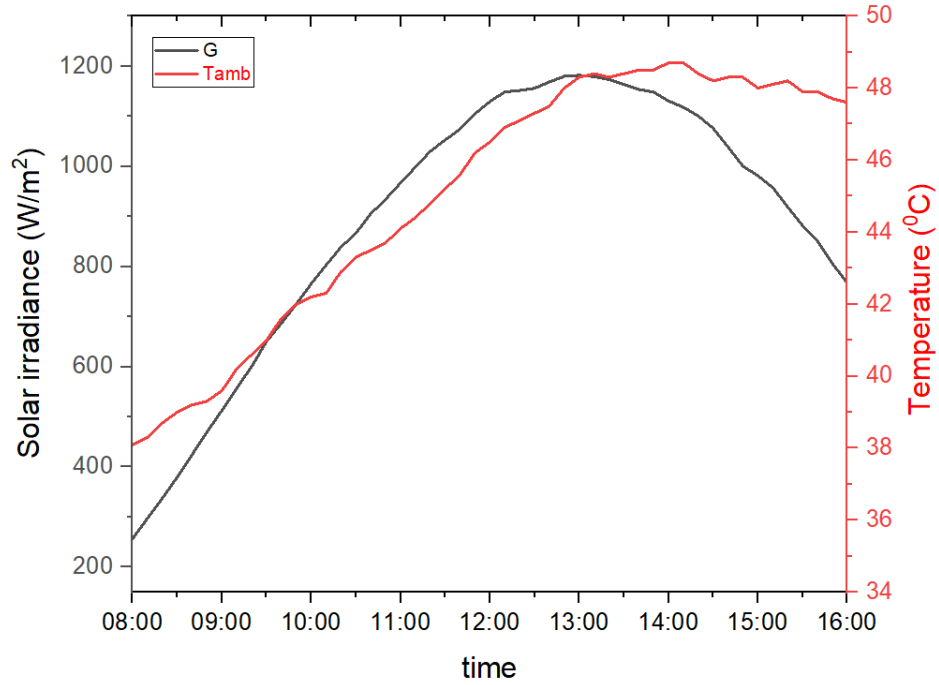
Figure a 3. Variations ambient temperature and solar radiation 7th July 2023.
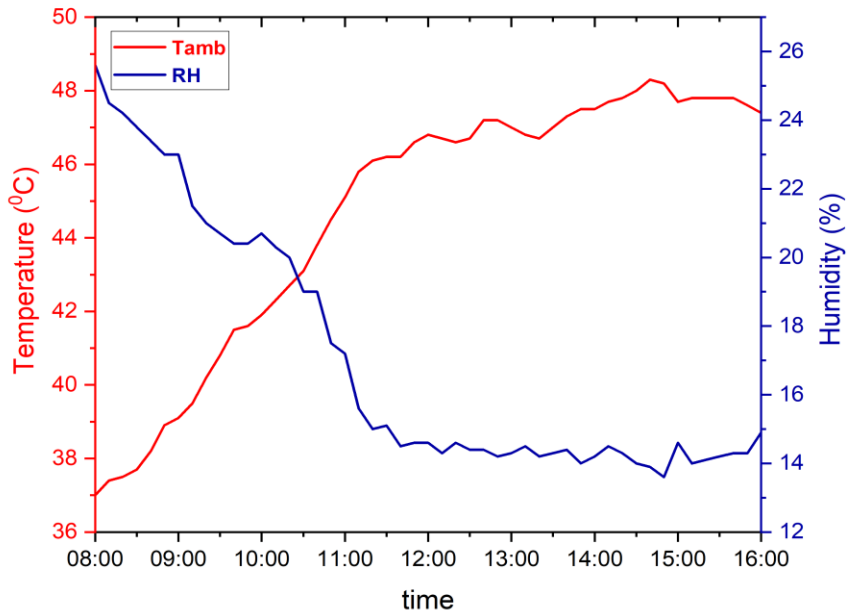
Figure a 4. Relative humidity and ambient temperature 26th June 2023.
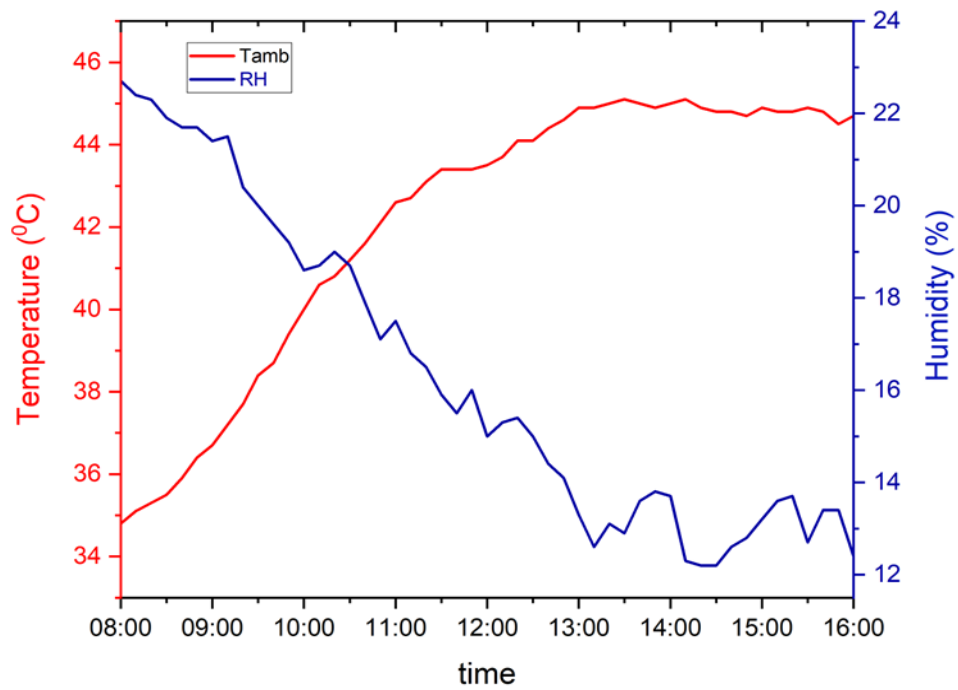
Figure a 5. Relative humidity and ambient temperature 27th June 2023.
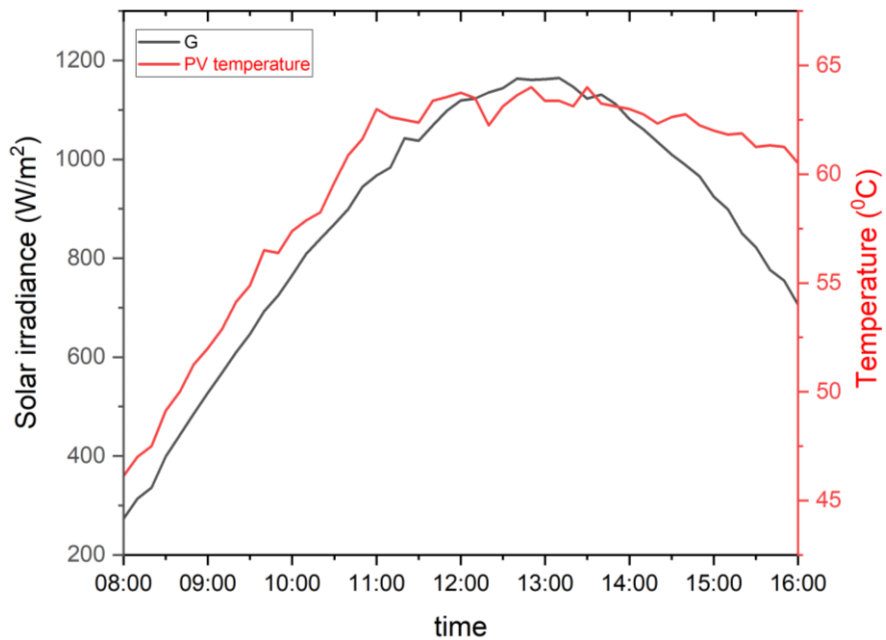
Figure a 6. PV module temperature and solar radiation 24th June 2023.
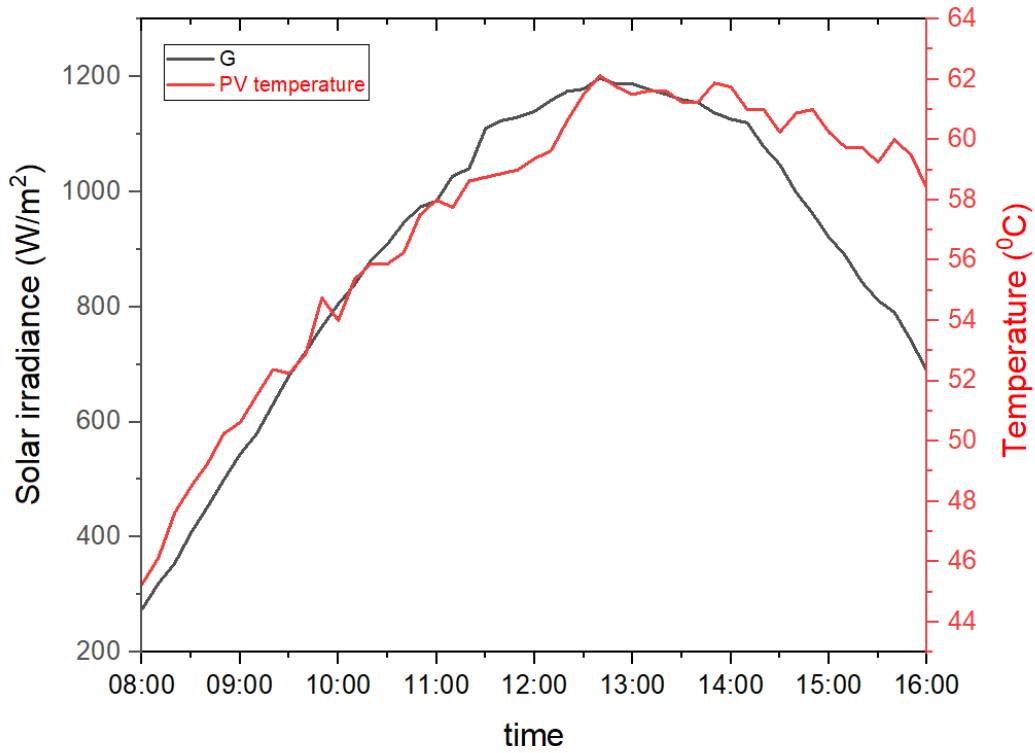
Figure a 7. PV module temperature and solar radiation 26th June 2023.
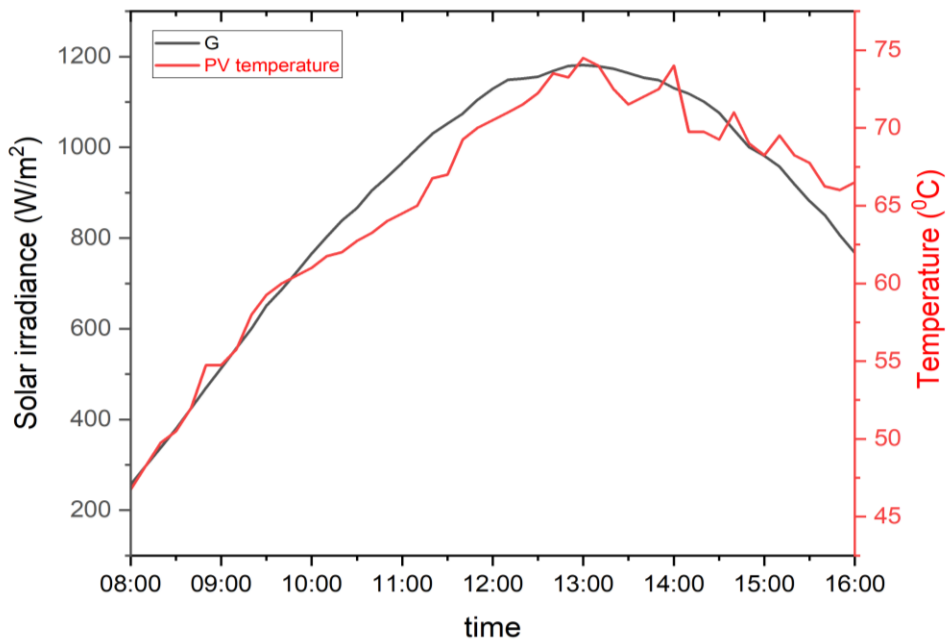
Figure a 8. PV module temperature and solar radiation 7th July.
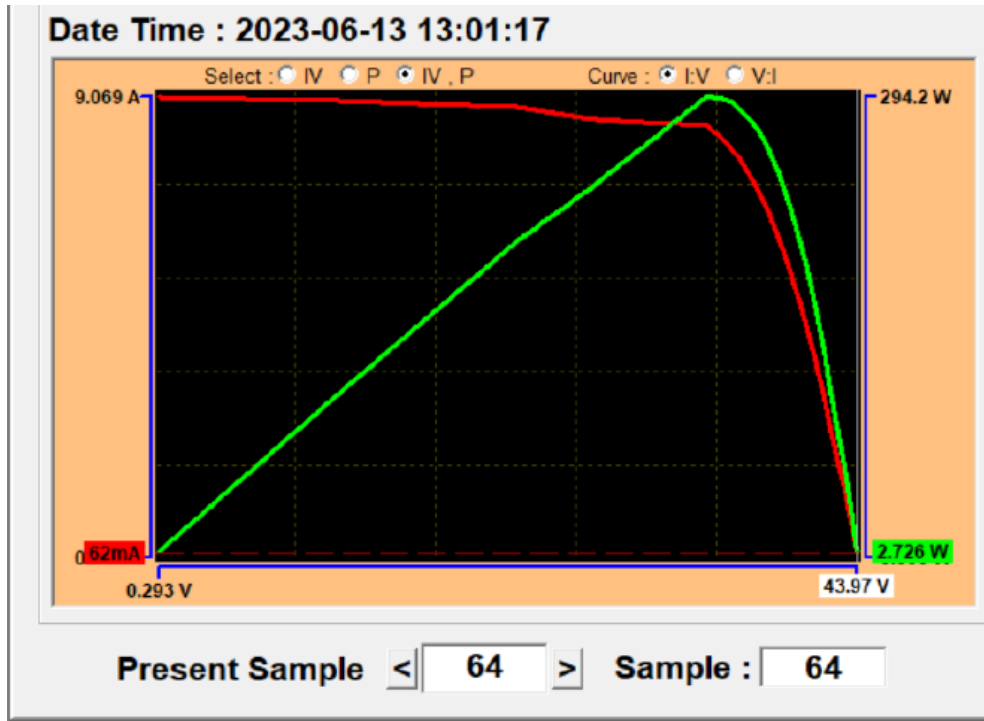
Figure a 9. IV, P curve for PV analyzer.
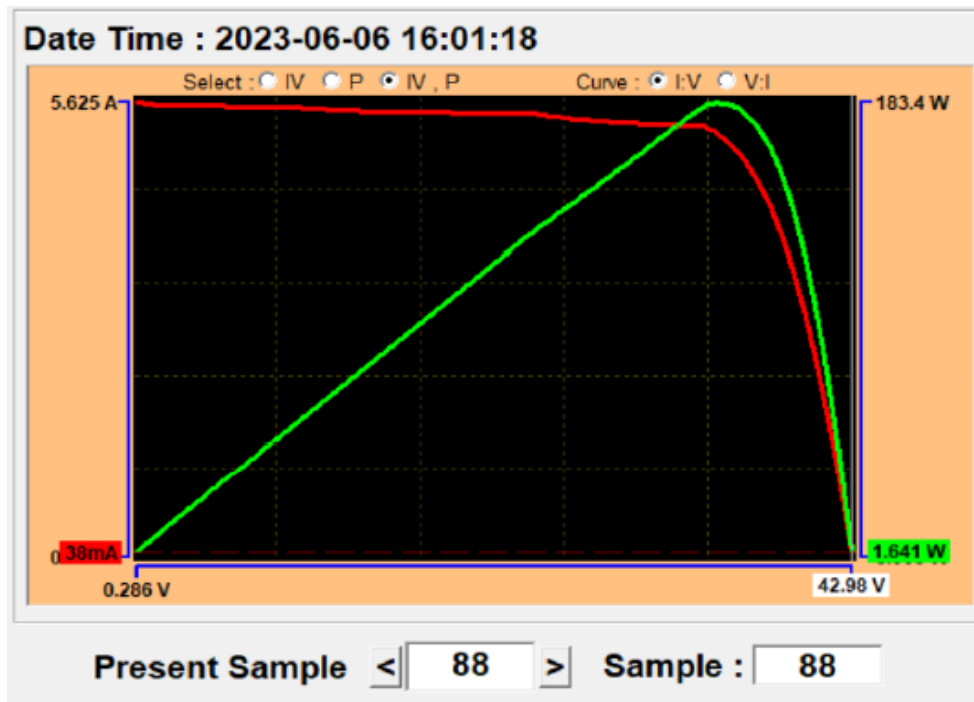
Figure a 10. IV, P curve for PV analyzer.
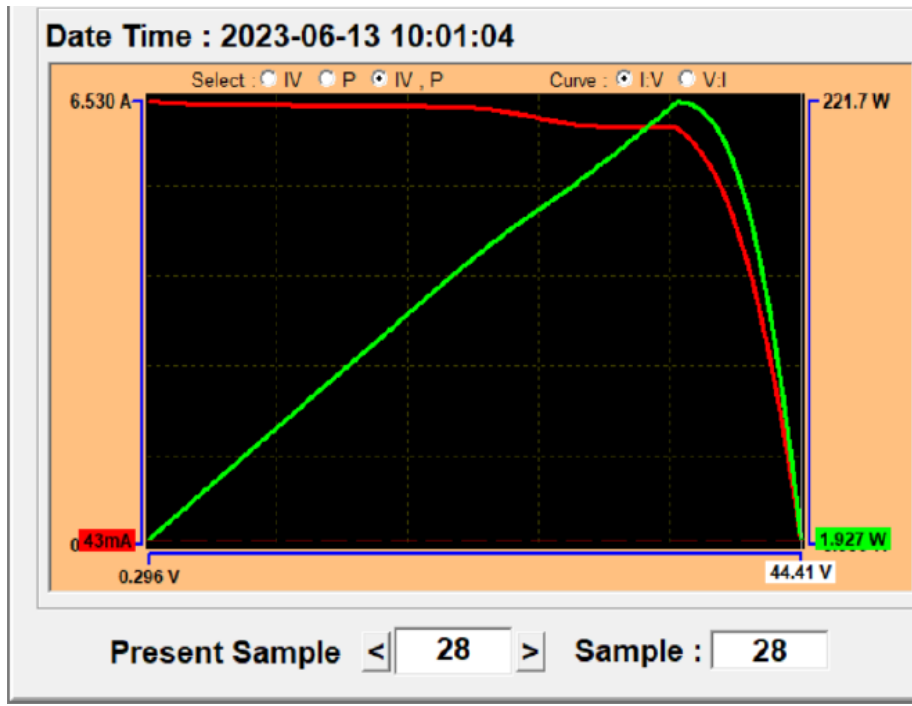
Figure a 11. IV, P curve for PV analyzer.
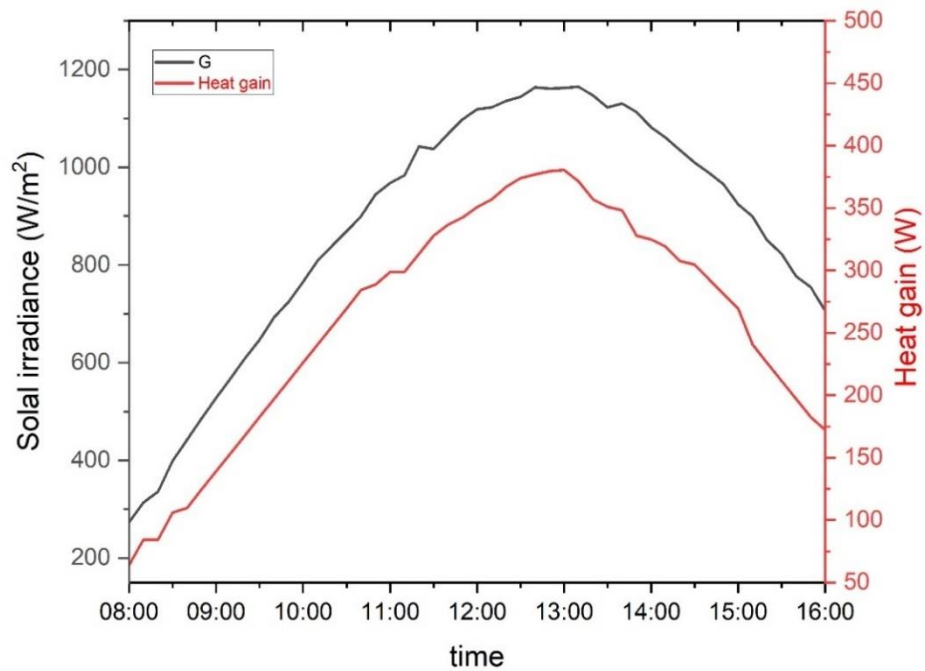
Figure a 12. Heat gain and solar radiation 26th June 2023.
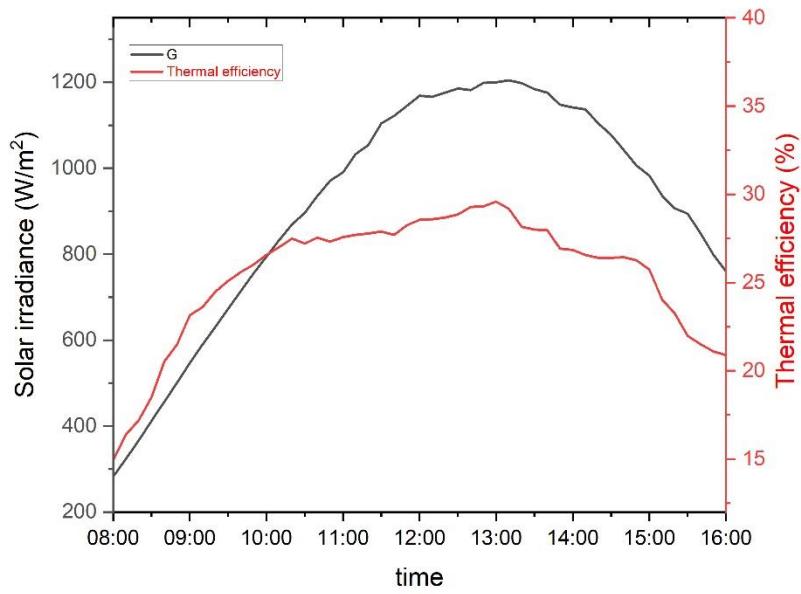
Figure a 13. Thermal efficiency and solar radiation 27th June 2023.
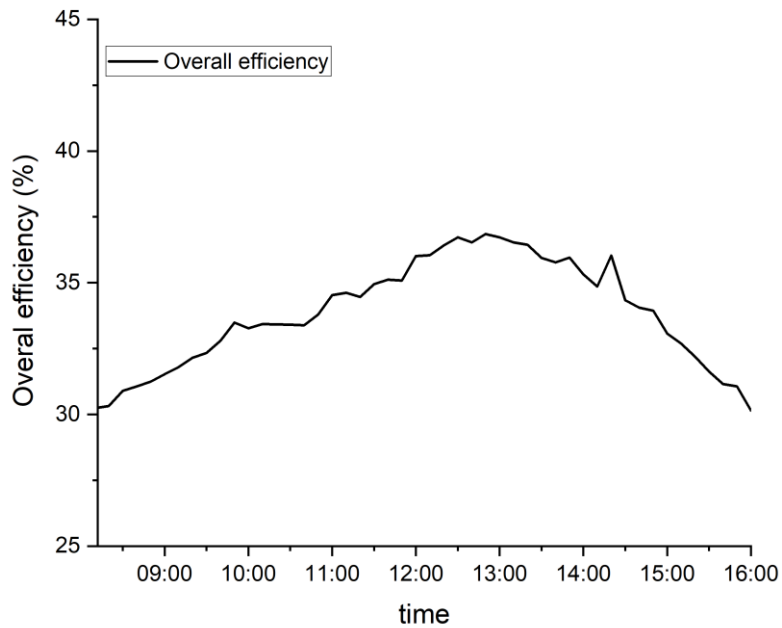
Figure a 14. Overall efficiency of PV/T module 24th June 2023.
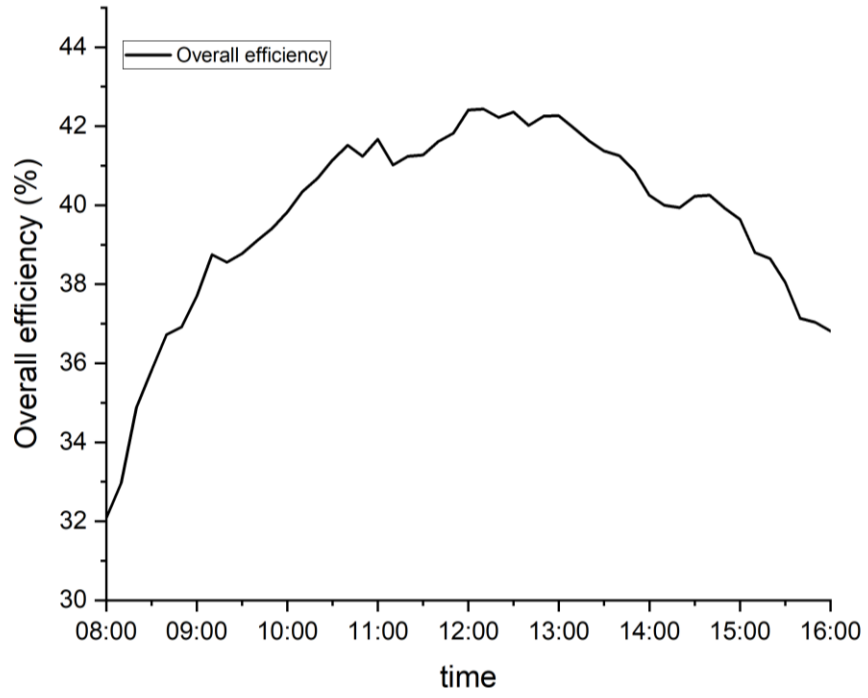
Figure a 15. Overall efficiency of PV/T module 26th June 2023.

Appendix (b): Comparison of thermal and electrical properties for for PV unit and PV/T system
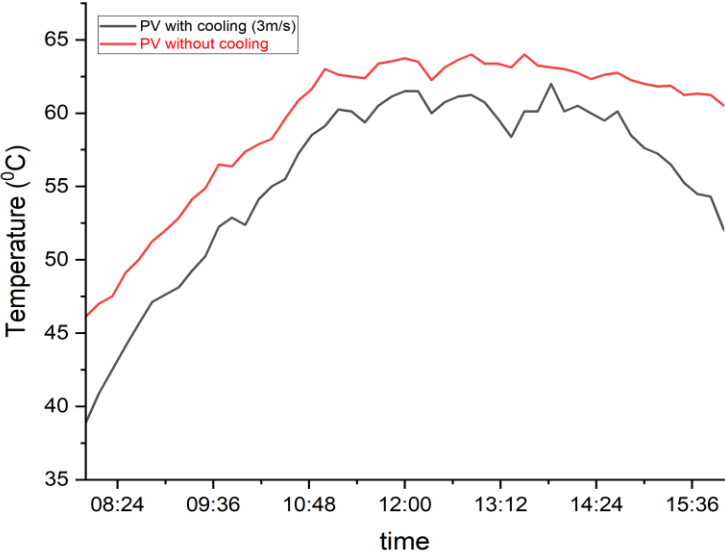
Figure b 1. Panel temperature with and without cooling 24th June 2023.
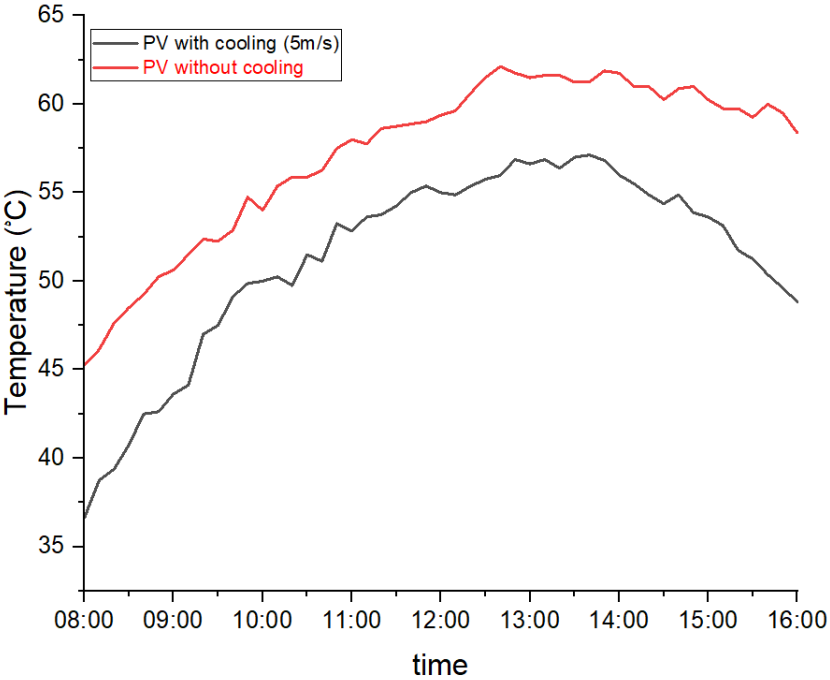
Figure b 2. PV panels temperature with and without cooling 26th June 2023.
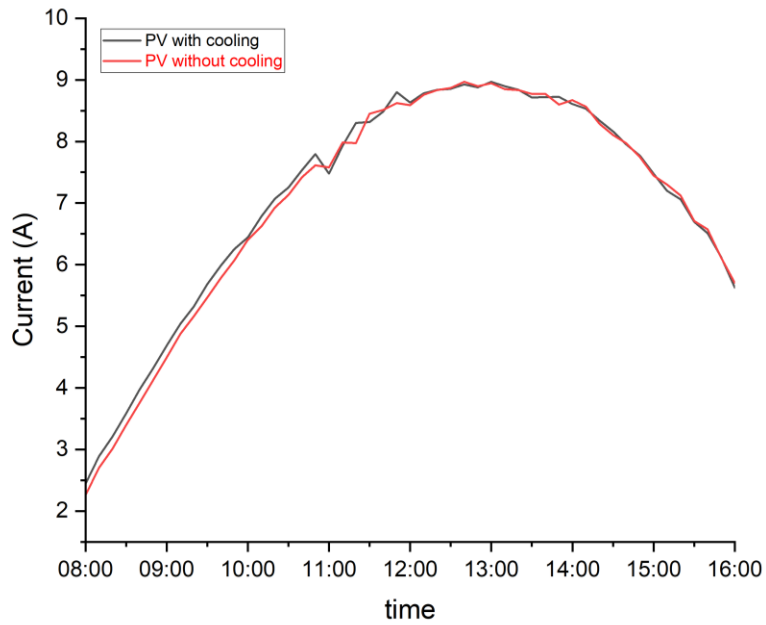
Figure b 3. Current PV with and without cooling 26th June 2023.
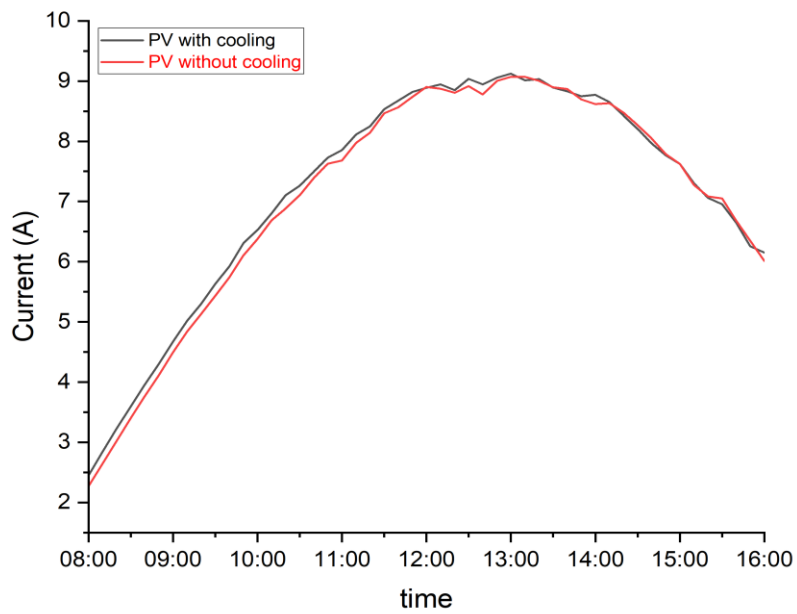
Figure b 4 Current PV with and without cooling 27th June 2023.
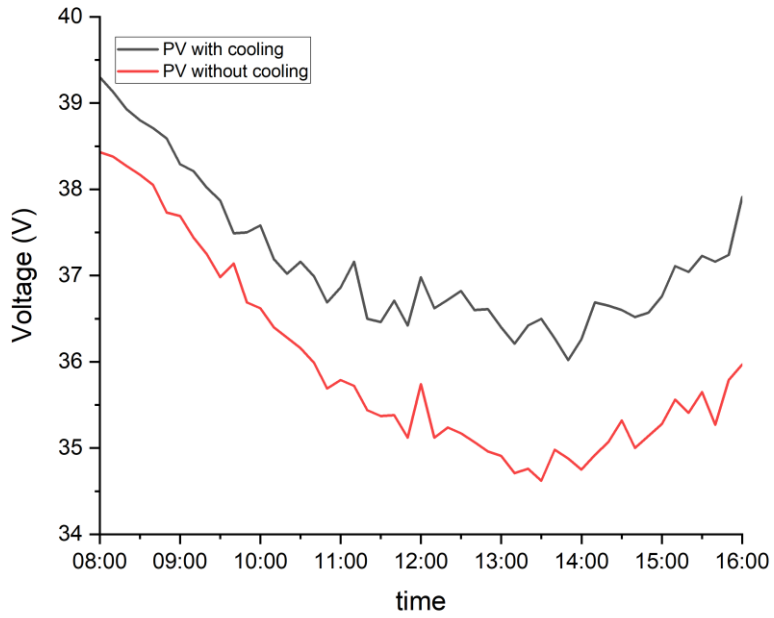
Figure b 5. Voltage PV with and without cooling 26th June 2023.
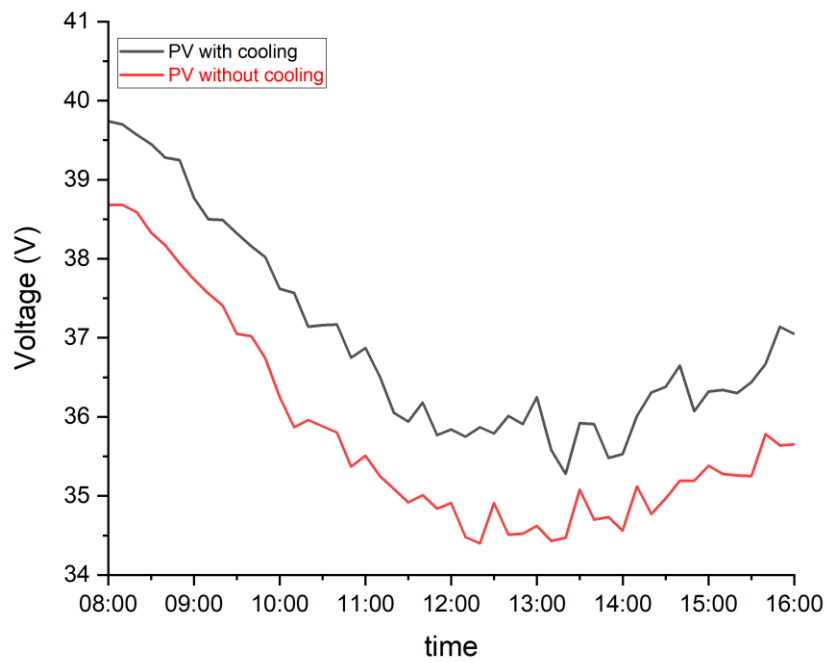
Figure b 6. . Voltage PV with and without cooling 27th June.
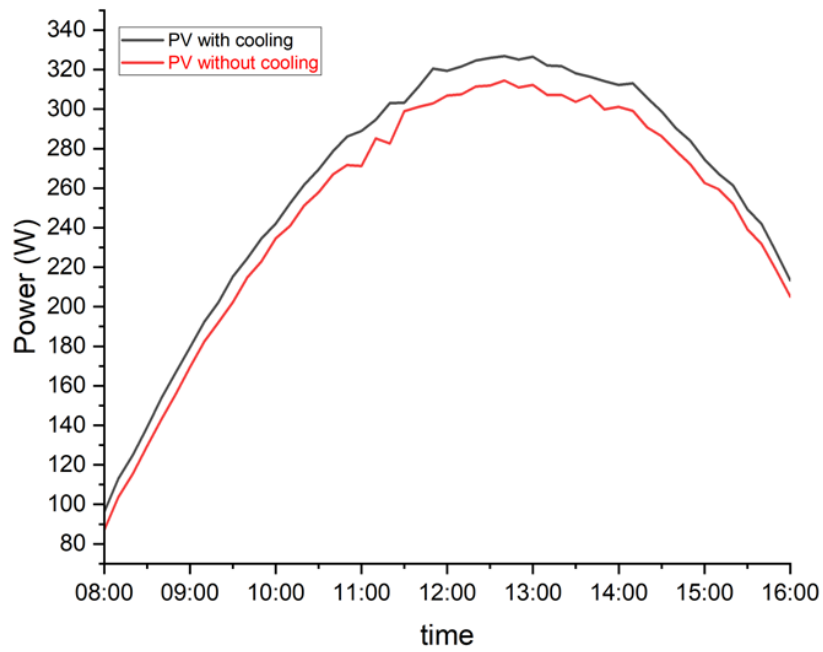
Figure b 7. Power PV with and without cooling 26th June 2023.
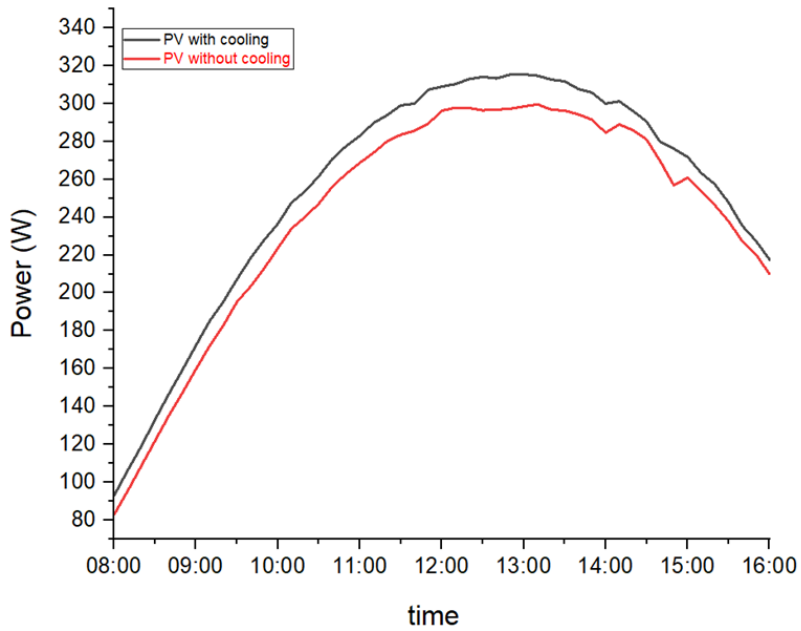
Figure b 8. Power PV with and without cooling 7th July 2023.
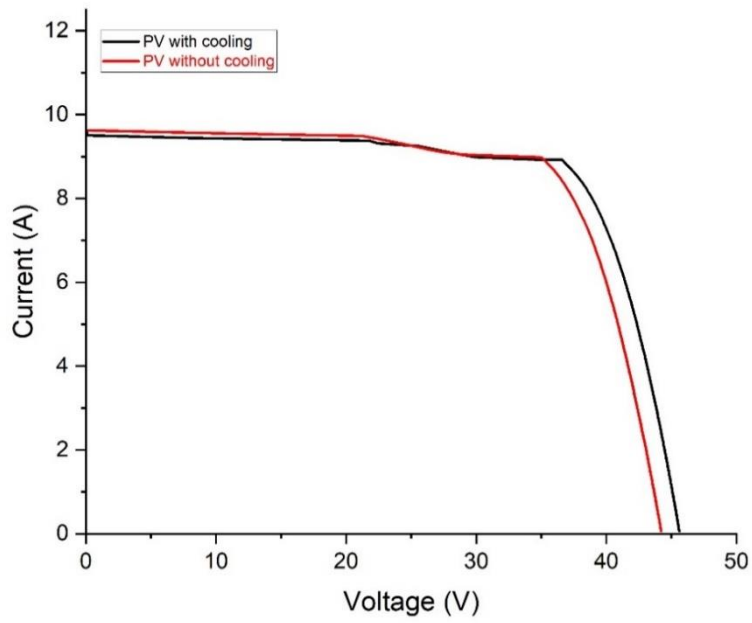
Figure b 9. I-V curve for PV with and without cooling 26th June 2023.

..
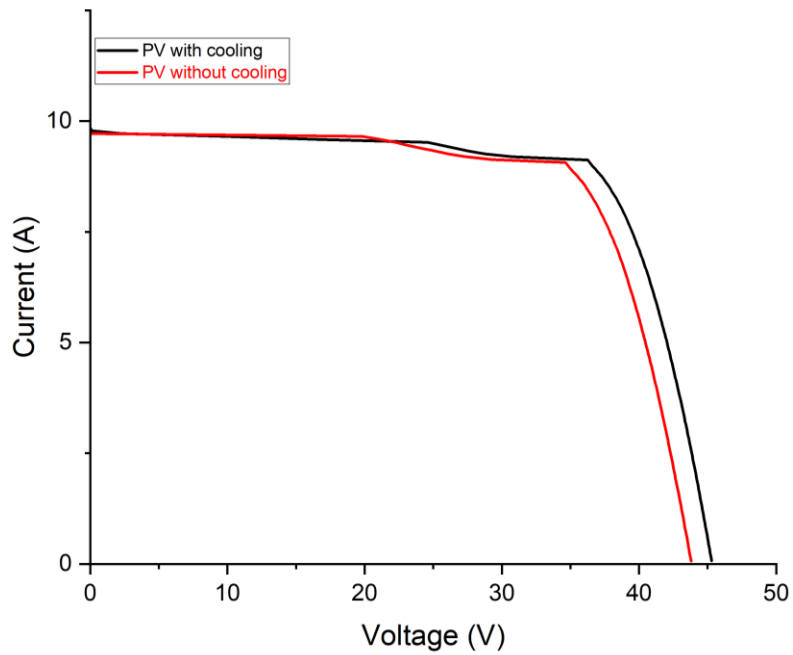
Figure b 10. I-V curve for PV with and without cooling 27th June 2023.
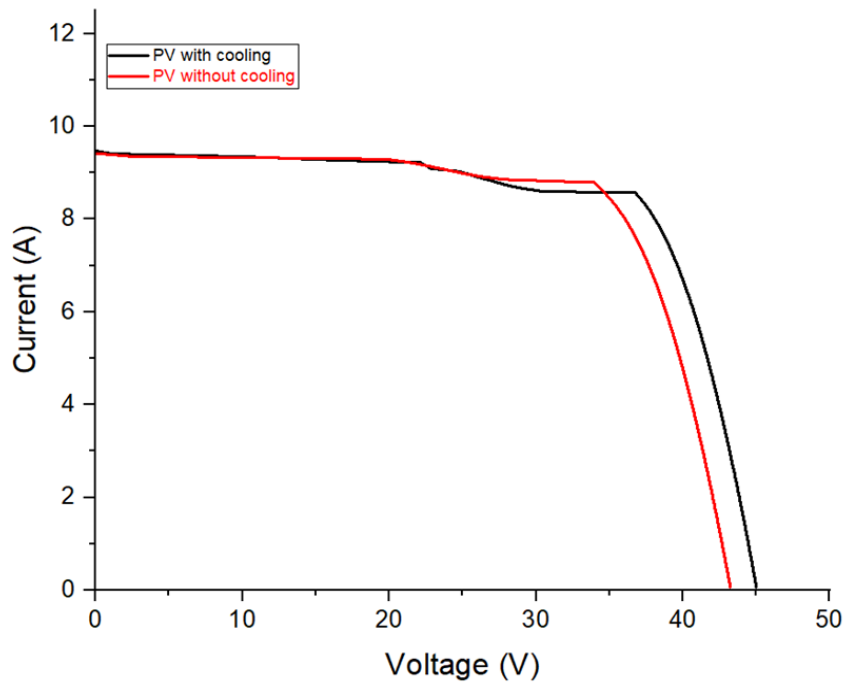
Figure b 11. I-V curve for PV with and without cooling 7th July 2023.
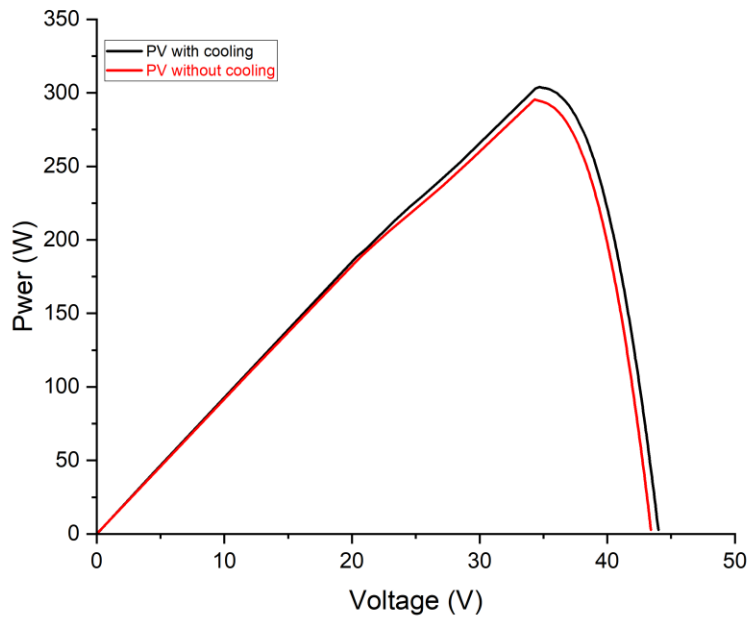
Figure b 12. P-V curve for PV with and without cooling 24th June 2023.
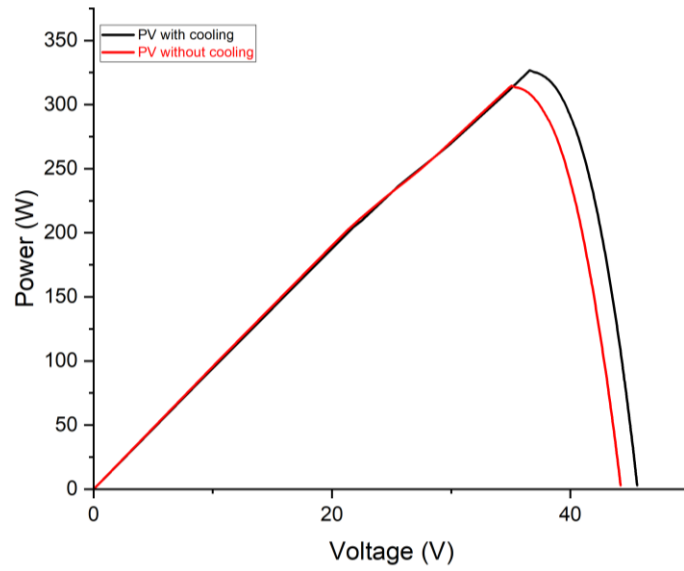
Figure b 13. curve for PV with and without cooling 26th June 2023.
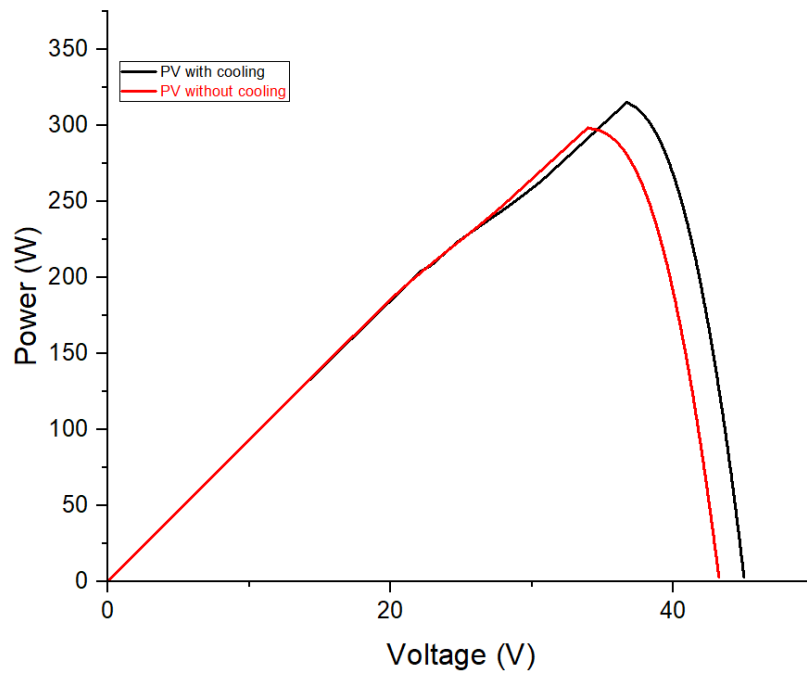
Figure b 14. . P-V curve for PV with and without cooling 7th July 2023.
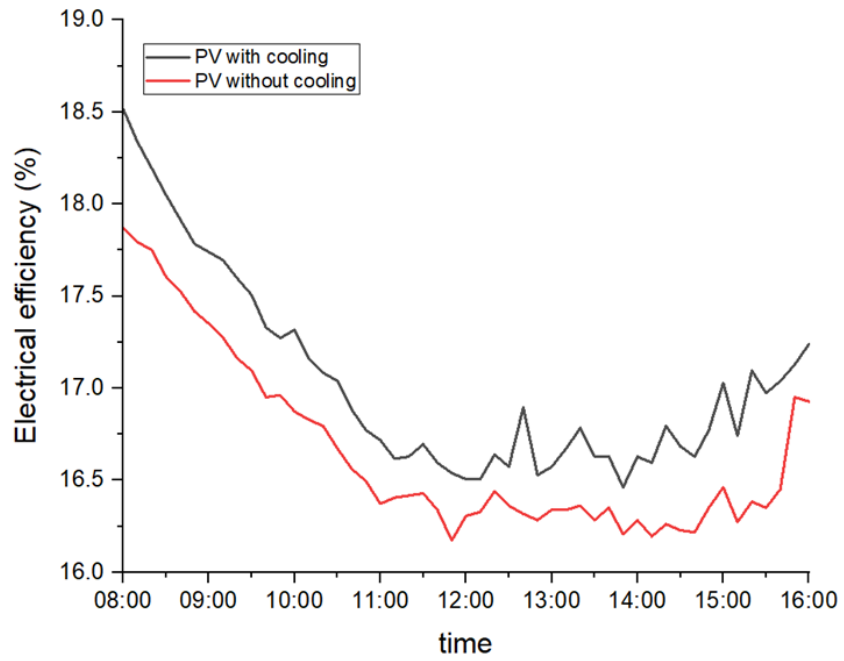
Figure b 15. Electrical efficiency with and without cooling 24th June 2023.
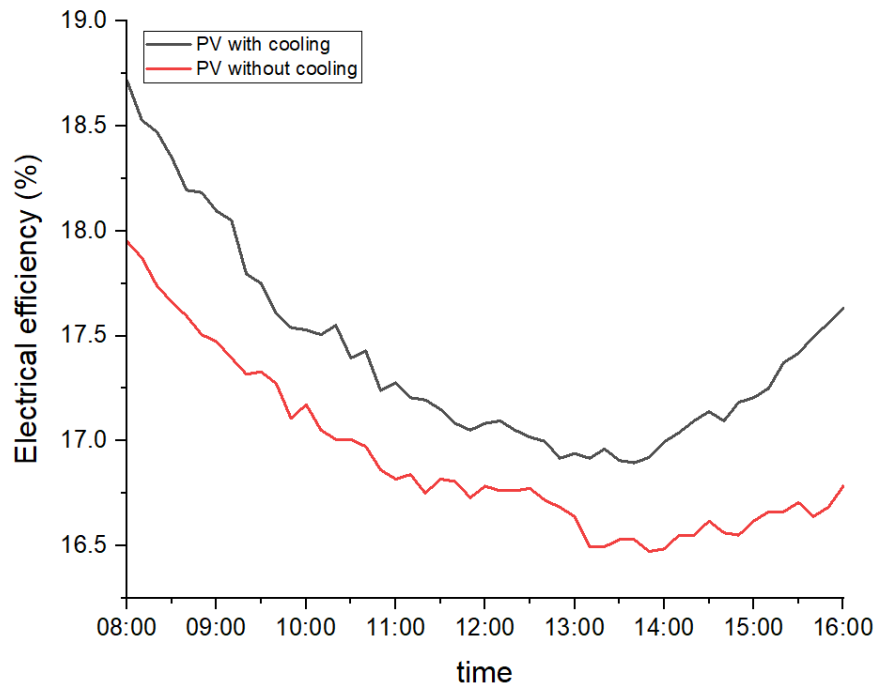
Figure b 16. Electrical efficiency with and without cooling 24th June 2023.
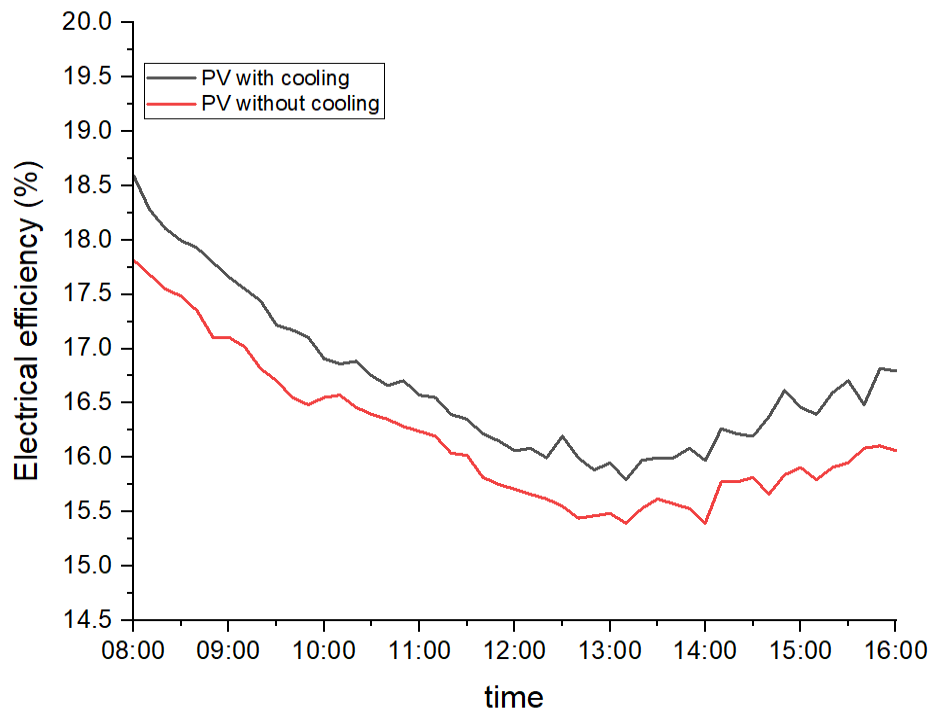
Figure b 17. Electrical efficiency with and without cooling 7th July 2023.

Appendix (c): Experimental setup of the PV unit and PV/T system

Figure c 1. Rear view of the PVunit and PV/T module.

Figure c 2. Side view of the PVunit and PV/T module.

Figure c 3. Air fan and airspeed sensor.

Figure c 4. The Arduino device for experimental work.

Figure c 5. Photovoltaic panels characteristics.

Appendix (D): Calibration of Thermocouple , Solar power meter and Anemometer
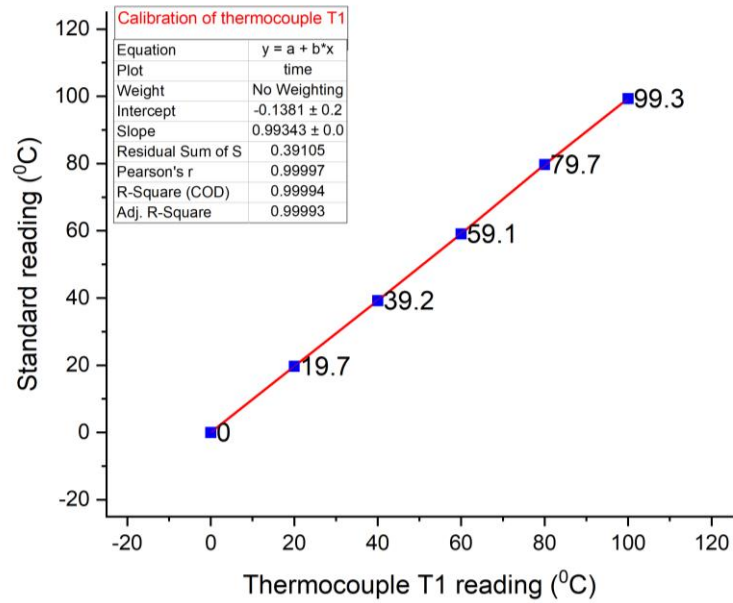
Figure D 1. Calibration of thermocouple (T1).
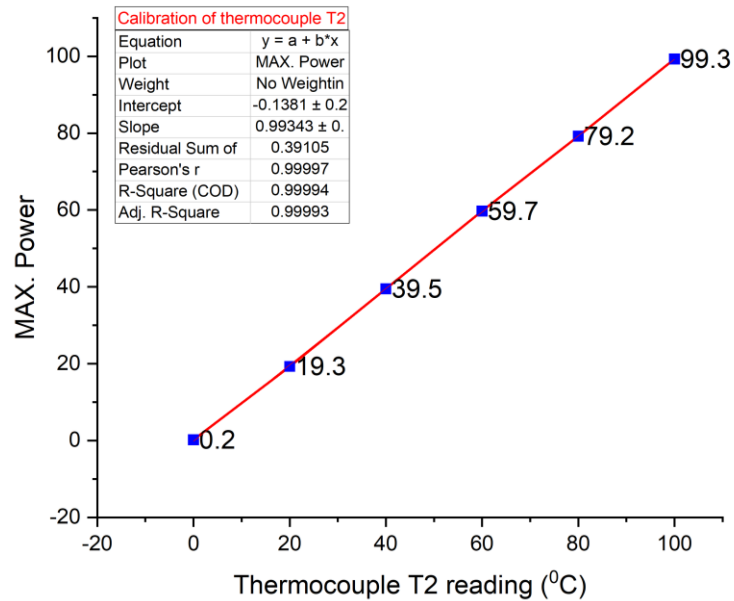
Figure D 2. Calibration of thermocouple (T2).
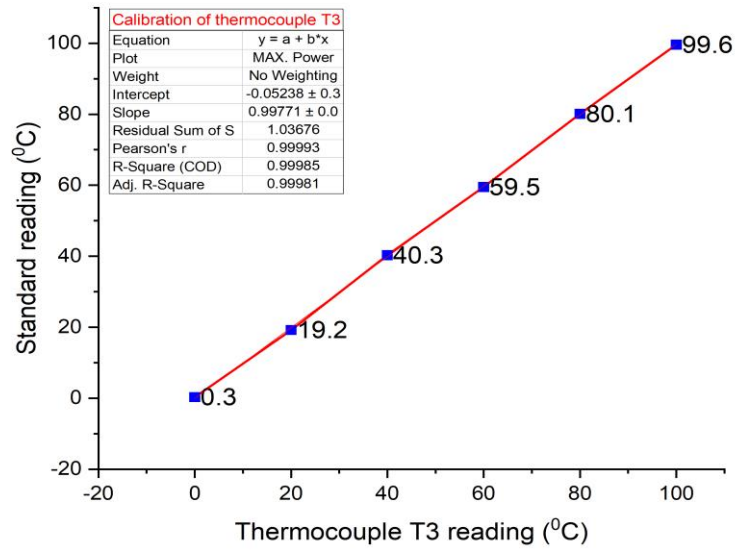
Figure D 3. Calibration of thermocouple (T3).

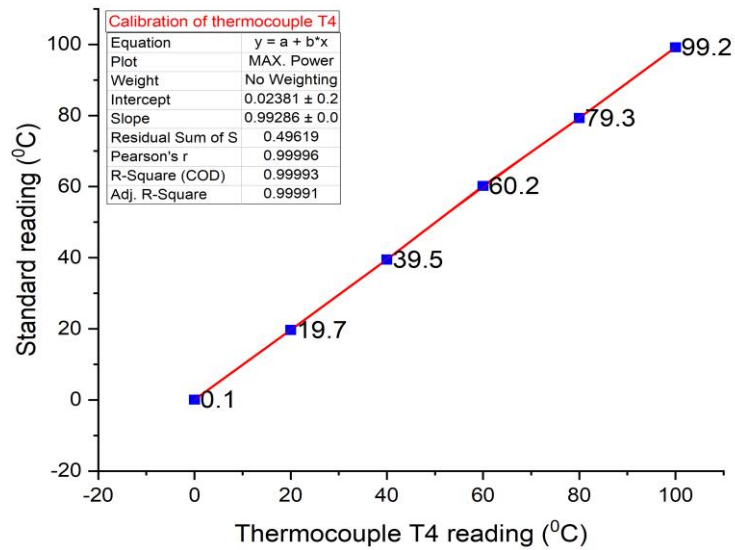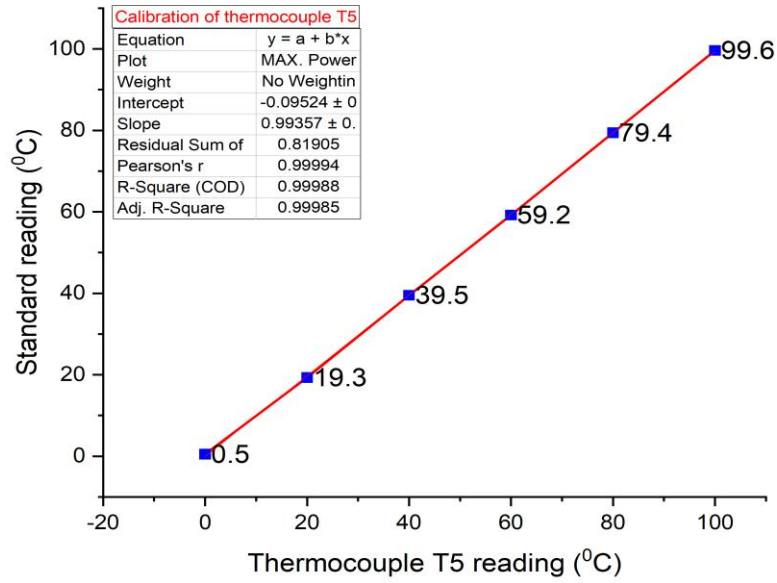Figure D 4. Calibration of thermocouple (T4).

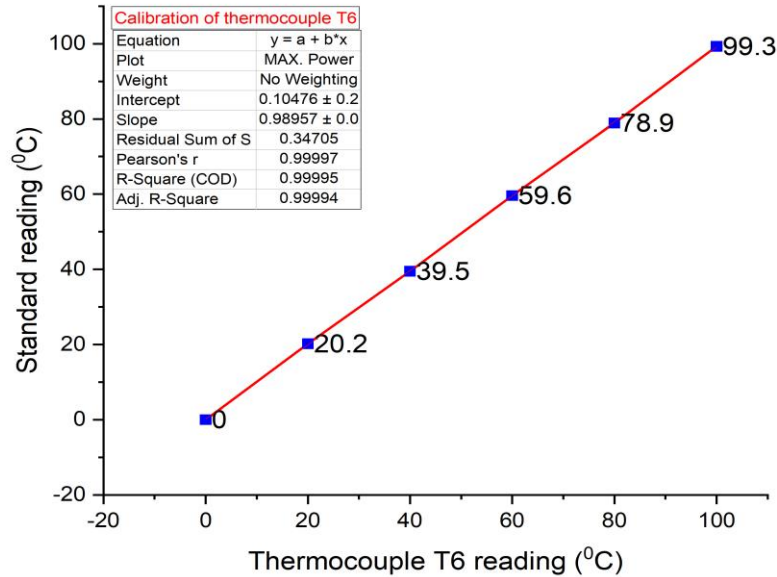Figure D 5. Calibration of thermocouple (T5).
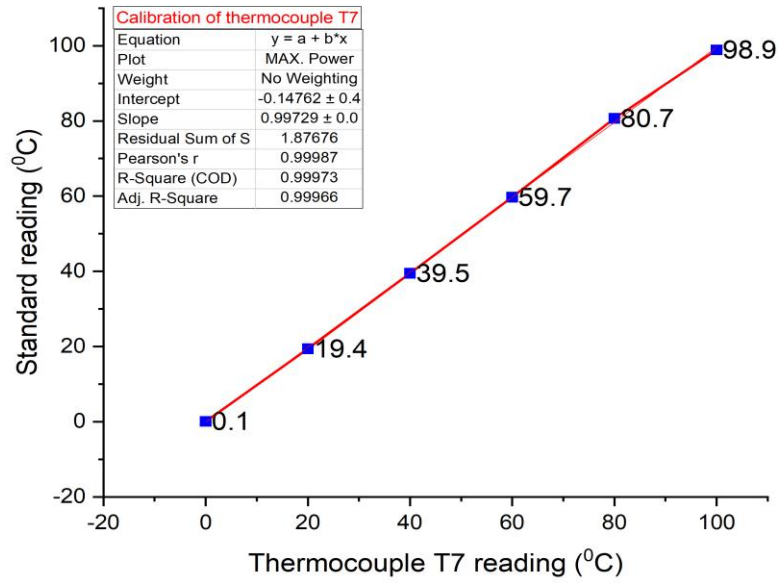

Figure D 6. Calibration of thermocouple (T6).

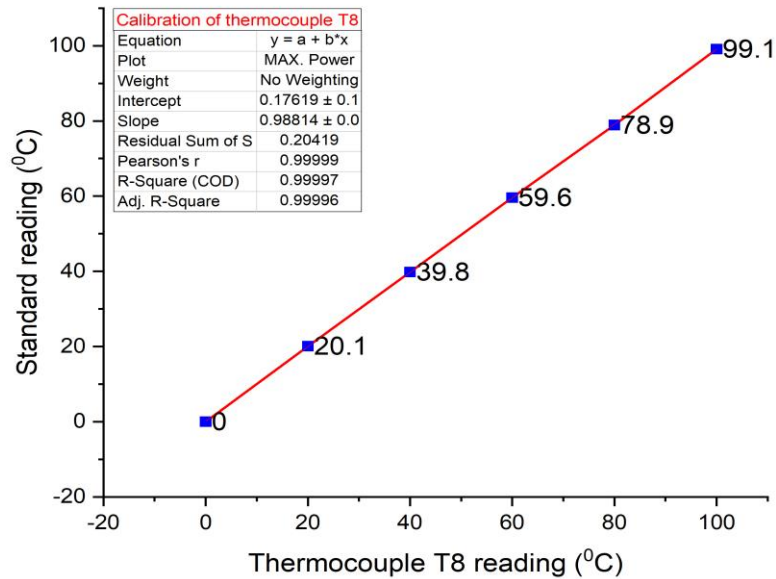Figure D 7. Calibration of thermocouple (T7).

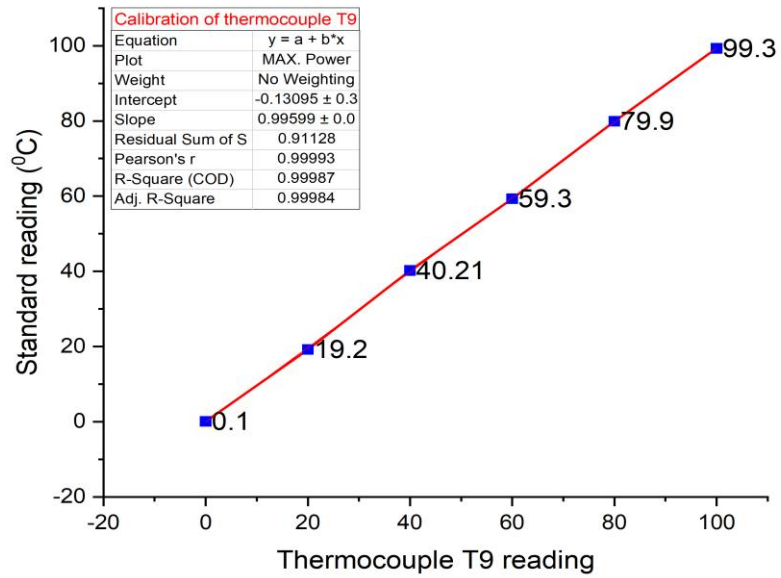Figure D 8. Calibration of thermocouple (T8).

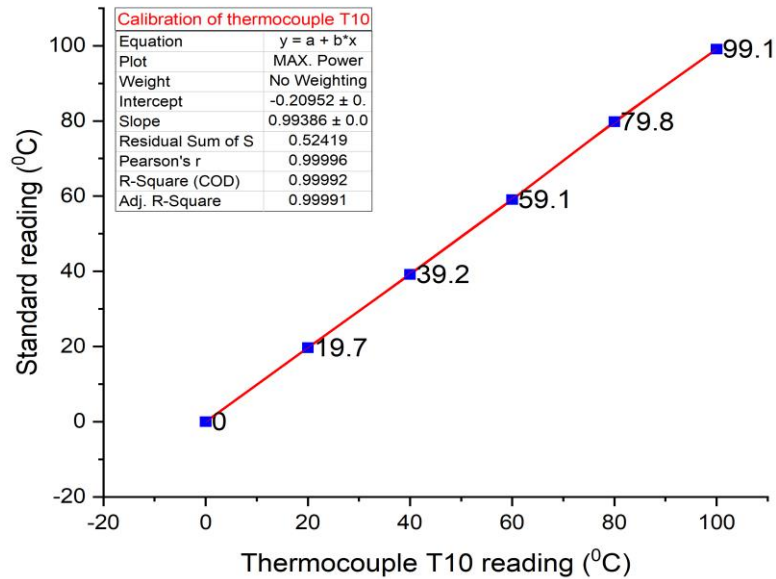Figure D 9. Calibration of thermocouple (T9).

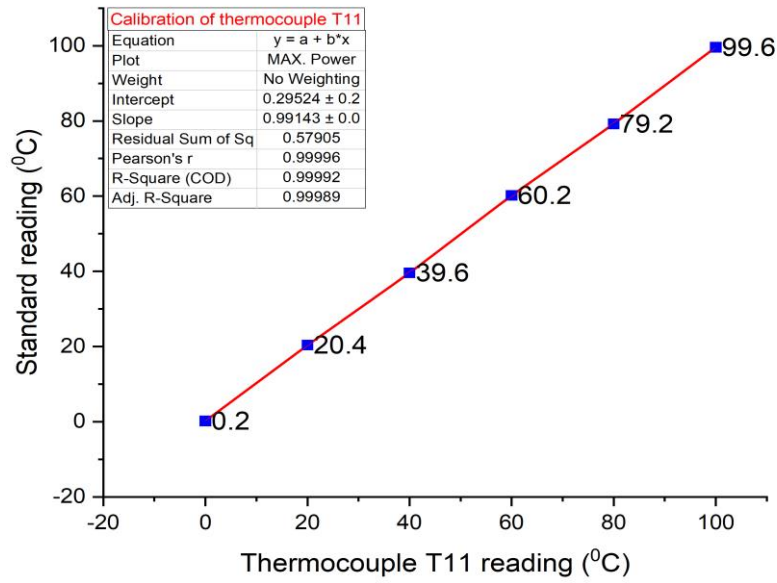Figure D 10. Calibration of thermocouple (T10).

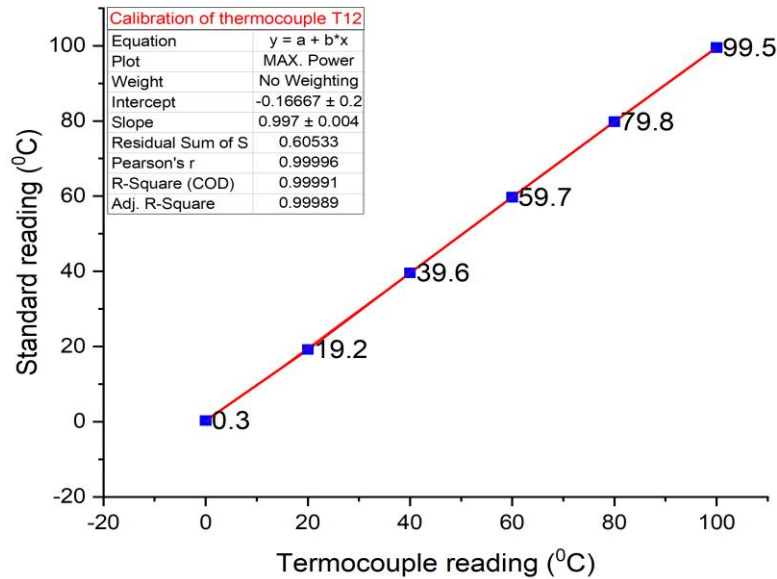Figure D 11. Calibration of thermocouple (T11).

Figure D 12. Calibration of thermocouple (T12).
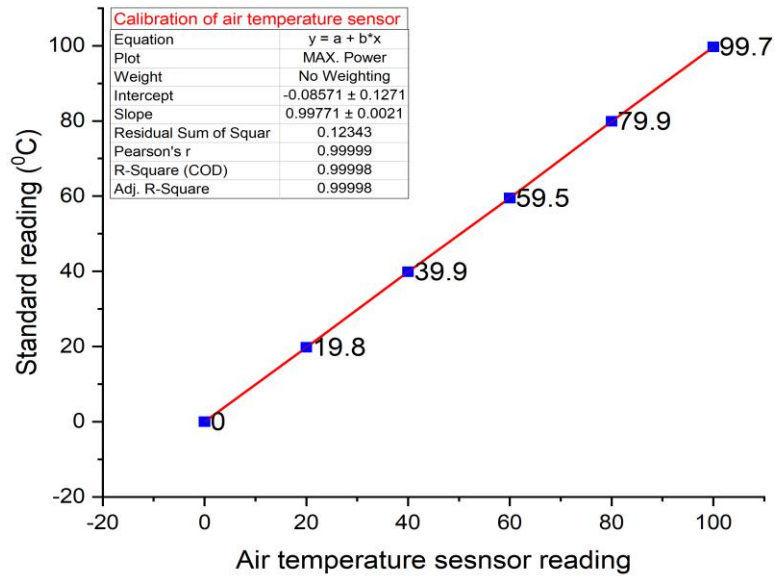
Figure D 13. Calibration of air temperature sensor.
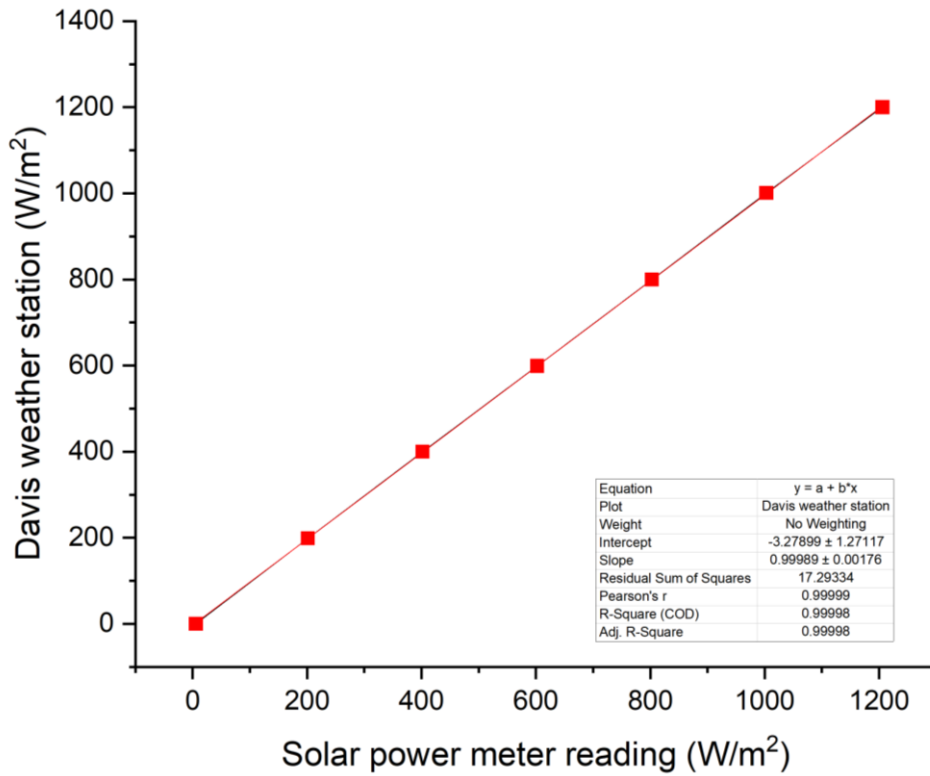
Figure D 14. Calibration of Solar power meter.
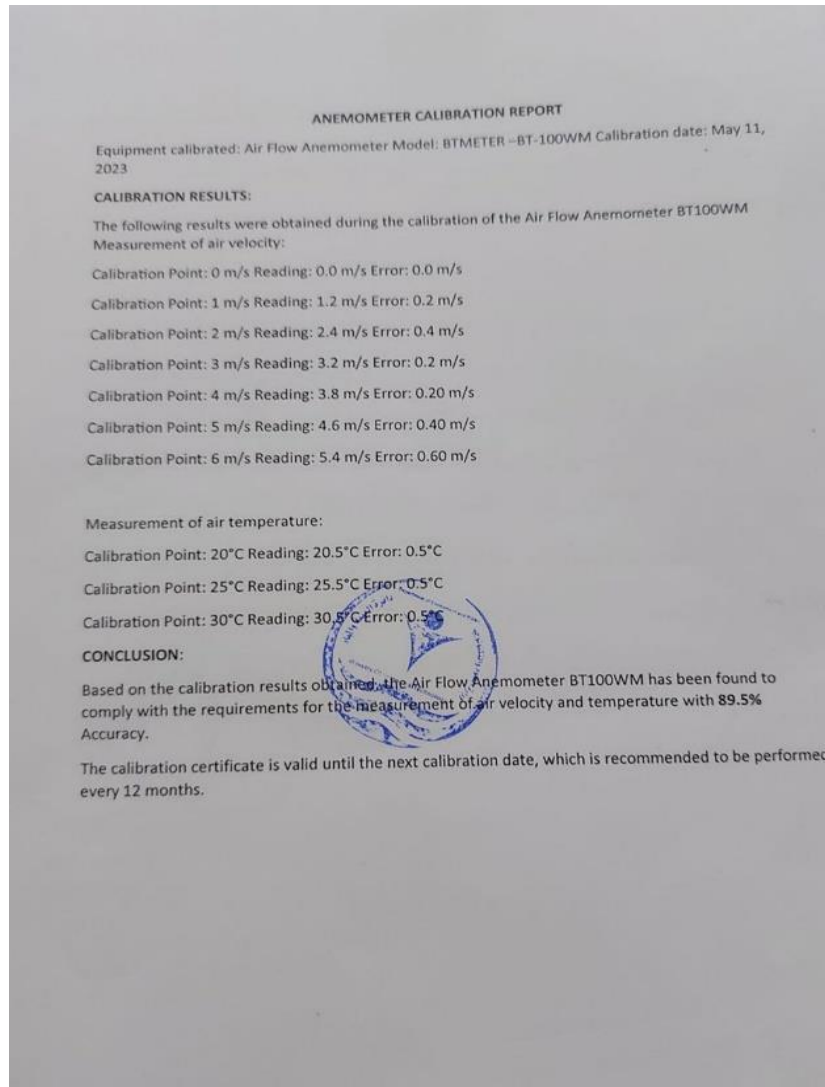
Figure D 15. Calibration of Anemometer.

Appendix (E): Uncertainty and accuracy for the measuring instruments

Instruments	Accuracy	Range	Uncertainty	Resolution
Solar power meter	$\pm$ 10 W/m^2	0 .1– 1999 W/m^2	5.77 W/m^2	0.1W/m^2
Anemometer	$\pm$ 0.2 m/s	0 – 32.4 m/sec	0.115 m/s	0.1m/s
Thermocouples	$\pm$ 1.2 ^{o}C	0 – 1200 ^{o}C	0.692 ^{o}C	0.1 ^{o}C
PV analyzer	$\pm$ 0.01V	0 – 60 V	0.01V	0.01 V
	$\pm$ 0.01 A	0 –12 A	0.01A	10 mA

Appendix (F): List of Publications

1- Numerical investigation on the performance analysis of thermophotovoltaic by using COMSOL

University POLITEHNICA of Bucharest
Faculty of Mechanical Engineering and Mechatronics
Department of Thermotechnics, Engines, Thermal and Refrigeration Equipments

Bucharest, 30.09.2023

Dear Authors:

Amjad H. HAMZAW and Qahtan A ABED

On behalf of the Organizing Committee, it is my pleasure to announce you that your paper entitled

NUMERICAL INVESTIGATION ON THE PERFORMANCE ANALYSIS OF THERMOPHOTOVOLTAIC BY USING COMSOL

has been accepted by the Scientific Committee and was presented by at least one author at the *11th International Conference on Thermal Equipments, Renewable Energy and Rural Development TE-RE-RD 2023*, organized in the period 8-10 June 2023 (onsite & online) by a consortium of Romanian Institutions led by University Politehnica of Bucharest.

Accepted and presented papers to TE-RE-RD 2023 are to be submitted to "Technium Romanian Journal of Applied Sciences and Technology" (ISSN: 2668-778X,#
https://techniumscience.com/index.php/technium/issue/archive,# in order to be published , and submitted to be indexed in prestigious scientific databases.

More details related to the Conference can be found on the webpage www.tererd.upb.ro .

Yours sincerely,

Professor Dr.ing. Gabriel Negreanu
Chair TE-RE-RD 2023

2- A Review of cooling Techniques for Photovoltaic Modules

2nd **International Conference on Engineering, and Science to Achieve the Sustainable Development Goals**

(9th – 10th) July 2023 in Tabriz - Iran

Final Acceptance Letter

Manuscript Number: 314

Dear: Amjad H. Hamzawy

Co-Authors: Qahtan A. Abedb

Congratulations!

It is a great pleasure to inform you that, following the peer review process, your manuscript titled

(A review of cooling techniques for Photovoltaic modules)

Had been **ACCEPTED** for participating in the 2nd **International Conference on Engineering, and Science to Achieve the Sustainable Development Goals,** and considered for publication in **(AIP Conference proceeding).**

Thank you for your significant contribution to the ICASDG2023 conference.

Prof. Dr. Ahmed G. Wadday
ICASDG2023 Scientific Committee Chair | AIP Conference Proceeding Editor
9th – 10th **July 2023 | Tabriz | Iran**

3- An experimental study on the impact of porous media in improving the heat transfer performance characteristics of photovolatic - thermal

Manuscript Details

Manuscript Details

Manuscript Id	: **JTEN-2023-359**
Title	: An experimental study on the impact of porous media in improving the heat transfer performance characteristics of photovoltaic-thermal
Scope(Resarch Sub Area)	: Heat and mass transfer, Single-phase and multi-phase flow , Renewable energy systems
Version:	: 1
Journal	: Journal of Thermal Engineering
Issue	: 2025-11-2-Special Issue 21 ICETMIE 2022 Emerging Trends in Thermal Engineering
First Submission Start Date	: 8.11.2023(0)
Peer Review status	: Initial Submission 8.11.2023(0)
Corresponding Author	: Amjad Hamzawy
Author(s)	: Amjad Hamzawy-

Assigned Editor

Assigned Reviewer(s)

Uploaded File List

1- An experimental study of photovoltaic-thermal.docx

الخلاصة

نظرا للآثار الضارة المرتبطة باستخدام الوقود الأحفوري، أصبح من الضروري تحديد مصادر بديلة للطاقة. إحدى الطرق الرئيسية لتوليد الطاقة المتجددة هي الطاقة الشمسية. حيث يمكن تحويل الطاقة الشمسية إلى طاقة كهربائية باستخدام الخلايا الشمسية (الخلايا الكهروضوئية). تتأثر كفاءة الخلايا الشمسية بشكل كبير بدرجة حرارة تشغيلها، لذلك أصبح من الضروري جدا تقليل درجات حرارة التشغيل المرتفعة لتعزيز أدائها. في هذه الدراسة، تم إجراء بحث نظري وعملي واسع النطاق بهدف تقليل درجة حرارة تشغيل الألواح الكهروضوئية وزيادة كفاءتها الإجمالية.

يتضمن الموديل الرياضي المقترح استخدام تدفق الهواء القسري داخل مجرى الهواء الذي يحتوي بداخله على المعدن المسامي المثبت على السطح الخلفي للوح الكهروضوئي. تم تحديد التصميم الأمثل للنظام الكهروضوئي/الحراري من خلال التحليل النظري باستخدام COMSOL Multiphysics 5.5 ، والذي سهل لاحقًا العمل التجريبي. وأشارت نتائج المحاكاة إلى أن وجود 14 ضلعًا (7 مجاري) من الوسائط المسامية أدت إلى الحصول على نتائج جيدة .

أجريت الدراسة التجريبية في معهد التقني الرميثة، جامعة الفرات الأوسط التقنية في العراق (الإحداثيات: 42°31′ - 12°45′). وأثناء العمل التجريبي، تم استخدام لوحين شمسيين من السيليكون أحادي البلورية، احدهما في النظام الكهروضوئي الحراري (PV/T) يستخدم نظام التبريد، بينما كانت اللوحة الأخرى بدون استخدام تبريد حيث استخدمت لغرض المقارنة. تم تصنيع مجرى الهواء (وهو جزء مهم من اجزاء النظام الكهروضوئي الحراري) من معدن الألومنيوم بسمك 0.7 مم، وعمق 115 مم، وطول 2000 مم، وعرض 1000 مم. كما تم استخدام مروحة لسحب الهواء .

وتم اجراء التجارب العملية على مدار عدة أيام مختلفة من السنة، وأظهرت النتائج أن الحد الأقصى للكفاءة الكهربائية المحققة وصل إلى 19%، وهو ما يمثل تعزيزًا بنسبة 6.9%، مع طاقة إنتاجية قصوى تبلغ 330.7 واط.

علاوة على ذلك، تم قياس الحد الأقصى للإشعاع الساقط حيث بلغ 1192.14 واط/م2، مع اختلاف في درجات الحرارة قدرها 6.7 درجة مئوية بين الهواء الداخل والخارج. حيث بلغت كمية الحرارة المكتسبة حوالي 378.6 واط، الكفاءة الحرارية حوالي 29.57%، بذلك، تم تحقيق كفاءة إجمالية بنسبة 48.53%، مما يؤكد فعالية النظام الكهروضوئي الحراري المطبق.

تعزيز الكفاءة الحرارية والكهربائية للنظام الكهروضوئي الحراري

بأستخدام معدن مسامي

رسالة مقدمة الى

قسم هندسة تقنيات ميكانيك القوى

كجزء من متطلبات نيل درجة الماجستير في

هندسة تقنيات ميكانيك القوى/ الحراريات

تقدم بها

أمجد حميد حمزاوي

ماجستير في هندسة تقنيات ميكانيك القوى

اشراف

الاستاذ الدكتور

قحطان عدنان عبد الفتلاوي

1445

جمهورية العراق

وزارة التعليم العالي والبحث العلمي

جامعة الفرات الاوسط التقنية

الكلية التقنية الهندسية/النجف

تعزيز الكفاءة الحرارية والكهربائية للنظام الكهروضوئي الحراري

بأستخدام معدن مسامي

أمجد حميد حمزاوي

ماجستير في هندسة تقنيات ميكانيك القوى

1445